ANALYSIS METHOD FOR THE DESIGN OF REINFORCED CONCRETE BRIDGE BARRIER AND CANTILEVER DECK UNDER RAILING LOADS AS SPECIFIED IN CAN/CSA-S6-00 (CANADIAN HIGHWAY BRIDGE DESIGN CODE)

by

JOE WONG

B.A.Sc., University of British Columbia, Canada, 2002

A THESIS SUBMITTED IN PARTIAL FULFILLMENT OF
THE REQUIREMENT FOR THE DEGREE OF

MASTER OF APPLIED SCIENCE

in

THE FACULTY OF GRADUATE STUDIES

Civil Engineering

THE UNIVERSITY OF BRITISH COLUMBIA

August 2005

Abstract

The objective of this thesis is to develop a rational and effective method for designing reinforced concrete bridge parapets and cantilevered decks so that such a method could be easily applied in practice against railing loads, as specified in the CAN/CSA-S6-00 *Canadian Highway Bridge Design Code.*

The maximum moment dispersal angle (MMDA) is the most promising overall of the methods being considered for this task, including yield line analysis (YLA), finite element analysis (FEA) and the dispersal angle method. The MMDA provides a means of approximating maximum moments, which were evaluated using the linear elastic FEA at locations of interest on both the traffic barriers and the deck overhang using dispersal angles, which are provided in the form of tables. The MMDA is an improved version of the maximum moment envelope (MME) method, which had been initially developed based on concepts from the dispersal angle method as well as the FEA. The improved MMDA method takes advantage of the accuracy of FEA and the simplicity of the classic concept of load dispersion, while eliminating some of the issues of unconventionality found in the dispersal angle method. Hence, MMDA is an improvement on the dispersal angle method, as was suggested in the *Commentary* of S6-00. It minimizes possible inconsistencies between the code design methods and the FEA results.

This thesis summarizes the design criteria, methods of analysis, and load applications for bridge traffic barriers and deck overhang design that has been suggested by various jurisdictions, including *AASHTO LRFD Bridge Design Specifications 2004,* Washington State DOT *Bridge Design Manual LRFD,* CAN/CSA-S6-88 *Design of Highway Bridges* and CAN/CSA-S6-00 *Canadian Highway Bridge Design Code.*

Table of Contents

List of Tables

List of Figures

Acknowledgment

I would like to express my deepest gratitude to Mr. Kevin Basin (Chief Bridge Engineer) and Ms. Sharlie Huffman (Bridge Seismic Engineer) from the Ministry of Transportation of British Columbia. Their support and contributions to this research have been invaluable to my work.

I would also like to acknowledge my research supervisor, Dr. S. F. Stiemer, for his continual guidance and for the immense effort he has put into making this research an interesting and enlightening experience for me. His wisdom and sense of humor have helped me to overcome challenges, and delighted me in many ways.

Further, I would like to express my appreciation for my fellow students: Nathan Loewen and Chun Hai (Sean) Xiao, both of whom participated in this project.

Last, but not least then, I sincerely thank my family and friends for the time and effort they have put into encouraging me and supporting me throughout my journey.

Chapter 1: Introduction

The objective of this research is to develop an effective tool that is practical and which can be easily used to design reinforced concrete parapets, as well as the cantilever portion of bridge decks, against railing loads as specified in the CAN/CSA-S6-00 *Canadian Highway Bridge Design Code*. This design tool should allow designers to calculate the design forces of both the cantilevered deck and the traffic barrier/parapet system with minimum effort. It should also seek a compromise with the current code *S6-00*, and should effectively improve, or upgrade, the current code's proposed methods. The method developed in this research combines the concepts of finite element analysis and the dispersal angle method, called the maximum moment dispersal angle (MMDA) method. The scope of this research focuses on the design criteria for performance level 2 and 3. These two performance levels have the highest load magnitude and the widest area of affect, based on the standards of the *S6-00*.

This report will include a general discussion of the methods suggested by various jurisdictions, such as *AASHTO LRFD Bridge Design Specifications 2004*, Washington State DOT *Bridge Design Manual LRFD*, CAN/CSA-S6-88 *Design of Highway Bridges* and CAN/CSA-S6-00 *Canadian Highway Bridge Design Code*. Background information such as site condition ranking systems, specified design loads and their applications, design criteria, and analysis methods are topics included in that review. A discussion of the strengths and weaknesses found in each jurisdiction is also essential for contributing towards the improvement of current methods.

For the purposes of this research, several methods of analysis have been used for study, including yield line analysis (YLA), finite element analysis (FEA), and dispersal

1

angle methods. The theory behind each method is reviewed in detail, then following by a discussion and an investigation of their advantages and disadvantages. In order to come up with a method that takes advantages of the above methods while minimizing their drawbacks, a new method called "maximum moment envelope" (MME) will be introduced. However, this new concept deviates from a possible ideal outcome of this research because of its complexity and difficulty when applying to practice. As a result, a further improved version of this method, called the "maximum moment dispersal angle" (MMDA) will be established. This one has proven to be more useful and effective than other methods. The results of the MMDA will then be presented in the form of a table for easy and efficient application. Finally, examples usage of this new method as well as examples of some of the traditional methods will be shown in a correlation study.

Chapter 2: Background Research and Literature Review

As part of the literature review, relevant jurisdictions will be studied and discussed in detail in the following section in order to provide background information on this topic. The jurisdictions being reviewed are the *AASHTO LRFD Bridge Design Specifications*, Washington State DOT *Bridge Design Manual LRFD, CAN/CSA-S6-88 Design of Highway Bridges* and *CAN/CSA-S6-00 Canadian Highway Bridge Design Code.* Methods of analysis, loading criteria, traffic barriers and bridge deck overhang designs are all issues included in this discussion. Although the design methods suggested by each jurisdiction have their own distinct advantages, only a few of them have been selected for the following discussion as the scope of this research. Ultimately one method is proposed for further studies as far as the scope of this research allows. The review of various codes provides solid background information in making such a decision. Details of the recommended design methods can be found in Chapter 3 "Methods of Analysis."

2.1 AASHTO LRFD Bridge Design Specifications

The third edition of the *American Association of State and Highway and Transportation Officials (AASHTO)* published in 2004 is considered in this study. In general, *AASHTO* codes are well recognized and are used as the basis of many other official codes in different municipalities. For example, the *Canadian Highway Bridge Design Code* CAN/CSA-S6-00, which is discussed in a later section, makes many references to the *AASHTO* as a supporting document. Reviewing this code is needed in order to understand the philosophy behind various design methods in other codes.

2.1.1 Limit States and Resistance Factors

ASSTHO Clause 13.6.1 states that the strength limit should be applied according to load

combinations specified in *ASSTHO* Table 3.4.1-1, using resistance factors as specified in

ASSTHO Articles 5.5.4, 6.5.4, 7.5.4, and 8.5.2. For an extreme event limit state, the

bridge deck design forces may be determined by an ultimate strength analysis using the

loads specified in Table 1 and applied as illustrated in Figure 1 as factored loads.

Table 1 - Design Forces for Traffic Railings

(Data source: AASHTO Table A13.2-1)

Design Forces and Designations	Railing Test Levels						
	TL-1	TL-2	TL-3	TL-4	TL-5A	TL-5	TL-6
F_t, Transverse (kip)	13.5	27	54	54	116	124	175
F_L, Longitudinal (kip)	4.5	9.0	18.0	18	39	41	58
F_v, Vertical (kip) Down	4.5	4.5	4.5	18	50	80	80
L_t and L_L (ft)	4.0	4.0	4.0	3.5	8.0	8.0	8.0
L_v (ft)	18.0	18.0	18.0	18.0	40.0	40.0	40.0
H_e (min)(in)	18	20	24	32	40	42	56
Min. H Height of Rail (in)	27	27	27	32	40	54	90
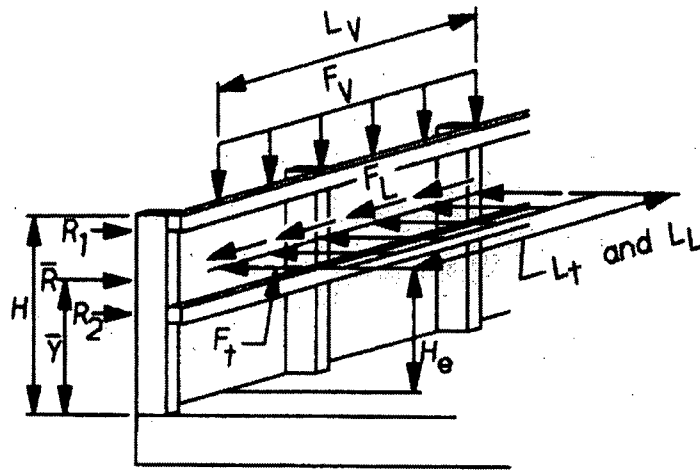
Figure 1 - Bridge Railing Design Forces, Locations and Distribution Length

(Data source: AASHTO Figure A13.2-1)

2.1.2 Test Levels

AASHTO has introduced seven test levels in correspondence with the *NCHRP Report 350, Recommended Procedures for the Safety Performance Evaluation of Highway Features*. The seven test levels in *AASHTO* Clause 13.7.2 are specified so as to evaluate the performance factors of bridge railings, which include structural adequacy, occupant risk, and post-impact behavior of the test vehicles. The seven test levels being considered are TL-1, TL-2, TL-3, TL-4, TL-5A, TL-5, and TL-6 as ranked from the lowest level of TL-1 to the highest level of TL-6. TL-1 is generally acceptable for a work zone with low posted speed limits, and for very low-volume, low-speed local streets. TL-6 on the other hand, is generally acceptable for applications on freeways with high speed, high traffic volume, a higher ratio of heavy vehicles, and otherwise unfavorable site conditions. *AASHTO Commentary* Clause C13.7.2 also states that the TL-4 railing is expected to satisfy the majority of interstate design requirements. Table 2 provides corresponding

5

vehicle weights, speeds, and angles of impact as the testing criteria for the different test levels.

Table 2 - Bridge Railing Test Levels and Crash Test Criteria

(Data source: AASHTO Table 13.7.2.1)

Vehicle Characteristics	Small Automobiles		Pickup Truck	Single-Unit Van Truck	Van-Type Tractor-Trailers		Tractor-Tanker Trailers
W(kip)	1.55	1.8	4.5	18.0	50.0	80.0	80.0
B(ft)	5.5	5.5	6.5	7.5	8.0	8.0	8.0
G (in)	22	22	27	49	64	73	81
Crash angle, Θ	20°	20°	25o	15°	15°	15°	15°
Test Level	Test Speeds (mph)						
TL-1	30	30	30	N/A	N/A	N/A	N/A
TL-2	45	45	45	N/A	N/A	N/A	N/A
TL-3	60	60	60	N/A	N/A	N/A	N/A
TL-4	60	60	60	50	N/A	N/A	N/A
TL-5A	60	60	60	N/A	50	N/A	N/A
TL-5	60	60	60	N/A	N/A	50	N/A
TL-6	60	60	60	N/A	N/A	N/A	50

2.1.3 Traffic Barrier

AASHTO Clause 13.7.3 gives detailed design criteria for traffic railings. An existing railing system can be used without further analysis or testing if it has been previously tested and proven crashworthy. However, a new system can only be used if it is first approved by full-scale crash tests. The specifications on minimal edge thickness for concrete deck overhangs supporting deck-mounted post systems or concrete barriers are 8 inches, and 12 inches for a side-mounted post system. The height of concrete railings with slopping surfaces should be greater than, or equal to, 27 inches for TL-3 and 32

6

inches for TL-4. Furthermore, concrete railing with a vertical surface should have a minimum height of 27 inches.

Appendix A in *AASHTO* Chapter 13 provides detail information on the specifications of railing geometry and anchorages, railing design forces, and barrier and deck overhang designs. In short, anchorages and reinforcement in concrete barriers should be properly designed, using, amongst other things, bond, honks, embedded plates, and sufficient embedment length, so that the yield strength of the connections can be fully developed. Pull-out failure is an example of immature failure where the yield strength of the connections is not fully developed.

The design loads for barriers under the impact of different test levels should be taken as specified in Table 1, and should be applied as illustrated in Figure 1. The transverse and longitudinal loads are applied at the effective height of the vehicle rollover force, H_e such that:

$$H_e = G - \frac{WB}{2F_t} \qquad (1)$$

Where:

G   =   height of vehicle center of gravity above bridge deck, as specified in Table 2 (ft)

W   =   weight of vehicle corresponding to the required test level, as specified in Table 2 (kip)

B   =   out-to-out wheel spacing on an axle, as specified in Table 2 (kip)

F_t =   transverse force corresponding to the required test level as specified in Table 1 (kip)

The vertical loads are applied on top of the railing but need not be applied in conjunction with the transverse and longitudinal loads.

AASHTO makes use of yield line analysis (YLA) in the capacity design of reinforced concrete and prestressed concrete barriers, or parapets, as described in *AASHTO* Clause A13.3.1. The concept of yield line analysis is explained later under Section 3.1 "Yield Line Analysis." According to the yield line patterns predefined by *ASSTHO* as shown in Figure 2 and 3, though, a unique parameter called the critical length of failure pattern, L_C, is introduced so as to determine the total transverse resistance of the railing, R_W, as described by Equations (2) – (5).
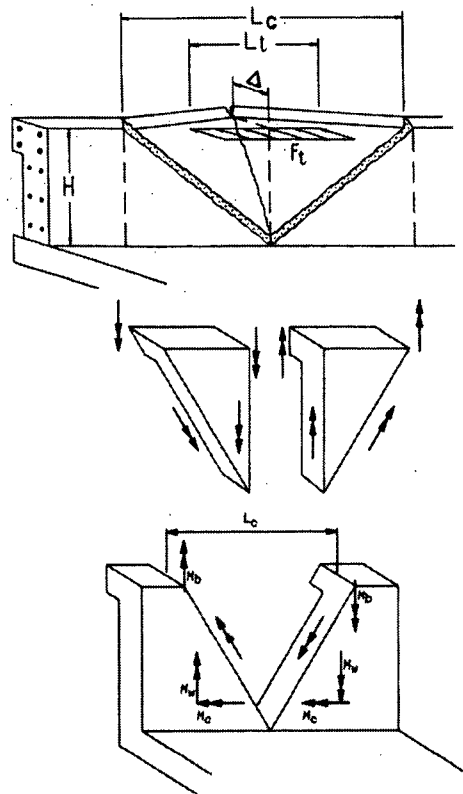
Figure 2 - YLA of Barrier for Inner Portion

(Data source: AASHTO Figure CA13.3.1-1)

8

For inner portion analysis:

$$R_w = \left(\frac{2}{2L_c - L_t}\right)\left(8M_b + 8M_w + \frac{M_c L_c 2}{H}\right)$$ (2)

The critical wall length L_C is taken as:

$$L_c = \frac{L_t}{2} + \sqrt{\left(\frac{L_t}{2}\right)^2 + \frac{8H(M_b + M_w)}{M_c}}$$ (3)
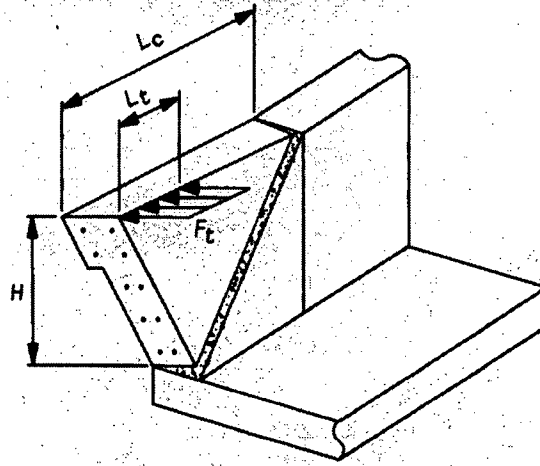
Figure 3 - YLA of Barrier for End Portion

(Data source: AASHTO Figure CA13.3.1-2)

For end portion analysis:

$$R_w = \left(\frac{2}{2L_c - L_t}\right)\left(M_b + M_w + \frac{M_c L_c 2}{H}\right)$$ (4)

$$L_c = \frac{L_t}{2} + \sqrt{\left(\frac{L_t}{2}\right)^2 + H\left(\frac{M_b + M_w}{M_c}\right)}$$ (5)

Where:

H   =   height of wall (ft)

9

L_c = critical length of yield line failure pattern (ft)

L_t = longitudinal length of distribution of impact force F_t (ft)

R_w = total transverse resistance of the railing (kip)

M_b = additional flexural resistance of beam in addition to M_w, if any, at top of wall (kip-ft)

M_c = flexural resistance of cantilevered walls about an axis parallel to the longitudinal axis of the bridge (kip-ft/ft)

M_w = flexural resistance of the wall about its vertical axis (kip-ft/ft)

F_t = transverse force specified in Table 1 (kip)

It is important to note then, that this YLA has assumed that the failure mechanism occurs within the barrier and does not extend to the deck. In other words, the deck must be designed to properly resist the impact loads so that it does not fail before the barrier does, otherwise Equation (2) – (5) are not valid. Also, the longitudinal length of the barrier should be sufficient, meaning that it should be greater than or equal to the critical length, L_C, for the assumed yield line pattern to take place within the barrier. As such, some other means of analysis should be used for capacity calculations if the barrier is considered to be short. For example, a precasted discontinuous barrier may be considered short based on its flexural resistances.

Lastly, it is assumed that the negative and positive resisting moments of barriers are equal. The resisting moment of a barrier depends on its geometry, its material, and on the layout of reinforcement. Ideally, a perfectly symmetrical barrier, with respect to its vertical axis, would yield the same negative and positive resisting moments. However, barriers used in practice are usually perfectly vertical on the outer surface while having the inner surface slightly sloped, meaning that the negative and positive resisting

moments may not in fact be equal. In this case, adjustment of Equation (2) – (5) may be necessary to ensure the accuracy of the barrier capacity calculations. When the total transverse resistance of the railing, R_W, is determined, it is to be subsequently compared with the specified loads in Table 1 for structural adequacy.

2.1.4 Deck Overhang

Deck overhang design should be performed as suggested under *ASSTHO* Article A13.4, with considerations for three separate design cases. The first case is an ultimate limit state design, with an application of the transverse and longitudinal loads as specified in Table 1 and Figure 1. The second case also involves an ultimate limit state design, but this one takes only the vertical loads specified in Table 1 and Figure 1. The last case is a strength limit state design, with applied loads as specified in *ASSTHO* Article 3.6.1. For the first design case, the deck may be expected to provide flexural resistance, acting coincidently with the tensile force, T, which can be calculated using the following equation:

$$T = \frac{R_w}{L_c + 2H} \qquad (6)$$

Where:

R_W = barrier resistance specified in Equation (2) or (4)

L_C = critical length of yield line failure pattern (ft)

H = height of barrier (ft)

T = tensile force per unit of deck length (kip/ft)

2.1.5 Comments

The design philosophy of *AASHTO* YLA can be well applied to the predefined yield line pattern if we assume that a failure occurred only within the barrier and that it did not extend to the deck. This assumption, while it is valid, would take full advantage of the power of YLA. However, design procedures must be clearly defined to ensure such assumptions continue to work towards the safety of designs. In addition, this method becomes invalid if the barrier is considered short, or at least shorter than the critical length, L_C. In some cases, precasted barriers may be considered short barriers and should therefore be checked carefully before the application of the YLA method, as suggested by Equation (2) – (5). Furthermore, the drawback of this design method lies in the limitations of YLA, which are discussed later in Section 3.1 "Yield Line Analysis."

Also, *AASHTO* makes use of rather conservative design criteria in their designs for the deck overhang. They state that the deck overhang capacity, which acting coincident with the tensile force specified in Equation (6), may be designed to exceed the transverse flexural resistance of the barrier. Since the crash test system is oriented towards improving the likelihood of survival in an accident and not necessary the ultimate limit state design, the barrier is likely to be over-designed, which would lead to an over-design of the deck. On the other hand, localized failure at the edge of the deck is a mode of brittle failure which may lead to casualties, so conservative design procedures may, in fact, be necessary to ensure the deck is capable of resisting the forces transferred down from the barriers.

Overall, the design methods specified in this code work well if all of its assumptions prove accurate, although that is a far-fetched possibility in some

12

circumstances. The instructions are easy to follow though, and are easy to carry out in practice as well.

2.2 Washington State DOT Bridge Design Manual LRFD

The Washington State Department of Transportation (WSDOT) *Bridge Design Manual* (*BDM*) *2005* is a guide for those who design bridges in Washington State. In association with that guide, the *ASSTHO LRFD Bridge Design Specifications* is the second of the two basic documents for highway bridge and structure design in Washington State. *BDM* supplements *ASSTHO* by providing additional directions, design aides, and examples. It also takes precedence when conflicts arise between the two documents' standards.

2.2.1 Traffic Barrier

Design guidelines for the bridge traffic barriers, which can be found in Chapter 10.2 of the BDM, are developed in accordance with Chapter 13 of the *AASHTO LRFD Bridge Design Specifications*. *BDM* Clause 10.2.1 gives general guidelines for the types and heights of the barriers to be used on highway bridges depending on the different traffic conditions involved. TL-4 is the test level adopted by *BDM* from *AASHTO*, and so, standard bridge traffic barriers in Washington State are commonly designed to accommodate it. Similar to *ASSTHO*, *BDM* also carries over the railing test level grading system according to site conditions. Two samples of the standard TL-4 concrete barriers, which have been previously crash tested and are now commonly used in Washington State, are shown in Figure 4. The "Shape F" traffic barrier has been crash tested twice,

first in late 1996 under *NCHRP 230*, and then again more recently under *NCHRP 350*. It was proven to have met the safety requirements. A newer traffic barrier, "Single Slope," was introduced later in the '90s to speed up construction by using the 'slip forming' method. However, the drawback of that 'slip forming' method was that it resulted in an increase of the concrete cover required by WSDOT on the traffic side of the barrier.
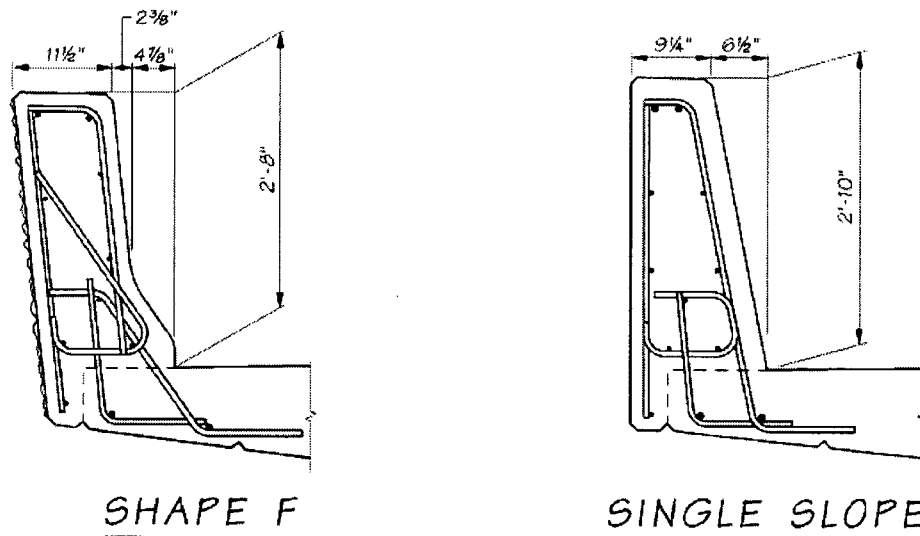
Figure 4 - Sample Standard Concrete Barriers Commonly Used in Washington State

(Data source: WSDOT Bridge Design Manual Figure 10.2.3.2)

2.2.2 Deck Overhang

BDM Clause 10.2.4 "Design Criteria" states that the WSDOT barriers are reinforced as per the crash test results in *NCHRP Report 350*. This may lead to an over-design of the traffic barrier though, and hence an over-design of deck overhangs. Therefore, the nominal transverse barrier resistance, R_W, that is transferred from the barrier to the deck should be equal to 120% of the transverse loads, F_t, as specified in Table 1. This prevents

the over-design of deck overhangs. *BDM* also requires, as does *ASSTHO*, that the flexural resistance of the deck exceed that of the barrier at its base, so that the yield line pattern remains valid by having failures occur within the barrier.

2.2.3 Design Criteria

By inheriting the method of analysis used in *ASSTHO*, *BDM* produces its own table of impact design forces for traffic barriers and deck overhangs based on the few types of barriers that are most commonly used in Washington State. This can be found in Table 3.

Table 3 - Impact Design Forces for Traffic Barriers and Deck Overhang

(Data source: WSDOT Bridge Design Manual Section 10.2.4, pg. 10-18)

Traffic Barrier/Cantilevered Slab Design		Yield Line Theory							
	Parameters	Shape F		Single Slope		Shape F 42"		Single Slope 42"	
		Interior	End	Interior	End	Interior	End	Interior	End
Traffic Barrier Design	Mc (ft-kips/ft)	20.62	20.62	19.39	19.39	29.18	29.18	25.22	25.22
	MwH (ft-kips)	42.48	45.98	44.72	42.17	97.83	96.91	81.06	77.50
	Lc (ft)	8.61	4.75	9.19	4.79	14.48	9.26	14.30	9.17
	Rw (kips)	133.09	73.48	125.79	65.53	241.47	154.33	205.99	132.17
	Ft (kips)	54.00	54.00	54.00	54.00	124.00	124.00	124.00	124.00
Deck Overhand Design	Ms (ft-kips/ft)	12.40	17.13	12.36	17.56	24.24	32.04	24.46	28.60
	T (kips/ft)	4.65	6.43	4.36	6.20	6.93	9.15	6.99	8.17
	1.2*Ft (kips)	64.80	64.80	64.80	64.80	148.80	148.80	148.80	148.80
Deck to Barrier Reinforcement	As required (in^2/ft)	0.29	0.41	0.29	0.42	0.44	0.59	0.50	0.59
	As provided (in^2/ft)	0.41	0.41	0.41	0.41	0.66	0.66	0.66	0.66
	S1 Bars	#5 @ 9in		#5 @ 9in		#6 @ 8in		#6 @ 8in	
	S2 Bars	#4 @ 18in		#4 @ 18in		#5 @ 16in		#5 @ 16in	
Weight Area	W (lbs/ft)	472.5		505.3		729.0		692.2	
	A (in ^2)	425.2		454.8		656.1		623.0	

2.2.4 Comments

The WSDOT *Bridge Design Manual*, using *ASSTHO Bridge Design Specifications* as its backbone, is a useful resource for traffic barrier and deck overhang design. It provides

extensive background information and clear design criteria. It also went one step further in solidifying the impact design forces, by applying some of the design methods proposed in *ASSTHO* for the standard traffic barriers used in Washington State. These design forces are presented in Table 3, making them easy to follow and to use in practice. However, this table is only valid for certain types of barriers, making it less useful for those who are outside of Washington State. Nonetheless, *BDM* is a good example of making full use of the *ASSTHO Bridge Design Specifications*.

2.3 CAN/CSA-S6-00 and CAN/CSA-S6-88

The *Canadian Highway Bridge Design* code *S6-00* and the *Design of Highway Bridges S6-88* are both prepared by the Canadian Standards Association (CSA) for highway bridge design in Canada. *CAN/CSA-S6-00* combines with and replaces both *CAN/CSA-S6-88 Design of Highway Bridges*, and *OHBDC-91-01 Ontario Highway Bridge Design Code*, becoming the standard national code used in Canada. This section reviews mainly the design methods and criteria suggested in *S6-00*, while also including some materials from *S6-88* for reference.

2.3.1 Traffic Barrier

S6-00 Clause 12.5.1 states that traffic barriers shall be crash tested to determine their effectiveness in reducing the consequences of vehicles leaving the highway upon the occurrence of an accident. *S6-00* Clause 12.5.2.3 provides detailed information on crash test requirements. The adequacy of a barrier that has the same details as those of an

existing barrier can be determined from an evaluation of the performance of the existing barrier.

2.3.2 Performance Level

Performance levels (PL) 1, 2, and 3 are the ranking systems used in *S6-00* to determine the site condition for a bridge. Alongside that, the barrier exposure index is used in accordance with *S6-00* Clauses 12.5.2.1.2 and 12.5.2.1.3 to determine the performance level of a bridge site. This exposure index is evaluated based on the estimated average annual daily traffic for the first year after construction, as well as on the highway type, curvature, and grade, and superstructure height factors which are shown in *S6-00* Tables 12.5.2.1.2 (a) – (d). With that, then, the barrier exposure index is used, along with barrier clearance, design speed, and ratio of trucks as shown in *S6-00* Tables 12.5.2.1.3 (a) – (c), to determine the performance level suitable for the bridge site. The minimum barrier heights for PL-1, 2, and 3 traffic barriers are 0.68 m, 0.80 m, and 1.05 m respectively, as laid out in *S6-00* Table 12.5.2.2.

2.3.3 Design Criteria

Under *S6-00* Clause 12.5.2.4, traffic barrier anchorages should be designed to resist the unfactored loads as specified in Table 4, and applied as illustrated in Figure 5. These are also used in the calculation of design forces for deck overhang. Unlike *AASHTO*, where the vertical load is applied independently of the other two loads, the transverse and longitudinal loads are to be applied in tandem with the vertical load on the barrier, as

specified in *S6-00*. For reference, the transverse load used in *S6-88* was much lower; 35 kN and 45 kN for roadway widths of 9m or less, and greater than 9m, respectively. Also, the transverse load should be distributed over a longitudinal length of 1.5 m.

Table 4 - Unfactored Loads on Traffic Barriers

(Data source: S6-00 Table 3.8.8.1)

Performance Level	Transverse Load - PT (kN)	Longitudinal Load - PL (kN)	Vertical Load - PV (kN)
PL-1	50	20	10
PL-2	100	30	30
PL-3	210	70	90
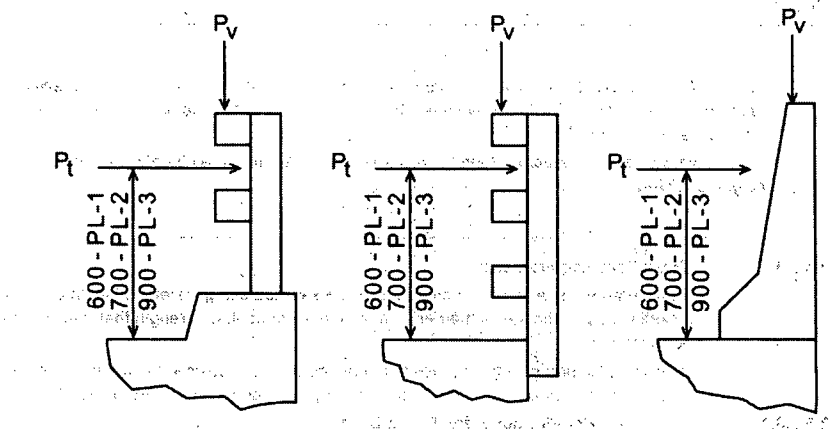
Note:

(a)   Traffic barrier types are illustrative only and other types may be used.

(b)   Transverse load "P_t" shall be applied over a barrier length of 1200 mm for PL-1 barriers, 1050 mm for PL-2 barriers, and 2400 mm for PL-3 barriers.

(c)   Longitudinal load "P_l" shall be applied at the same locations and over the same barrier lengths as P_t. For post and railing barriers, the longitudinal load shall not be distributed to more than 3 posts.

(d)   Vertical load "P_v" shall be applied over a barrier length of 5500 mm for PL-1 and PL-2 barriers and 12000 mm for PL-3 barriers.

(e)   These loads shall be used for the design of traffic barrier anchorages and decks only.

Figure 5 - Application of Railing Loads

(Data source: S6-00 Figure 12.5.2.4)

2.3.4 Deck Overhang

According to S6-00 Clause 5.4.7, analysis of deck overhang under railing loads should be carried out using the methods given in *S6-00* Clause 5.7.1.6.3. Those include refined methods in accordance with *S6-00* Clause 5.9, and yield line analysis.

2.3.4.1 Refined Methods

The refined methods suggested by Clause 5.9 are divided into four categories. The first category includes methods for general applications, such as grillage analogy, orthotropic plate theory, finite element analysis, finite strip, folded plate, and semi-continuum method, in accordance with *S6-00* Clause 5.9.1. The second category is a specific application of influence surfaces in accordance with *S6-00* Clause 5.9.2. Model Analysis is the third category specified under *S6-00* Clause 5.9.3, and it involves the testing of a physical model. Lastly, *S6-00* suggests that other methods may be used upon approval. The limitations of applicability for the above methods can be found in *S6-00* Table 5.9.4.

2.3.4.2 Simplified Methods

S6-00 Clause C5.7.1.6.3 in the *Commentary* recalls a simplified method from the *OHBDC* and *S6-88* which was used for determining moments in the deck due to concentrated horizontal railing loads. This method assumes that the horizontal loads transferred down from the barrier to the deck are distributed over a constant length of 1.5m at the outer edge of the deck. As the moments progress into the deck due to the horizontal loads, this length is increased by 0.8 times the distance between the outer edge

19
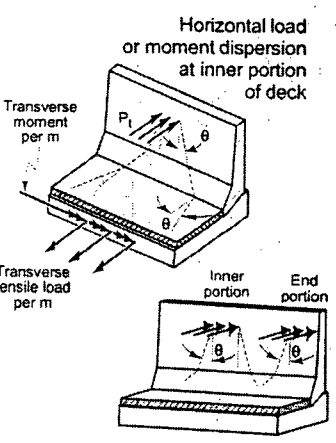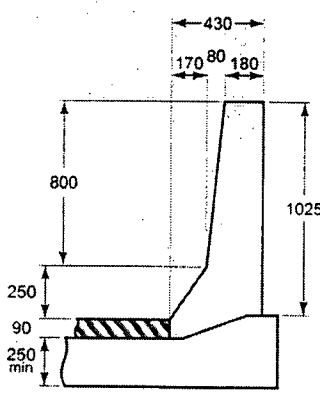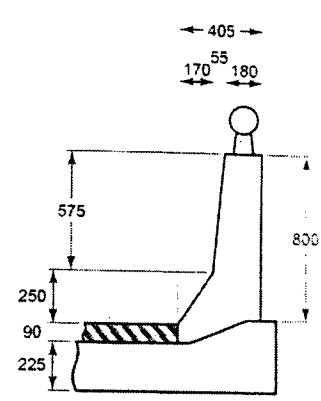
of the deck and the section of the deck being analyzed. That results in a dispersal angle of 21°. Since the design loads in the previous code were much lower than those specified in this code, it is necessary to perform the more rational, refined methods that were suggested in *S6-00* Clause 5.9

2.3.4.3 Dispersal Angle Method

The *S6-00 Commentary* also mentions the use of dispersal angles, resulting from FEA, in some Canadian provinces. This is shown in Table 5. Details of this dispersal angle method are presented in Section 3.3 "Dispersal Angle Method." A point worth noting here is that although load dispersal is an old concept from the previous code, when it is used in combination with the FEA results, it becomes an effective tool for approximating the dispersion of forces on the deck.

Table 5 - Transverse Moments in Cantilever Slabs Due to Horizontal Railing Loads

(Data source: S6-00 Commentary Table C5.7.1.6.3)

Horizontal Load or Moment Dispersion at Inner Portion of Deck		Performance Level 3 Barrier		Performance Level 2 Barrier with Rail	
Factored Horizontal Load P_t (Clause 3.8.8.1)		357 kN		170 kN	
Length of Load Application (Clause 12.5.2.4)		2400 mm		1050 mm	
Height of Load Application Above Deck (clause 12.5.2.4)		900 mm		700 mm	
Moment in Inner Portions of Deck per metre at Face of Barrier		83 kN-m/m		38 kN-m/m	
Dispersal Angle for Barrier	Dispersal Angle for Deck	$\theta = 42°$	$\theta = 47°$	$\theta = 56°$	$\theta = 55°$
Tensile Force in Inner Portion of Deck at Deck Edge		144 kN/m		100 kN/m	
Dispersal Angle for Barrier	Dispersal Angle for Deck	$\theta = 3°$	$\theta = 10°$	$\theta = 25°$	$\theta = 20°$
Moment in End Portion of Deck per metre at Face of Barrier		102 kN-m/m		52 kN-m/m	
Dispersal Angle for Barrier	Dispersal Angle for Deck	$\theta = 48°$	$\theta = 45°$	$\theta = 55°$	$\theta = 55°$
Tensile Force in End Portion of Deck at Deck Edge		161 kN/m		142 kN/m	
Dispersal Angle for Barrier	Dispersal Angle for Deck	$\theta = 0°$	$\theta = 0°$	$\theta = 8°$	$\theta = 8°$

2.3.5 Comments

In general, *S6-00* and its *Commentary* provide users with great flexibility in the design of traffic barriers, anchorages, and deck overhangs by offering a varied range of suggested methods. However, the list of available analysis methods may be too broad for most users, and so may lead to confusion when being applied in practice. Without a standardized method of analysis, the resulting design loads may vary significantly from one designer to another simply because they have been calculated using very different methods. While flexibility is valuable, one standard design method should be created as tool for the majority of designers to use in common. Of course, in order for a tool to be used commonly by people, it must also be effective and easy to apply. Hence, finding such a design method becomes the objective of this research. Certainly is is also sensible that users who demand more sophisticated methods of analysis, such as those suggested by the code, are still given the authority to do so.

Chapter 3: Methods of Analysis

There are a number of methods available for carrying out the traffic barrier and deck overhang design calculations, as we saw in the pervious section. Some are better than others. While studying every method in detail is not possible here, considering the scope of this thesis, a few of the better, more well-known methods have been selected for review in this section. Those methods include yield line analysis, finite element analysis, and the dispersal angle method. In addition, two new and improved concepts will be introduced as having evolved from some of the existing methods through this research. They are referred to as the maximum moment envelope (MME) method and the maximum moment dispersal angle (MMDA) method. As suggested by their names, these two new methods act as a means of approximating "maximum" moment intensities for the design forces, which would in effect, give the design an additional level of safety. The MMDA method is recognized as the most useful of the available methods for the purposes of this research, because of its overall strength. Then finally, some design examples will be presented and the results will be compared using the different methods mentioned before.

3.1 Yield Line Analysis (YLA)

According to *S6-00* Clause 5.4.7, YLA may be used in the ultimate limit state design along with elastic analysis for the analysis of decks. Clause 5.11.3.2 also briefly explains the theory of YLA and puts forward the criteria used by YLA to determine inelastic-dynamic responses.

3.1.1 Design Philosophy

In short, YLA is basically another form of plastic analysis that uses the principle of virtual work. With an assumed yield-line pattern for the reinforced concrete slab, the ultimate plastic capacity of the slab can be determined by equating external work to internal work without knowing the actual load. This is illustrated as follows:

$$\sum P\delta = \int M\kappa ds + \sum M\phi \qquad (7)$$

where P is the concentrated external load, δ is the deformation, M is any distributed moments that satisfy equilibrium with P, κ is any distributed curvature that is compatible with hinge rotation, ϕ, and s is the length of each member.

This analysis gives an upper bound solution such that the collapsed load obtained is either higher or equal to the true failure load of the system. Therefore, if an incorrect set of yield-line patterns is assumed, the collapsed load obtained could potentially be overestimated for the given slab reinforcements.

3.1.2 Sample Application

The model can be set up using some variables to represent the geometry of the yield-line pattern, instead of requiring the use of some assumed actual values. Hence, the true yield-line pattern can be determined by optimizing the load with respect to these variables. A model of the deck has been set up as shown in the following figure, with two variables (a and b) to represent its yield-line pattern.
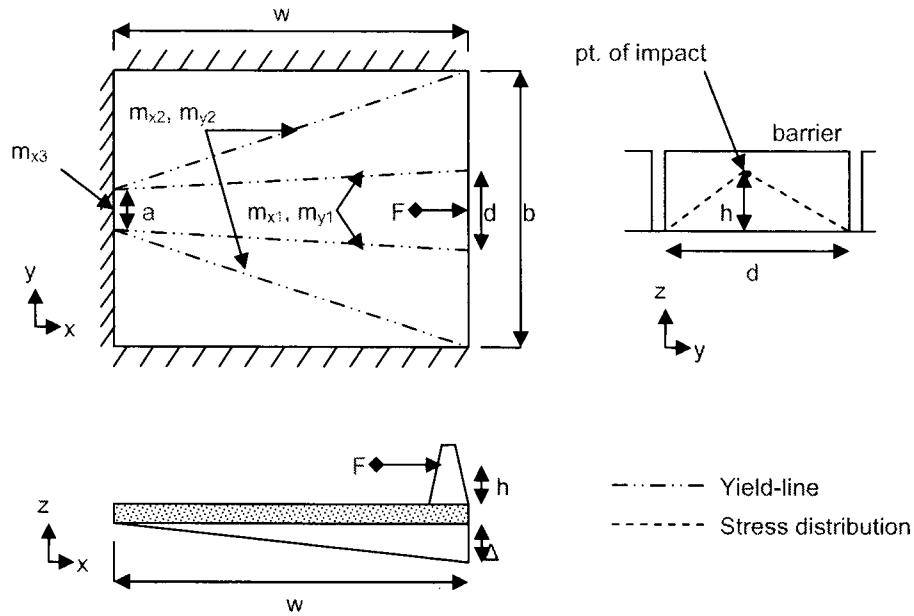
Figure 6 - YLA Model for Deck

The model in Figure 6 is developed using many assumptions. First, the deck fails in

flexural, not in shear, so that YLA is applicable. Second, only the force in x-direction

contributes to the external work applied to the system, while the force in y-direction is

not considered. Also, both the barrier and the connection between the barrier and the

deck must be properly designed so that they survive the impact; hence, the impact force

can be successfully transferred down to the deck. Lastly, both the barrier and the

connection suffer minor damage, such that little or no energy is lost there. Based on

these assumptions, the following equation is derived:

$$F(a,b) = \frac{m_{x3} \cdot a}{2h} + \frac{(b-a)}{2h(b-d)}\left[m_{x2}(b-a) + m_{x1}(d-a)\right] + \frac{2w^2}{h(b-d)}\left(m_{y1} + m_{y2}\right) \qquad (8)$$

Where:

d	=	the assumed width of the deck subjected to the impact load transferred from the barrier attached to it (m)

w	=	the distance from the edge of the deck to the nearest girder underneath the deck, where negative bending moment is max (m)

m_x1 = height of impact location to the deck (m)

m_y1 = positive plastic moment of the deck in x-direction (kN*m/m)

m_x2 = negative plastic moment of the deck in x-direction (kN*m/m)

m_y2 = negative plastic moment of the deck in y-direction (kN*m/m)

m_x3	=	negative plastic moment of the deck in x-direction at the location above the girder (kN*m/m)

a = variable representing the yield-line pattern

b = variable representing the yield-line pattern

F = failure load of the deck; a function of a and b (kN)

Δ = virtual displacement (m)

3.1.3 Comments

Note, however, that this method is only valid if the corrected set of yield line patterns can be predicted in advance. Therefore, it should be used in conjunction with other methods to ensure that the assumptions are correct. For example, it could be used with FEA. In that case, the result of a simple FEA shows an undesirable localize failure mechanism that YLA is not capable of dealing with. However, if the outer portion of the deck is reinforced, the next failure mechanism should take place at the girder and hence YLA can be used to predict such a failure load. Again, the accuracy of the YLA solution depends heavily on the accuracy of the predicted yield line pattern. But for an element as large as a bridge deck, with its irregular loadings and configuration, the yield line pattern can be

very complicated and difficult to predict. Also, the fact that YLA gives an upper bound solution makes the design unconservative. Therefore, it may not be the best tool to use for a method of analysis in this case, as compared to the FEA.

3.2 Finite Element Analysis (FEA)

FEA is listed as one of the most feasible methods of analysis in *S6-00* because of its ability to simulate very complicated, three-dimensional structures. The concept of FEA was first introduced in the 1950s, and has been thoroughly used and improved over the last five decades. Although the technique may appear complex to begin with, the basic theory is actually rather straightforward.

3.2.1 Basic Principle

The basic principle of the FEA is to divide the actual geometry of a structure into discrete pieces called finite elements. These elements are then joined together by nodes to form a mesh. The number and the type of elements should be chosen in a way that allows the best approximation of the overall geometry to be achieved through the combined elemental representations. As a structure is divided into its discrete pieces, the governing equation of each element is calculated and then they are combined to determine the system equations. Those system equations describe the behavior of the whole structure. As such, variables such as temperature, displacement, and stress can be evaluated.

In this case, the force and stress distribution of a system containing two planes (the barrier and deck overhang) that intersect at a 90 degree angle with specified loads in

27

three directions, can best be evaluated using FEA. For this reason, a linear elastic finite element model (FEM) of the traffic barrier and bridge deck system was developed. That was done in preparation for this research by me and my fellow student, Sean Xiao, using SAP2000. Besides the following, further information on the development of the FEM can also be found in Xiao's paper, listed in the References.

3.2.2 Finite Element Model

This section describes the various modeling details involved in the development of the FEM. Note that the detailing of the FEM plays a big part in the accuracy of the FEA results. Although two FEMs may be set up to simulate the same structures, the difference in their detailing may yield significantly different results. Therefore, one needs to take precautions when making decisions regarding each detail of a FEM, so as to ensure the accuracy of the FEA.

3.2.2.1 Element Properties

Shell elements are chosen for the FEM for their ability to carry forces and moments lying both in their plane as well as transverse to their plane. These shell objects are defined as thick plates which can also demonstrate transverse shear deformation. Compared to solid elements, shell elements achieve greater accuracy with greater comfort, and are therefore more commonly used. As for the geometry of these, quadrilateral elements are used because they are more reliable than triangular elements. However, the shell elements are linear, instead of quadratic, meaning that the mesh density must actually be much higher to ensure the accuracy of results.

Table 6 - Element Properties

	PL-2	PL3
Element type	Thick shell (linear)	
Material	Reinforced concrete	
Actual deck thickness	250mm	275mm
Modeled deck thickness	170mm	195mm
Modeled barrier thickness – top	140mm	
Modeled barrier thickness – middle	195mm	
Modeled barrier thickness – bottom	260mm	

3.2.2.2 Deck Overhang

The variation between actual and modeled deck thickness is a result of minimum cover, rebar size, and the deck's neutral axis. Since the difference in deck thickness for different performance levels may lead to inconsistent results, a series of tests were run in order to determine the sensitivity of deck thickness on stress distribution. The results show that the effects are minimal, as compared to other factors such as cantilever length. This is because the range of possible deck thickness is very narrow.

3.2.2.3 Traffic Barrier

The barrier is modeled in three sections with various thicknesses, in an attempt to reflect the actual varying thickness that arises from a sloped surface. In terms of the barrier types, precasted reinforced concrete barriers are used for PL-2 FEM and Cast-In-Place reinforced concrete barriers are used for PL-3 FEM. Note that it is possible to use other types of barriers on each performance level. For example, Cast-In-Place reinforced concrete barriers can be used for both PL-2 and 3, or a post type barrier could be used for PL-2. However, taking into consideration all possible barrier-PLs, combinations of

different ones would result in too much data being generated by the FEA and would therefore make them unmanageable. In doing so, it would also violate the simplicity objective of this research. Consequently, for simplicity's sake as well as for convenience, just one barrier type will be specified for each performance level.

3.2.2.4 Connection/Anchorages

As for anchorages, connections between barriers and decks are assumed to be continuous, instead of in a series of discrete joints. This assumption may be valid for PL-3 because rebar connections resemble continuous connections under certain circumstances. For PL-2, in the meantime, the effect of discrete joints on force distribution may or may not be significant, but further investigation is suggested for future studies.

3.2.2.5 Overall Dimensions

The FEM that was constructed is 14m in length (the direction parallel to traffic), and varies from 2.6m to 3.8m in depth (the direction perpendicular to the traffic). This variance depends upon the cantilever length. As mentioned above, the barriers are attached to the deck as continuous connections. Their heights, for PL-1, 2, and 3, are 0.68m, 0.80m, and 1.05m respectively, as specified in *S6-00* Table 12.5.2.2. The deck then, is rested on two bridge girders, which are located 2m apart. The outer girder is represented by a series of roller supports that allow all rotations and horizontal translations in both x and y directions, although translations in z directions are restrained. The inner girder is modeled by a series of fixed supports, which serve to prevent all rotations and translations.

3.2.2.6 Material

The material property table below provides detailed information about all of the default materials. Regular, reinforced concrete is used as the FEM material for the purpose of load calculation only. Capacity designs should then be performed using the design loads calculated without regard for this default material. However, it is essential to check the two materials at the end to ensure the discrepancy between their properties is within a reasonable range.

Table 7 - Material Properties

Material type	Reinforced concrete – Isotropic	
Mass per volume	2.4	$\dfrac{kN \cdot s^2}{m^4}$
Weight per volume	23.6	$\dfrac{kN}{m^3}$
Modulus of elasticity	24800000	$\dfrac{kN}{m^2}$
Passion's ratio	0.2	Unitless
Shear modulus	10300000	$\dfrac{kN}{m^2}$
Specified compressive strength, fc	27600	$\dfrac{kN}{m^2}$
Bending reinforced yield strength, fy	414000	$\dfrac{kN}{m^2}$
Shear reinforced yield strength, fys	275000	$\dfrac{kN}{m^2}$

3.2.2.7 Mesh and Geometry

Mesh is a collection of elements joined together by nodes. As two of the basic properties of a FEM, mesh size and geometry have great effects on the FEA results. Shell elements usually have an aspect ratio of 1:1 to 1:2 as is the convention. For this reason, the basic

31

framework of the FEM is built using 0.35mx0.35m shell elements. However, a much

denser mesh is commonly applied in an area of interest to ensure the accuracy of the

results produced by the FEA. In order to determine the mesh size then, a series of tests

were conducted for convergence. The testing contained two parts: increasing mesh

density in the x-direction, and then increasing it in the y-direction independently. A point

of reference at the base of the barrier (node 16 in the FEM) was selected to be used for

comparing the results. The results of PL-2 test are presented in the following tables.

Table 8 – Simple Cantilever Testing Results for Increasing Mesh Density in Y-Direction

Mesh size (mxm)	Max moment intensity(kN*m/m)	Vertical displacement (mm)
0.35X0.35	145	-0.835
0.35x0.18	168	-0.842
0.35X0.088	194	-0.847
0.35x0.044	217	-0.849
0.35x0.022	233	-0.85
0.35x0.011	242	-0.85
0.35x0.0055	245	-0.85
0.35x0.0028	246	-0.85

Table 9 – Simple Cantilever Testing Results for Increasing Mesh Density in X-Direction

Mesh size (mxm)	Max moment intensity(kN*m/m)	Vertical displacement (mm)
0.18x0.011	345	-0.85
0.088x0.011	452	-0.85
0.044x0.011	536	-0.85
0.022x0.011	590	-0.85
0.011x0.011	614	-0.85

For clarification, x-direction in this FEM is parallel to the direction of traffic, while

y-direction is perpendicular to the direction of traffic. As shown in the above tables, both

the force and displacement yield converge at higher mesh densities in the y-direction. In the case of the x-direction, only displacement converged at higher mesh densities and the forces kept increasing as mesh density increased. In order to explain this phenomenon and to ensure the FEM is error-free, a much simpler FEM was built so that results could be hand-calculated for comparison with the FEA results under the same testing conditions as the original FEM. This mini-model was a simple cantilever model built using shell elements, as shown in Appendix A. The cantilever is 1.4m in length and 0.35m in width and has 2 point loads of 10 kN applied to the end. Hence, the moment at the fixed support can be calculated easily by hand. Again, this FEA is tested in two parts as before and the results are shown in the following tables.

Table 10 - Deck Test Results for Increasing Mesh Density in X-Direction

Mesh size (mxm)	Max moment intensity(kN*m/m)
0.35x0.35	-78.95
0.18x0.35	-78.96
0.088x0.35	-78.97
0.044x0.35	-79
0.022x0.35	-79.06
Hand calculation	-80

Table 11 - Deck Test Results for Increasing Mesh Density in Y-Direction

Mesh size (mxm)	Max moment intensity(kN*m/m)
0.22x0.35	-78.95
0.22x0.18	-81.1
0.22x0.088	-82.4
0.22x0.044	-84.6
0.22x0.022	-86.9
Hand Calculation	-80

Similar to the original FEA results, this simple cantilever FEM yields results (which are forces, in this case) that converge when meshing in the x-direction, but not when in the y-direction. This simple test shows that by increasing the mesh density in one direction, which is the direction parallel to the cantilever, it is enough to ensure that the force converges on the real solution. Over-meshing in the other direction only produces results that deviate from the real solution. The existence of this phenomenon is probably due to the FEA coding of SAP2000. The details of the connectivity between elements in SAP2000 are hidden factors that might have significant effects on the results.

For PL-3, the FEA results converged even when very coarse mesh was used, because of the simplicity of the model. The mesh size of 0.35m by 0.15m at the area of interest seemed to yield a convergence, while also using minimal computational effort. For PL-2, however, the use of a much denser mesh size of 0.35m by 0.011m was necessary for convergence. This was due to the more complex loading mechanism and structural configuration (Discontinuity of barriers).

3.2.2.8 Loads

According to *S6-00*, the anchorages and cantilever decks are to be designed for the possible forces that could be transmitted from the barrier subject to the impact loads, as specified in Table 4 and applied in Figure 5. The loads given in Table 4, are then distributed evenly amongst the nodes along the length of the barrier depending on the performance level, as is again specified in Figure 5. The safety factor is the 1.7 live load factor, as specified in Table 3.5.1(a) per *S6-00*.

Various loading combinations are set up while keeping under consideration the effect of cantilever length, the location of impact, and the performance levels. There are five different cantilever lengths being tested that range from 600mm to 1800mm, and there are two possible locations of impact: the inner portion and the end portion. In total, 80 various loading cases are being considered. The application of railing loads on PL-2's inner and end portions, and PL-3's inner and end portions of the bridges are presented in Appendices B, C, D, and E respectively.

3.2.3 Stress Averaging

Each element has its own forces or stresses, and typically they will be different at the common points of different elements. Thus, abrupt changes may be seen across those common points from element to element. The finer the mesh, the closer these common values will become, and vice-versa. SAP2000 has a function that averages the stresses at any given point by averaging the stresses from all of the surrounding shell elements that are both connected to the point and are visible in the active window, or on the plane at which the user is looking. Then, when SAP2000 plots the stresses for a particular shell element on screen, it plots those averaged stresses at the points that are under consideration instead of using the actual stresses calculated from the FEA. If the model has some kind of discontinuity, for example when two planes meet at an angle, one will need to perform this stress averaging function on each plane independently, by enabling this option during the plotting process. This will avoid the problem of averaging across the two planes, which would give incorrect results because the stress along the two planes is not continued relative to the element's local axes.

In addition, the stress averaging function provides an alternative way of checking the FEM for errors, if any. By turning this function off, the user can carefully observe and decide if the abrupt changes in stresses among elements are too great. If this change is much more apparent than the ones found with stress averaging, it is likely that the FEM contains errors such as inappropriate mesh sizes or connectivity problems. This "test" may be performed until the user is satisfied with the changes in the stresses across the elements. In this case, the model has discontinuity because the barriers are intersecting the deck at a right angle. Therefore, it is necessary to check for any possible errors that may exist in the FEM. That would be done through the use of the stress averaging function in each of the barrier planes and deck planes independently.

3.2.4 Comments

The data generated by the FEA are immense, although only part of them is actually useful for the purpose of this research. Therefore, data from only the areas of interest are being collected and stored in a spreadsheet. The spreadsheet itself is then completed by further data processing later in Section 3.5 "Maximum Moment Dispersal Angle." These data can be found in Appendices F, G, H, and I under the FEA results column. Sample graphs in which the forces vs. the distances have been plotted for a cantilever length of 1800mm, can be found in Appendix J.

In terms of the method of analysis, FEA is by far the most reliable way for determining load calculations. The results generated using FEA are usually more realistic than those generated through other methods, because of its ability to allow detailed specifications of each component, of realistic load assignments, and of

simultaneous load combinations. However, the drawback of its power is that the results are valid for only the very specific cases in which they are modeled. These results may or may not be applicable to other cases with slightly different specifications. That makes it a rather weak tool for general usage. In order to cover a reasonable scope, this method requires many individual remodelings and analyses for every possible case within the scope of interest. Hence, FEA requires too much time and effort, making it impractical to use in the course of regular design.

3.3 Dispersal Angle Method

The method of dispersal angle, which has been used in some Canadian provinces, is introduced in the *S6-00 Commentary* Clause C.5.7.1.6.3. Dispersal angles can be determined by a finite element analysis, and can be used to calculate barrier and deck overhang moment intensity based on the railing loads. This is a classic concept that tries to approximate the nature of load dispersion. To understand the strengths and weaknesses of this method, then, one must understand the concepts behind it. In the following sections, the behavior of true load dispersion is discussed in detail and compared to the assumed load dispersion described using the dispersal angle method.

3.3.1 Mechanic of Behavior

Figure 7 shows an inner portion cantilever bridge deck subjected to a concentrated load, P, as well as the actual moment intensity distribution along its two sections. The pattern of distribution of moment intensity comes out in the shape of a bell-curve, with a peak, or

maximum moment intensity. It can be seen that the moment intensity drops rapidly as it moves away from the peak and then drops more gradually as it reaches zero. Just as well, the maximum moment intensity increases as it moves towards the first support and away from the point load, P. On the other hand, the distance in the longitudinal direction, or x-direction, between the two end points where moment intensity diminishes to zero becomes greater as it progresses into the first support from the load P. The spread-out of the zone defined by the points where moment intensity reaches zero is know as load dispersion. This dispersion of load, however, is nonlinear and is dependent on the stiffness of the element. Also, note that the total area under each bell curve is equal to the total moment, which is determined by overall static equilibrium, at any given section. In this case, the total moment is the concentrated load, P, times the distance between the load and the section of interest.
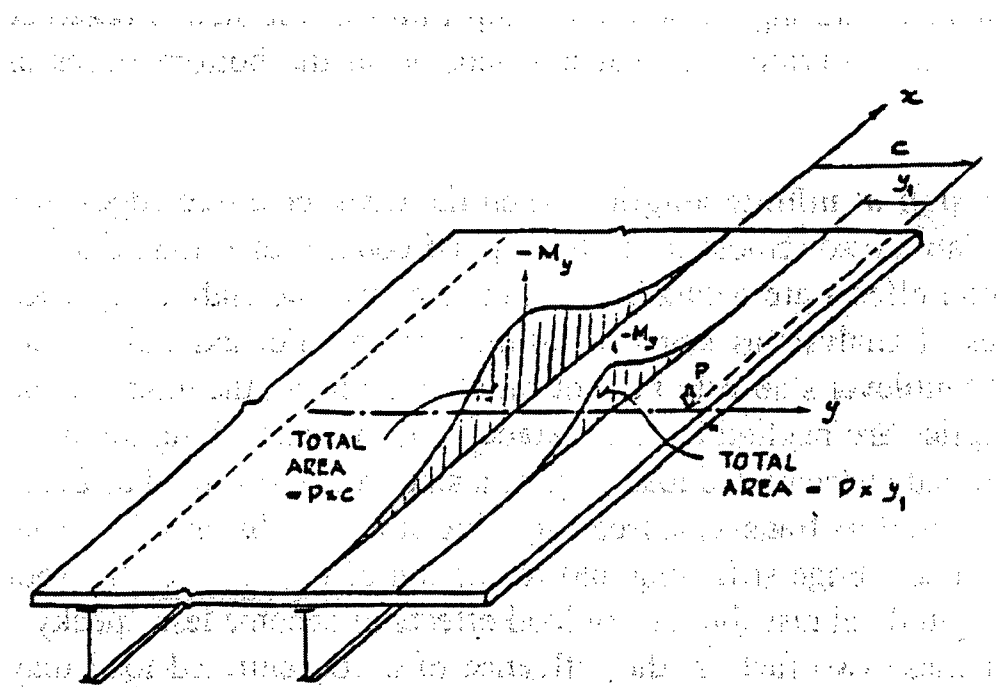
Figure 7 - Load Dispersion for Cantilever Deck Inner Portion

A cantilever deck at the end portion, which is shown in Figure 8(a), would have a slightly different moment intensity distribution than that of the inner portion. As mentioned above, the total area under the curve of any given section is equal to the total moment of that section, which equals to P*D, where P is the concentrated load and D is the distance from the load to the section being analyzed. In order to satisfy equilibrium then, the moment beyond the free edge represented by A_L must be redistributed within the cantilever deck. To do that, the area A_L is "reflected back," forming a mirror image that uses the free edge as the plane of reference, as shown in Figure 8(b), and that redistributes itself back into the moment represented by A_R as shown in Figure 8(c). As a result, the peak, or maximum moment intensity, as well as the moment in the region closest to the free edge, will be affected significantly. Therefore, a separate analysis for the inner and end portions should be carried out to ensure such effects are taken into account.
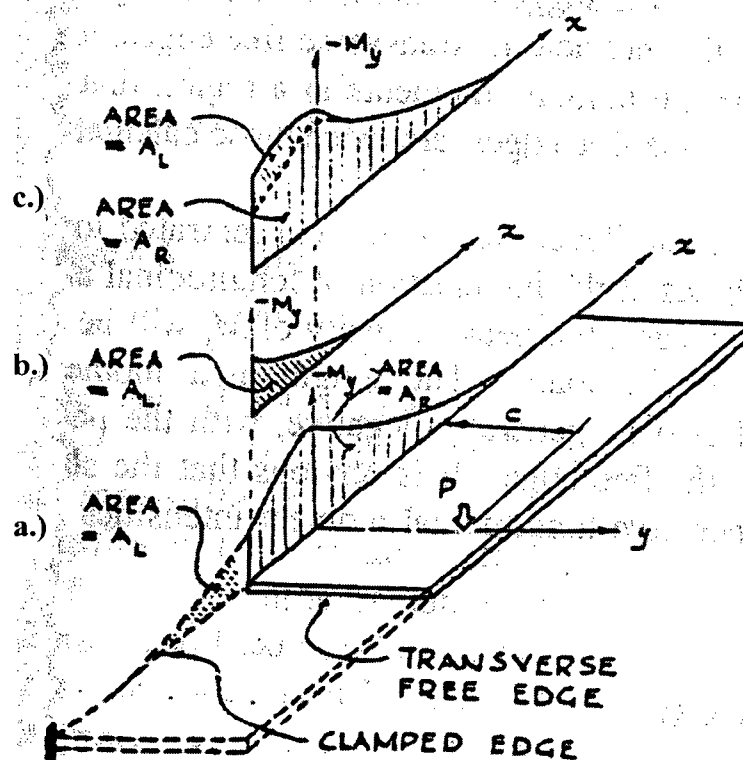
Figure 8 - Load Dispersion for Cantilever Deck End Portion.

3.3.2 Development of Dispersal Angle Method

Dispersal angle method is basically a simple method that was developed while "trying" to represent true load dispersions through the assignment of parameters called dispersal angles. It also assumes that the dispersion is linear, instead of nonlinear. In Figure 9, the dispersal angle, Θ, which can be defined by FEA, is used to calculate the moment intensity of the barrier and deck overhang based on the concentrated load, P. Note that this method is applicable for either the point load, or the distributed load. The zone of dispersion is represented by two lines that are determined by the given dispersal angle, Θ. Since the actual load dispersal is nonlinear and cannot be captured using one single dispersal angle, this method may produce results that are either overestimated or

40

underestimated depending on the location of the section making the design

unconservative in some cases.
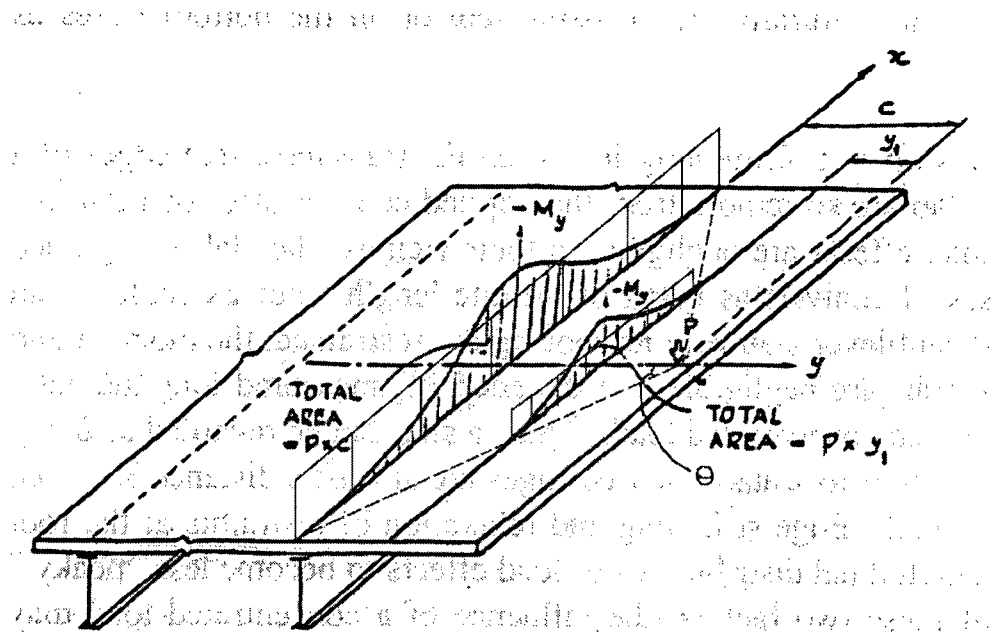
Figure 9 - Dispersal Angle Concept

The pattern of moment intensity distribution is assumed to be uniform instead of to

be the bell-curve distribution that it actually is. In order to satisfy equilibrium, the total

area under the uniform distribution is equal to the total moment of that particular section.

The total moment is simply P*D, where P is the load and D is the distance from the load

to the section being analyzed. However, this total moment is now evenly distributed

along the dispersal length and is bounded by the two lines that are defined in the dispersal

angle. At this point, it is clear that the uniform distributions are not good representations

of the original bell curve distributions, because they do not capture the peak, or maximum

moment intensity. The uniform distribution only serves as an approximation of the

average moment intensity of the original bell curve distribution. Hence, it underestimates

41

the moment at the center and overestimates the moment near the two sides, yielding

unconservative design loads.

A spreadsheet is set up to calculate the moment distribution at various sections of

the cantilever slab based on the railing loads. The dispersal angles are taken from the *S6-00 Commentary* Clauses C5.7.1.6.3 (which was determined by FEA) and are then applied

in the spreadsheet to different performance levels with the use of Equations (9) – (12)

using the parameters specified in Table 4 and Figure 5. Since there was no specific

information regarding PL-1, it was assumed to have dispersal angles similar to those of

PL-2. The dispersal angle for vertical loads is assumed to be zero at this point, and that is

verified later by the FEA. The torsion on the deck, due to longitudinal loads, is not

considered significant. Figures 10 to 12 show some examples of moment intensity

calculations for the inner portions of decks with overhang lengths of 1000mm using the

spreadsheet developed.

Transverse moment on barrier due to transverse load:

$$M = \frac{PT \times H}{DL + H \times TAN(\theta_{bPT})} \tag{9}$$

Transverse moment on deck due to transverse load:

$$MT = \frac{PT \times HB}{(DL + HB \times TAN(\theta_{bPT})) + (D \times TAN(\theta_{dPT}))} \tag{10}$$

Transverse moment on deck due to vertical load:

$$MV = \frac{PV \times D}{DL + D \times TAN(\theta_{dPV})} \tag{11}$$

Total transverse moment on deck due to transverse and vertical loads:

$$MC = (MT + MV) \tag{12}$$

Where:

M   =   transverse moment intensity on barrier due to transverse load (kN*m/m)

MT   =   transverse moment intensity on deck due to transverse load (kN*m/m)

MV   =   transverse moment intensity on deck due to vertical load (kN*m/m)

MC   =   transverse moment (kN*m/m) due to combined loads: PT, PV, and PL

PT   =   transverse load (kN) * safety factor (1.7)

PV   =   vertical load (kN) * safety factor (1.7)

H   =   height from the point of interest on the barrier to point of impact (m)

HB   =   height of barrier base to point of impact (m)

DL   =   dispersal length (m)

D   =   distance of deck from the point of interest to the barrier (m)

Θ_{bPT} =   dispersal angle of barrier (degree)

Θ_{dPT} =   dispersal angle of deck (degree)

Θ_{dPV} =   dispersal angle of deck (dgree)

Moment vs. Distance (PL-1)
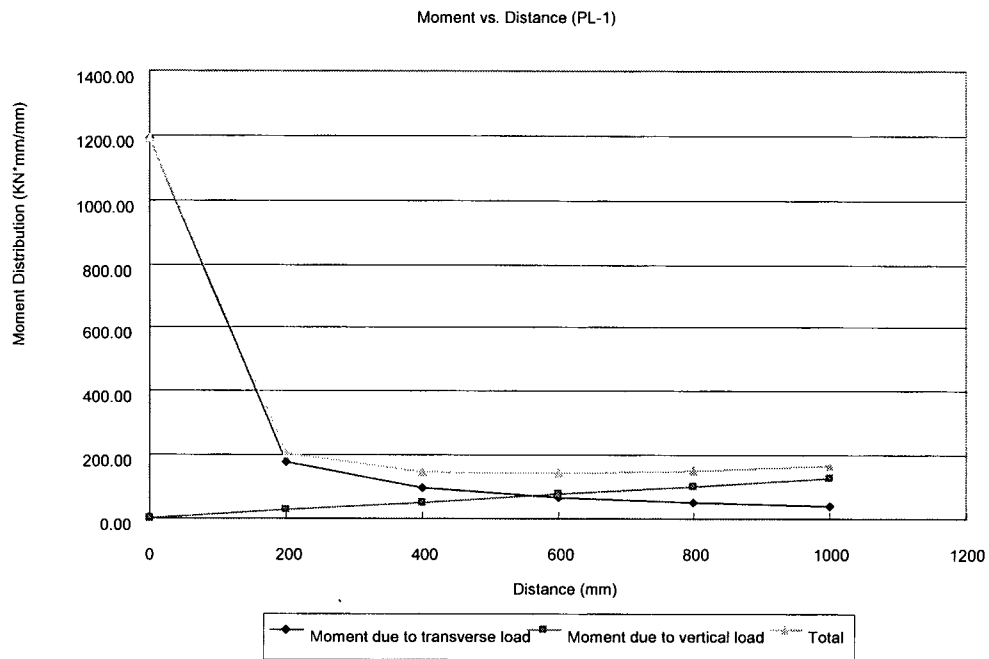
Figure 10 - Moment Intensity vs. Deck Distances Graph fro PL-1

Moment vs. Distance (PL-2)
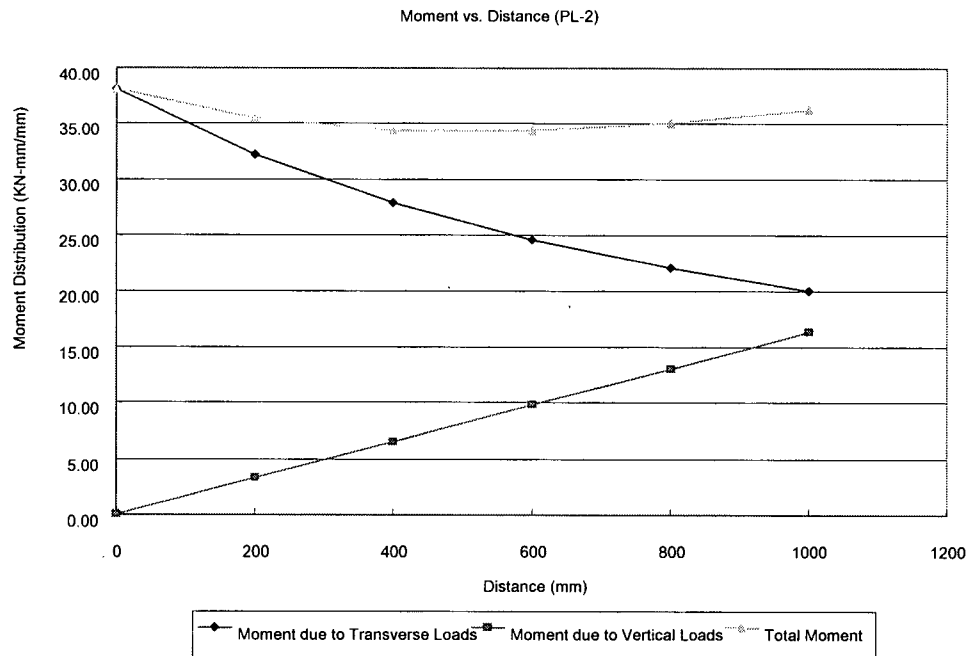
Figure 11 - Moment Intensity vs. Deck Distance Graph for PL-2

Moment vs. Distance (PL-3)
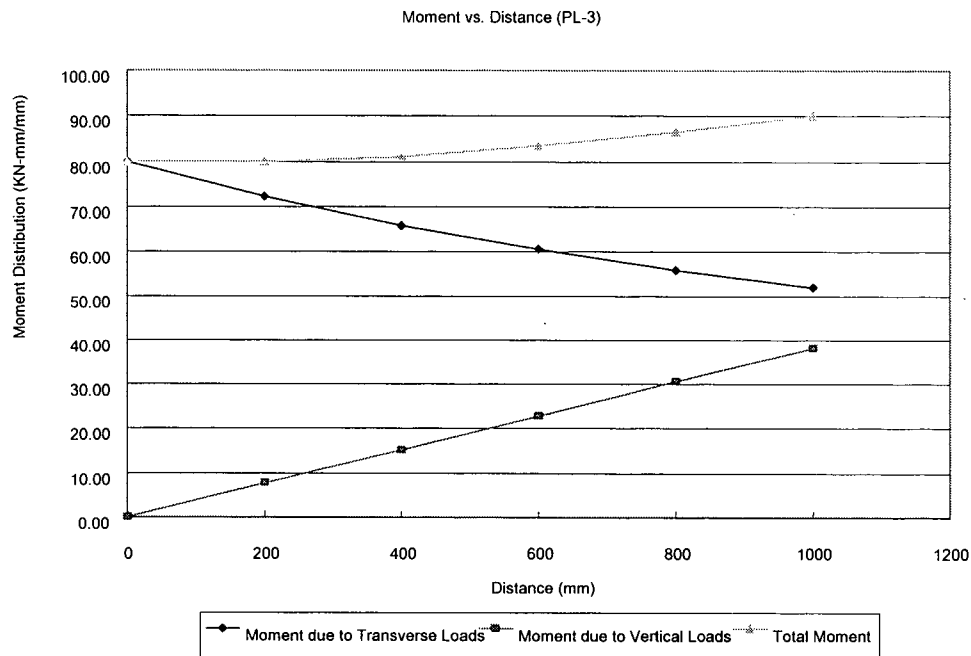
Figure 12 - Moment Intensity vs. Deck Distance Graph for PL-3

Since it appears as though the patterns associated with the change of moment intensity depend on the performance level, the following conclusion can be made. Figure 10 shows that the moment distribution for PL-1 (post-type barriers) is highly concentrated at the base of the posts but dissipates quickly as it extends outward onto the deck. Transverse loads dominate in this case. Local slab reinforcement should be designed properly to resist the high moment intensities here. Figure 11 shows that the moment distribution for PL-2 (precasted type barriers) is high at both the base of the barriers and the girder. In this case, both transverse loads and vertical loads dominate. Both areas also require additional reinforcement to deal with the railing loads, however. For PL-3, (Cast-In-Place barriers), the moment distribution is higher at the girder areas because of the much greater vertical loads which are being applied at the railings, causing

45

the vertical loads to dominate as shown in Figure 12. Meanwhile, the reinforcement of the whole cantilever slab may be designed around the highest moment in that area.

Although the dispersal angle method is a quick and efficient one for use in preliminary design processes where design moments are being estimated, it should still be checked for accuracy using other methods, such as the FEA.

3.3.3 Comments

The results generated using the dispersal angle method can be found in Appendix K. Also, Appendices F to I show results as calculated using the dispersal angle method, while further comparing that to the FEA. Note that the discrepancy between the results calculated using these two methods can be as great as 20%. The various assumptions inherent in the dispersal angle method are the main reason for these great differences in results. Also, because this method is based on FEA findings, it also inherits the advantages and disadvantages from the FEA method. This was discusses previously in Section 3.2 "Finite Element Analysis". However, the biggest strength of the dispersal angle method is that its concept is relatively simple and takes minimal effort to apply in practice.

3.4 Maximum Moment Envelope (MME)

A new method called the maximum moment envelope (MME) will be introduced here in as a means of capturing the true load dispersion on traffic barriers and deck overhangs. Unlike with the dispersal angle, the maximum moment intensity of each section can be

evaluated using this method, as shown in Figure 13. These maximum moment intensities can then be used as design loads in order to yield a safer design than would be had using the average moment intensities generated with uniform distribution in the dispersal angle method. The process of developing this method as well as the uses of the method, are presented in the following sections.
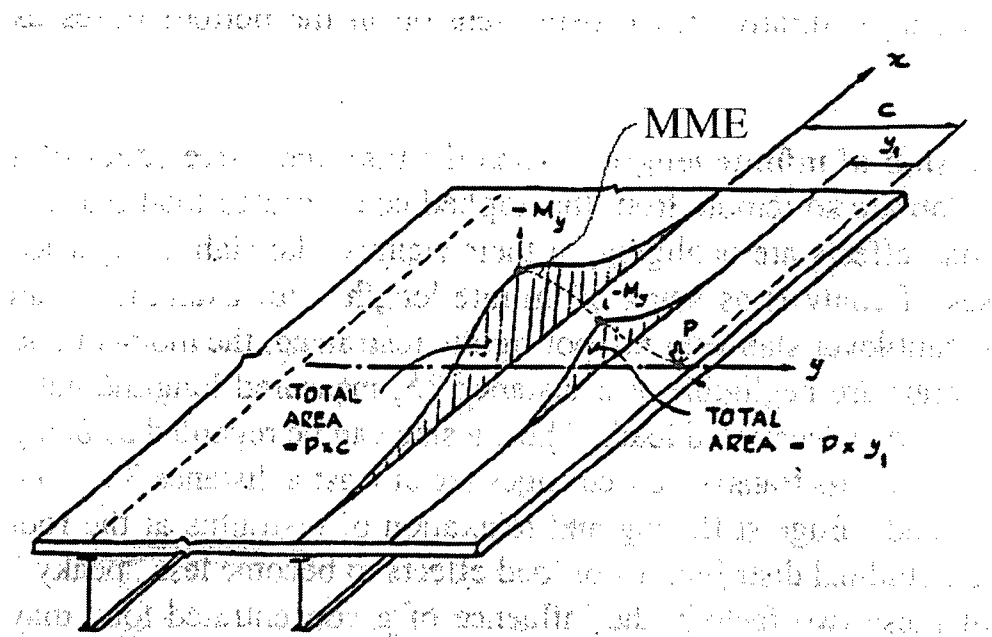
Figure 13 - MME Concept

3.4.1 Development

As mentioned before, the pattern of moment intensity distribution is a bell curve with a well-defined peak, or maximum moment intensity. The purpose of the MME is to capture these peaks using the FEA. As such, these peaks, which are collected and stored in a spreadsheet, form a distribution of maximum moment intensity all the way from the location of impact to the first support. This distribution is thus called the MME, and it is

represented by a chosen simple function. Different scenarios have different distributions and so are represented by different functions. For example, the transverse moment distribution of the PL-3 inner portion deck under transverse load is represented by a function different from that of the PL-2 end portion barrier under vertical load. These scenarios include combinations of various cantilever lengths (600mm, 900mm, 1200mm, 1500mm, or 1800mm), of different locations of impact (inner or end portion), of elements of interest (barrier or deck), of different loads (transverse, longitudinal, or vertical), and of various performance levels (1,2, or 3). They may be represented by either the same, or different, functions depending on the combinations. For example, varying cantilever length has a minor effect on the shape of the selected function, while a variance in the location of impact results in a change of the function itself.

The functions to be selected should be simple and should be represented by no more than a one or two constants, such as $A*sqrt(x)$, $sin(x^A)$, or $cos(A*x)$, where A is the constant that can be adjusted to fit the shape of the distribution, and x is the distance from the location of impact to the section being considered. Although the function type may or may not change depending on the situation, it can be predicted that the constants that define the functions will change from case to case. In particular, the constant of cantilever length is likely to undergo changes. In other words, both the function type and the constants are the basic parameters for determining the moment distribution of any scenario. The value of the constants, determined by matching the results of the FEA, is then represented by another set of functions that varying depending on the cantilever length, alone. Examples of this process are shown below in detail.

3.4.2 Applications

Figures 14 and 15 show a PL-3 barrier and the inner portion of a deck with a 1200mm overhang under a transverse load, and a corresponding transverse moment distribution. For the barrier, two functions (linear and square root) are proposed in Figure 16 in order to match the FEA results through the varying of constants A and B. It can be seen from Figure 17 that the linear approximation is a better representation of the FEA results. For the deck, only an exponential function is applicable, as seen in Figure 18. Figure 19 shows that the exponential function with one constant matches well with the FEA results. Examples of the relationship between the constants and the cantilever lengths can be found in Appendix L.
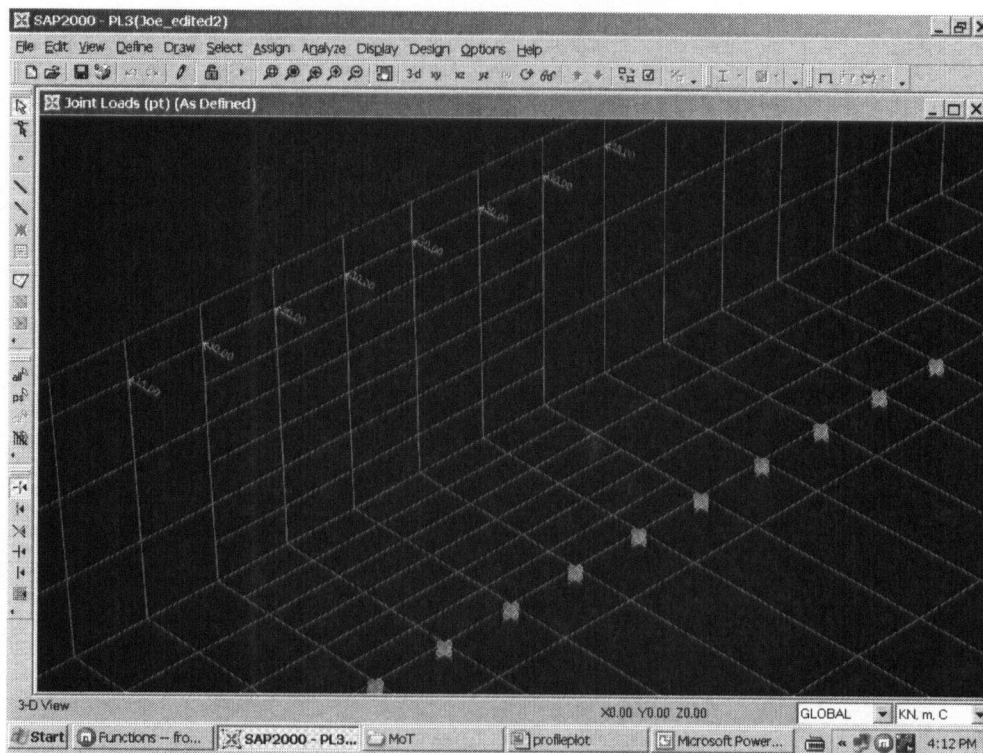
Figure 14 - Transverse Load on PL-3 Inner Portion Barrier and Deck with 1200mm Overhang

Figure 15 - Transverse Moment Distribution due to PL-3 Transverse load

Figure 16 - MME Spreadsheet for Barrier
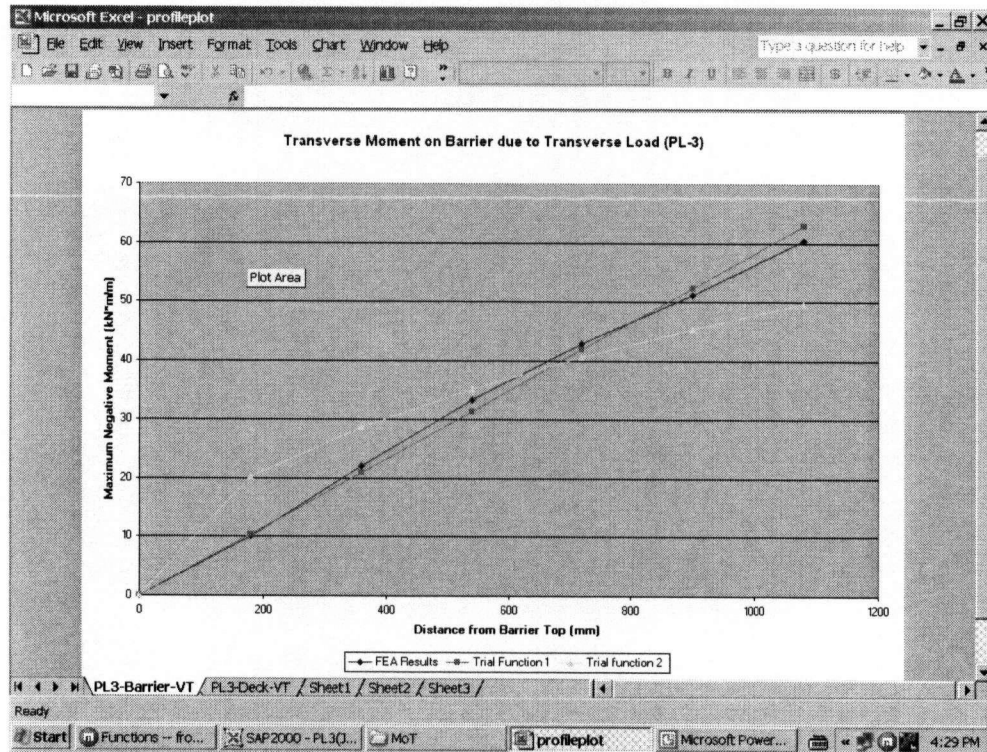
Figure 17 - Plots for Transverse Moment on Barrier

Figure 18 - MME Spreadsheet for Deck

51
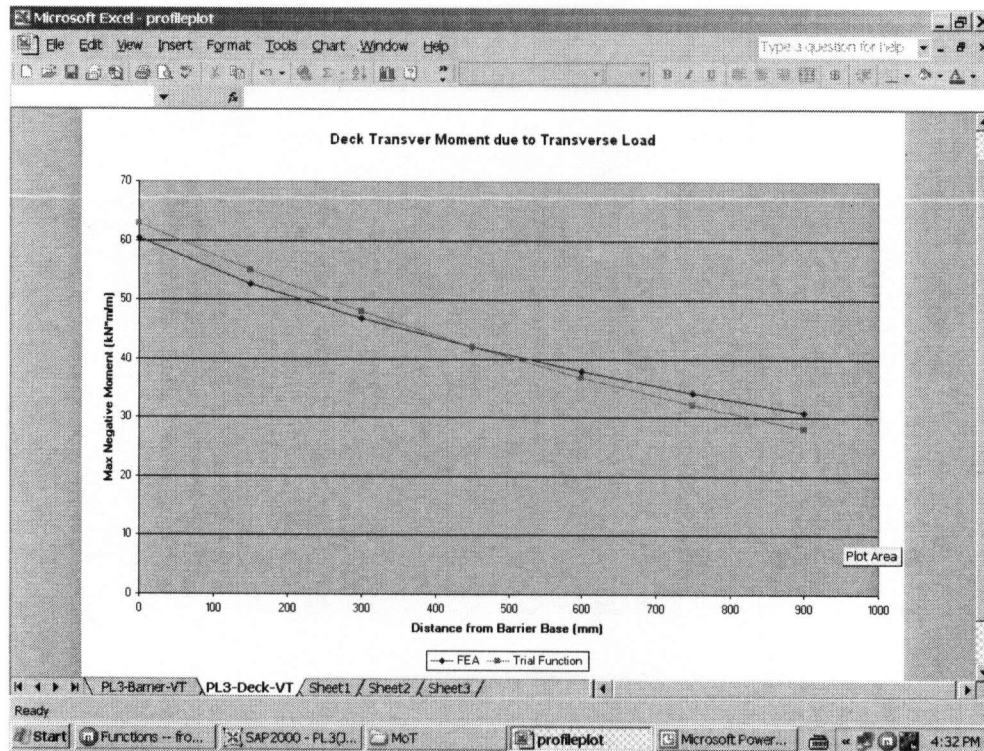
Figure 19 - Plot for Deck Transverse Moment

The results of this method ought to provide a table containing various constant functions that can be used to calculate the relevant constants. Depending on the scenario, those can then be used together with the distribution function to determine the MME needed for any particular design.

3.4.3 Comments

The MME is realistic in its representations of the true moment distribution along barriers and deck overhangs. This method also gives the maximum moments that designers should design for, instead of just the average values calculated using the dispersal angle method. As such, this design is a conservative one. Keep in mind what came up before, where the moment distribution yielded by the dispersal angle method was assumed to be

uniform and so it may have underestimated the design moments by as much as 20%. The application of this MME method, however, is much more involved and does require much more time and effort than the dispersal angle method, making it less practical. The various functions and constants that define the moment distribution curve may appear to be confusing for designers at first, as well. That might make people unwilling to adopt this new method. In general, MME provides an alternative way for mapping the distribution of the maximum moment intensity of the barrier and deck, although it does deviate slightly from one of the objectives of this research, which is to compromise with the current code design methods.

3.5 Maximum Moment Dispersal Angle (MMDA)

The dispersal angle method and the MME each have their own strengths and weaknesses. In order to counter the weaknesses of these two methods while preserving their strengths, a combined method called the maximum moment dispersal angle (MMDA) was developed during this research. MMDA takes advantages of the use of maximum moment intensity, while also using the dispersal angle theory as its backbone. In other words, the MMDA makes use of the basic concept of the dispersal angle while improving the results of that system, but without making it too much more complicated, as the MME did. There are two ways of achieving such an affect. The first way is by adding modification factors to the results generated by the current dispersal angles to scale or improve those results until they suit the FEA results. The second way is by determining new dispersal angles altogether, so that the results produced by these new angles would give the maximum moment intensity distribution as calculated by the FEA. Both

methods are presented in details in the following sections although only one method

(termed method 2) is recommended for further studies after consideration of their

advantages and disadvantages, and after consultation with the Ministry of Transportation

(MOT) of British Columbia.

3.5.1 Method 1 – Modification factors

The application of this method requires a calculation of the average moment intensity

using the current dispersal angles given by the *Commentary* of the *S6-00* code. As

mentioned before, a spreadsheet was developed so that by simply entering a few basic

input parameters such as performance level, live load factors, overhang distances, and

properties of the barriers, as shown in Appendix K, this calculation could be carried out.

Then, the results can be transferred into another spreadsheet for the purposes of further

developing this method.

3.5.1.1 Development and Application

Figure 20 shows the spreadsheet used to determine modification factor A by adjusting the

results that were calculated in the previous spreadsheet in order to better represent the

FEA results. The Cast-In-Place barrier located in the inner portion is subjected to

performance level 3 transverse loads. The modification factor A is in linear relationship

with the results calculated using current the dispersal angle and it is to be scaled by the

modification factor A of 1.17 in order to yield the maximum moment intensity results

produced by the FEA at the base of the barrier, where maximum moment usually occurs.

Figure 21 illustrates the concept best, as it shows the results plotted using the current

dispersal angle, FEA, along with the modification factor A. Although the modification

factor method does not capture the maximum moment intensity on every point along the

barrier, it does provide a better approximation than would the code dispersal angle at the

base of the barrier, where maximum moment occurs.

Figure 20 - Spreadsheet Used to Determine Modification Factor "A"
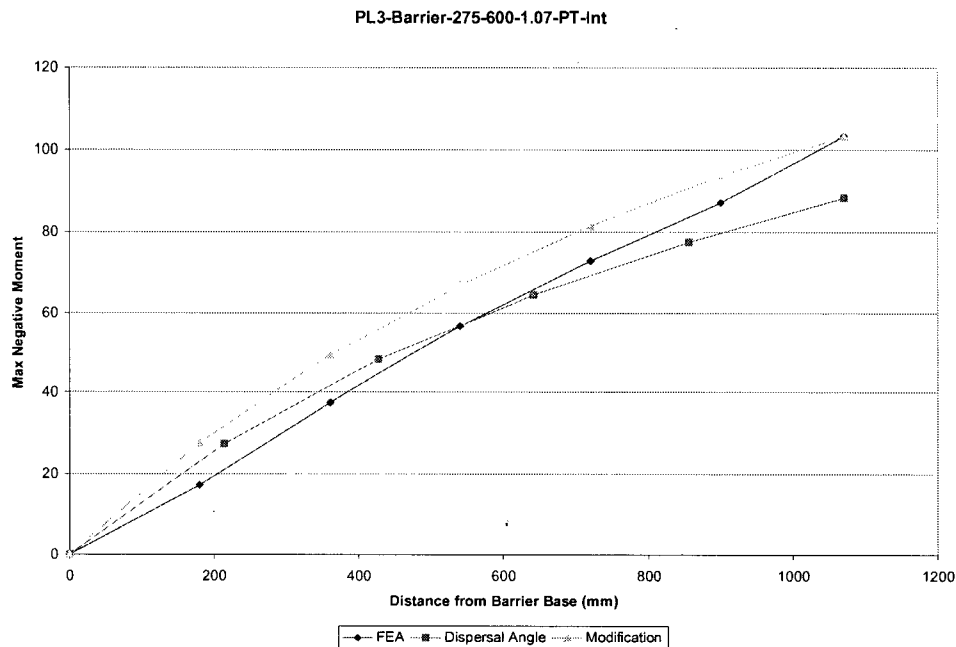
Figure 21 - Plot of FEA, Dispersal Angle, and Modification Factor "A" Results

However, not all modification factors are in a linear relationship with the results.

The relationship depends on how closely the new curve is able to simulate the original

one, which is described by the FEA results. Looking at the deck of the same system

under the same transverse loads, the moment calculated using the code dispersal angle

exponentially related to its modification factor B of 1.1E-3 as shown in Figure 22. It can

be seen from Figure 23 that the use of the exponential relationship in this case could yield

a good approximation of the FEA results. Note that, the use of a linear relationship here

would yield a bad approximation though, especially at the deck supports.

File Edit View Insert Format Tools Data Window Help

A22

	A	B	C	D	E	F	G	H	I
20	Y	=	A*N				Y	=	A*N
21							Deck Transverse Moment due to PT		
22			Modification Factor						Modificati
23	Distance from Barrier Base (mm)	FEA Max Negative Moment (kN*m/m)	Improved Max Negative Moment(kN*m/m)	Finite Differences			Distance from Barrier Base (mm)	FEA Max Negative Moment (kN*m/m)	Improved Max Negative Moment(kN*m/m)
24	0	103.4	103.40	0.00			0	128.2	128.20
25	75	91.4	91.83	0.43			75	123	126.0
26	150	82.7	81.66	-1.04			150	120	123.9
27	225	73.3	72.70	-0.60			225	120	121.9
28	300	63.6	64.80	1.20			300	120	120.00
29									
30	sum	=		0.00					
31									
32	Approximation								
33	A	=	1.17				A	=	1.20
34	B	=	1.10E-03				B	=	-4.73E-0
35	Trial Function								
36	Y	=	A*e^(-Bx)*N				Y	=	A*e^(-Bx)*N
37							Deck Transverse Moment due to PV		
38			No-Dispersion		Modification Factor				No-Disp
39	Distance from Barrier Base (mm)	FEA Max Negative Moment (kN*m/m)	Approximated Max Negative Moment(kN*m/m)	Finite Differences	Approximated Max Negative Moment(kN*m/m)	Finite Differences	Distance from Barrier Base (mm)	FEA Max Negative Moment (kN*m/m)	Approximated Max Negative Moment(kN*m
40	0	0	0.00	0.00	0.00	0.00	0	0	0.0

Constant B-Int / Constant C-Int \ MME-PL3 / MME-PL2 / MME-PL1 / DispersalAngle /

Ready   Sum=1579.97237

Figure 22 - Spreadsheet Used to Determine Modification Factor "B"

PL3-Deck-275-600-1.07-PT-Int
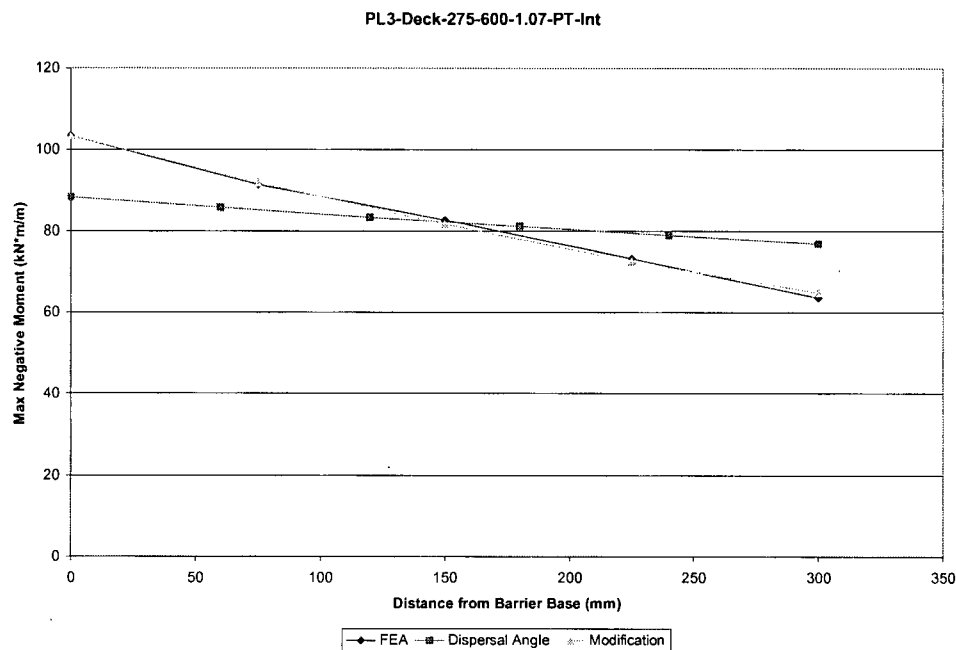
Figure 23 - Plot of FEA, Dispersal Angle, and Modification Factor "B" Results

57

The spreadsheet used to calculate the modification factor C in the case of the deck under the specified vertical loads, as well as the plotting of various analytical methods appear as shown in Figures 24 and 25, respectively. The modification factor C is in linear relationship with the results, and has been found to equal 0.96.

Figure 24 - Spreadsheet Used to Determine Modification Factor "C"

Deck Transverse Moment due to PV

	No-Dispersion			Modification Factor				No-Dis
Distance from Barrier Base (mm)	FEA Max Negative Moment (kN*m/m)	Approximated Max Negative Moment(kN*m/m)	Finite Differences	Approximated Max Negative Moment(kN*m/m)	Finite Differences	Distance from Barrier Base (mm)	FEA Max Negative Moment (kN*m/m)	Approximated Max Negative Moment(kN*m/m)
0	0	0.00	0.00	0.00	0.00	0	0	0.00
75	0.87	0.96	0.09	0.92	0.05	75	1.05	0.96
150	1.83	1.91	0.08	1.84	0.01	150	2.08	1.9
225	2.8	2.67	0.07	2.76	-0.04	225	3.19	2.8
300	3.7	3.83	0.13	3.68	-0.02	300	4.3	3.8
Sum =			0.3625		0.00			
Approximation								
C =		0.96				C	=	1.1
Trial Function								
Y =		C*N				Y	=	C*N

Deck Transverse Moment due to Combined loads

	Code Dispersal Angle			Combined Modifications				Code Disp
Distance from Barrier Base (mm)	FEA Max Negative Moment (kN*m/m)	Approximated Max Negative Moment(kN*m/m)	Finite Differences	Approximated Max Negative Moment(kN*m/m)	Finite Differences	Distance from Barrier Base (mm)	FEA Max Negative Moment (kN*m/m)	Approximated Max Negative Moment(kN*m/m)
0	103.6	88.28	-15.32	103.40	-0.20	0	127.9	106.4

Constant B-Int / Constant C-Int \ MME-PL3 / MME-PL2 / MME-PL1 / DispersalAngle

Sum=779.6495884

PL3-Deck-275-600-1.07-PV-Int

Figure 25 - Plot of FEA, Dispersal Angle, and Modification Factor "C" Results

Figure 26 is a table presenting, for comparison, the code dispersal angle results, the

modification factor results, and the FEA results of the deck moment intensity due to

combined loads. It is clear that the code dispersal angles yield results significantly

different from those of the FEA, especially at the two ends of the deck overhang.

Interestingly, the code dispersal angles have underestimated the results by 15.32 kN*m/m

(14.8%) at the location of the barrier and have overestimated the results by 13.18

kN*m/m (19.5%) at the first support. However, the contribution of the modification

factors did manage to greatly reduce these errors to 0.20 kN*m/m (0.002%) and 0.98

kN*m/m (0.01%) at the location of the barrier and the support, respectively. Figure 27

shows the plotted results as calculated using the three methods. It shows the improvement

that the modification factors have brought upon the current code dispersal angles.

Figure 26 - Spreadsheet Used to Present the Results of Various Methods

	A	B	C	D	E	F	G	H	I
46	sum	=		0.3625		0.00			
48	Approximation:								
49	C	=	0.96				C	=	1.1
51	Trial Function:								
52	Y	=	C*N				Y	=	C*N
53					Deck Transverse Moment due to Combined loads				
55		FEA Max	Code Dispersal Angle		Combined Modifications			FEA Max	Code Disp...
56	Distance from Barrier Base (mm)	Negative Moment (kN*m/m)	Approximated Max Negative Moment(kN*m/m)	Finite Differences	Approximated Max Negative Moment(kN*m/m)	Finite Differences	Distance from Barrier Base (mm)	Negative Moment (kN*m/m)	Approximated Max Negative Moment(kN*m/m)
57	0	103.6	88.28	-15.32	103.40	-0.20	0	127.9	106.4...
58	75	92.3	86.08	-6.22	92.75	0.45	75	123.4	105.2...
59	150	84.6	84.09	-0.51	83.50	-1.10	150	122.9	104.0...
60	225	76.2	82.29	6.09	75.46	-0.74	225	126	103.0...
61	300	67.5	80.68	13.18	68.48	0.98	300	129	102.0...
63	sum	=		-2.7817253		-0.60			
65			MME Approximation for Performance Level 3 (thk275-oh900-1.0...						
66			Barrier Transverse Moment						
67		Due to PT	Due to Combined		Modification Factor			Due to PT	Due to C...
68	Distance	FEA Max Negative	FEA Max		Improved Max		Distance	FEA Max Negative	FEA Max Negative

PL3-Deck-275-600-1.07-Combined-Int

Figure 27 - Plot of FEA, Dispersal Angle, and Modification Factors Results

3.5.1.2 Comments

Although, the results can be improved by adding modification factors while leaving the current dispersal angles unchanged, that does add complications to the method and in so doing, defeats the main objective of this research. The introduction of various relationship and modification factors could potentially lead to confusion similar to that found in the MME method. Therefore, another method is proposed below as a better alternative.

3.5.2 Method 2 – New Dispersal Angles

The second method functions to generate results that match those of the FEA at critical locations such as base of the barrier and the support of the deck overhang. This is done by changing the dispersal angle itself. The dispersal angle is adjusted so that the uniform moment intensity distribution ends up equal to the maximum moment intensity calculated by the FEA, as shown in Figure 28. The black line there represents the true bell-curve moment intensity distribution that has been calculated by the FEA. Additionally, the red line represents the results calculated using the code dispersal angle, and the blue line represents the new dispersal angle and the ways it has been adjusted to fit the FEA results, or the black line, at certain location. Keep in mind that the new dispersal angle is defined differently than the current one. Instead of describing the dispersion of forces, the new angle is used as a tool for finding the maximum moment intensity.
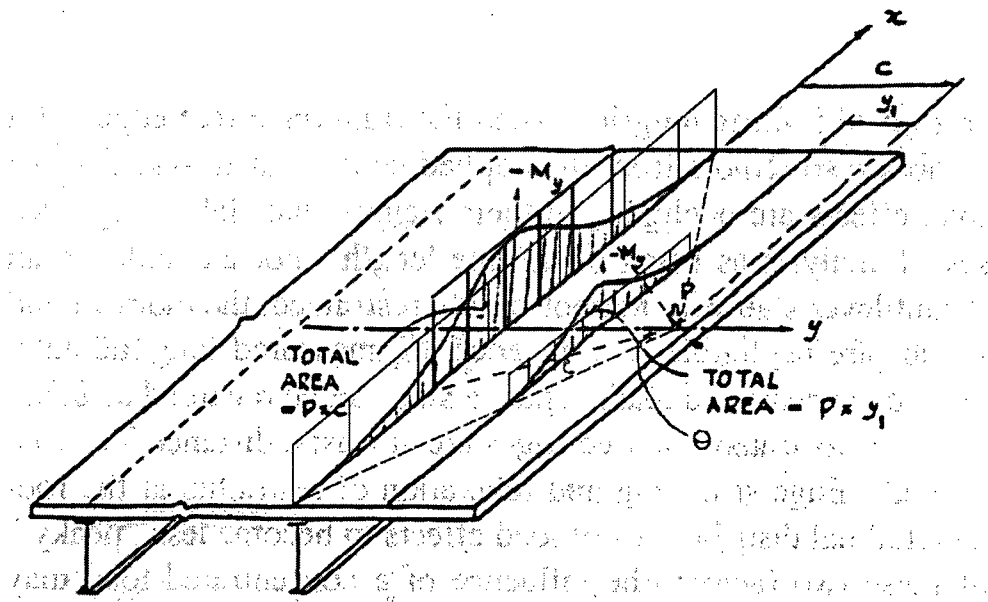
Figure 28 - MMDA Concept by Changing Dispersal Angles

3.5.2.1 Development and Application

Another spreadsheet was set up for the development of this method, and it can be found

in Appendices F to I. The new dispersal angle is to be optimized so that the moment

intensity at the location of interest comes out equal to the maximum moment intensity

calculated using the FEA.

The equations used in calculating moment intensities with the code dispersal angles

are slightly modified for the application of this method. A few new parameters have even

been added so that the new moment intensities can better approximate the FEA results.

Equation (13) is used to calculate the transverse moment, M, of the barrier resulting from

the specified transverse loads, PT, in the *S6-00* code. Θ_{bPT} is the new dispersal angle of

the barrier, which is ultimately to be determined by the spreadsheet. H and DL have the

same definitions as before, where H is the height measured from the location of impact to

the section being analyzed and DL is the distributed length of the transverse load. The only new parameter in this case is N, which depends upon the dispersion of forces: single-sided or double-sided. For the case of a PL-3 inner portion, the forces are freely dispersed onto both sides of the barrier because the Cast-In-Place barrier is a continuous element. Therefore, the dispersion must be multiplied by two to take those effects into account (N = 2). However, for other cases such as a PL-3 end portion, where one side is discontinuous, or a PL-2 inner and end portion, where the precasted barriers are discontinuous at the edge, the dispersion is limited to one side only. Recall that the worst loading condition is when the load is applied at the end of these elements, as shown in Appendices B to E. As a result, N equals unity. Note that the effects of vertical loads and longitudinal loads have very little or no contribution to the transverse moment of the barrier. Therefore, the transverse moment intensity, M, caused by a transverse load, is a good approximation for the total design moment intensity of a barrier.

$$M = \frac{PT \times H}{DL + H \times TAN(\theta_{bPT}) \times N1} \qquad (13)$$

Where:

M   =   transverse moment intensity (kN*m/m)

PT   =   transverse load (kN) * safety factor (1.7)

H   =   height from the point of interest on the barrier to point of impact (m)

DL   =   dispersal length (m)

θ_{bPT} =   dispersal angle of barrier (degree)

N1   =   2 for PL3 inner portion, 1 for other cases

Equation (14) calculates the transverse moment intensities, M, of the bridge deck that result from a transverse load, PT, as specified in the *S6-00* code. The fact that impact force transfers from the barrier down to the deck, caused the denominator of this equation to be divided into two parts. The first part describes the dispersion of loads on the barrier in ways similar to Equation (13) above, while the second part describes the load dispersion on the bridge deck itself. N1 and N2 are two parameters that determine whether the load dispersion is single or double-sided in the barrier and the deck, respectively, as was mentioned before. However, the dispersion across the connection between the barrier and the deck is not necessarily a smooth transition, meaning that the dispersal length on the barrier may not be equivalent to the dispersal length on the deck at the connection point. In fact, only in the case of a PL-3 does the connection between the barrier and the deck share the same dispersal length as would be predicted. However, in the case of PL-2s, the discontinuity of the precasted barrier forces the dispersions at the joint to behave quite differently. Similar to a case of fluid flowing from a narrow channel into an open water, as the fluid leaves the narrow channel it immediately spreads out and travels in all directions to fill the area. The impact load behaves like the fluid in this case. As the load transfers across the connection from the discontinuous barrier (narrow channel) into the continuous bridge deck (open area), the load immediately spreads out and disperses in all directions, causing an abrupt change in the dispersal length at the joint. After conducting a series of observations, this change in dispersal length is about two times the original length. In other words, the load disperses over a certain length as it approaches the connection, and this length doubles itself as the load subsequently moves across the connection, causing a great reduction in moment intensity on the deck. This phenomenon is defined by the new parameter, N3.

$$MT = \frac{PT \times HB}{(DL + HB \times TAN(\theta_{bPT}) \times N1) \times N3 + (D \times TAN(\theta_{dPT}) \times N2)} \quad (14)$$

Where:

MT   =   transverse moment intensity on deck due to transverse load (kN*m/m)

PT   =   transverse load (kN) * safety factor (1.7)

HB   =   height of barrier base to point of impact (m)

DL   =   dispersal length (m)

D   =   distance of deck from the point of interest to the barrier (m)

Θ_{bPT} =   dispersal angle of barrier (degree)

Θ_{dPT} =   dispersal angle of deck (degree)

N1   =   2 for PL3 inner portion, 1 for other cases

N2   =   1 for end portion, 2 for inner portion

N3   =   1 for PL3, 2 for PL2

Equation (15) is provided for the purpose of calculating moment intensities of decks based on vertical loads per the *S6-00* code. Unlike the transverse load, a vertical load transfers directly down the barrier onto the deck and creates a transverse moment in only the deck. By intuition, an axial load distributed over a long length would yield very little or no dispersion among an element. The distributed length is considered long when compared to the depth of the element. In this case, the length to depth ratio is as high as 8 and 13 for PL-2 and PL-3, respectively. Therefore, the barrier acts more as a medium for transmitting the load rather than means of dispersion. With this assumption, the dispersal length, DL, on the deck is set as equivalent to that of the barrier, which is specified in the code. N2, again, takes into consideration the dispersal affect; a single-sided dispersion for end portions and a double-sided dispersion for inner portions.

$$MV = \frac{PV \times D}{DL + D \times TAN(\theta_{dPV}) \times N2}$$ (15)

Where:

MV = transverse moment intensity on deck due to vertical load (kN*m/m)

PV = vertical load (kN) * safety factor (1.7)

D = distance of deck from the point of interest to the barrier (m)

DL = dispersal length (m)

θ_{dPV} = dispersal angle of deck (degree)

N2 = 1 for end portion, 2 for inner portion

The effect of longitudinal loads is minimal in some cases, although still significant enough to be considered in others. For PL-3, the longitudinal load was neglected for the inner portion cases because of its insignificant contribution, yet it was still considered for the end portion cases because of its affect was notable. The contribution of longitudinal loads is more significant for PL-2 scenarios, though, and in those cases it must be considered. However, the longitudinal load creates a twisting moment in the deck which is difficult to capture using the concept of a dispersal angle. Through observation, the proportion of transverse moment generated by the longitudinal load to the total transverse moment of the deck seems to be fairly constant. For the case of PL-3 with cantilever length equal to or greater than 900mm, this moment is approximately 7% of the total transverse moment. For cantilever length less than 900mm, this moment is insignificant and can be ignored for simplicity's sake. In terms of PL-2, the transverse moment of the deck resulting from longitudinal load at both the inner and end portions, with a cantilever length of 900mm or greater, is about 12% of the

total transverse moment. Just as well, for a cantilever length of less than 900mm, this ratio is reduced to approximately 5% for both inner and end potion. These proportions have been incorporated into the Equation (16) during the calculations for the total moment intensity that results from the combination of a transverse load, a vertical load, and a longitudinal load. The new parameter, NL, acts like a scale factor, and applies to the sum of moment intensities resulting from transverse and vertical loads. At this point, the total moment intensity, MC, takes into consideration the effect of all loads.

$$MC = (MT + MV)NL \qquad (16)$$

Where:

MC   =   transverse moment (kN*m/m) due to combined loads: PT, PV, and PL

MT   =   transverse moment (kN*m/m) due to PT

MV   =   transverse moment (kN*m/m) due to PV

NL   =   longitudinal load factor

  =   1 for PL3 inner portion

  =   1 for PL3 outer portion with cantilever length less than 900mm

  =   1.07 for PL3 outer portion with cantilever length equal or greater than 900mm

  =   1.05 for PL2 with cantilever length less than 900mm

  =   1.12 for PL2 with cantilever length equal or greater than 900mm

3.5.2.2 Comments

As mentioned before, the second method of finding new dispersal angles is preferred over the first, which involves the addition of modification factors. This is because of the simplicity and effectiveness of the second method, two characteristics which coincide

with the primary objective of this research. By directly applying the new dispersal angles using the equations presented above, one can easily determine the maximum moment intensities in any particular area of interest, unlike with the modification factor method, where one must calculate the moment intensities first, using the code dispersal angles, and then add scale factors into various relationships later on, so as to improve the results. Therefore, the new dispersal angle method is recommended for further studies. The overall superior results of this method are presented below.

3.5.3 Results

Loading conditions depend upon performance levels, overhang distances, and the properties of barriers and decks. Therefore, since load dispersion, or the dispersal angle, depends upon various parameters, including the loading conditions, many different combinations of these parameters must be tested for analysis to be thorough enough to ensure accuracy. For this reason, FEA has been performed repeatedly so that the necessary scenarios could all be completed. The data that have been used to carry out this research were collected in the spreadsheet available in Appendices F to I. To be precise, 80 different scenarios were performed in consideration of all the possible combinations of the important parameters. The resulting dispersal angles of the different scenarios are presented in the following tables.

Table 12 - Results of New Dispersal Angle Method for PL-3 Inner Portion

Overhang Distance (mm)	Angle of Barrier due to PT	Angle of Deck due to PT	Angle of Deck due to PV
600	31.2	75.5	34.1
900	30.8	77.2	32.0
1200	31.6	77.3	25.8
1500	32.8	77.6	24.9
1800	34.1	77.0	26.6
*All angles in degrees			

Table 13 - Results of New Dispersal Angle Method for PL-3 End Portion

Overhang Distance (mm)	Angle of Barrier due to PT	Angle of Deck due to PT	Angle of Deck due to PV
600	28.4	34.2	-77.2
900	31.6	46.5	-65.4
1200	31.0	50.9	-57.4
1500	31.5	55.1	-51.5
1800	32.5	57.1	-43.5
*All angles in degrees			

Table 14 - Results of New Dispersal Angle Method for PL-2 Inner Portion

Overhang Distance (mm)	Angle of Barrier due to PT	Angle of Deck due to PT	Angle of Deck due to PV
600	-25.1	70.9	62.5
900	-25.1	70.2	71.1
1200	-23.6	69.5	69.9
1500	-24.1	66.0	65.4
1800	-24.6	65.2	61.8
*All angles in degrees			

Table 15 – Results of New Dispersal Angle Method for PL-2 End Portion

Overhang Distance (mm)	Angle of Barrier due to PT	Angle of Deck due to PT	Angle of Deck due to PV
600	7.5	-10.2	-36.7
900	-7.1	48.0	-20.5
1200	-14.1	63.1	-70.3
1500	-19.4	70.1	-77.6
1800	-23.0	74.5	-79.7
*All angles in degrees			

Notice that the dispersal angles obtained in some cases are negative. This phenomenon is inevitable, for reasons given below. As mentioned before, the new dispersal angle has a slightly different definition than that of the current dispersal angle. While the current angles try to capture the load dispersion to a certain extent, the new angle is a means of calculating maximum moment intensity at specific locations of interest. Instead of providing the average moment intensity calculated using the current angles, the new angles provide the designer with a tool for approximating the critical moment intensity that should be designed for. To achieve such a goal, the new angles are adjusted so that the resulting dispersal length within which the load is distributed would produce a moment intensity that matches that maximum intensity obtained by the FEA as shown in Figure 28. For this reason, negative dispersal angles do seem to be possible based on the FEA results. For example, if the FEA moment intensity at a location of interest is so large that the dispersal length, calculated using a positive dispersal angle which cannot be produced if the total load is distributed evenly throughout, was needing to be shortened, then the dispersal angle would have to go in a negative direction to cause the resulting moment intensity to increase until it reached the FEA results. In fact, cases where the dispersal angles became negative occurred for the same reasons as given

70

above. It can be seen from the Tables 12 - 15 that the two scenarios involving negative

dispersal angles took place at the deck overhangs located at the end portion for both PL-3

and PL-2, and at the barrier for PL-2 at both the inner and end portions. The results of

the FEA, which can be found in Appendices F to I, indicate that extremely high moment

concentrations exist in both of the above scenarios. For deck end portion systems, this

high moment intensity is concentrated at the end of the first support, meaning that the

force flows toward this location as it travels across the deck. That is possibly due to the

discontinuity of the deck. For the case of PL-2 barriers at the inner portions, which are

shown in Figures 29 and 30, the extremely high moment concentration occurs at the

bottom corners of the barrier, meaning they are most likely due to barrier discontinuity.
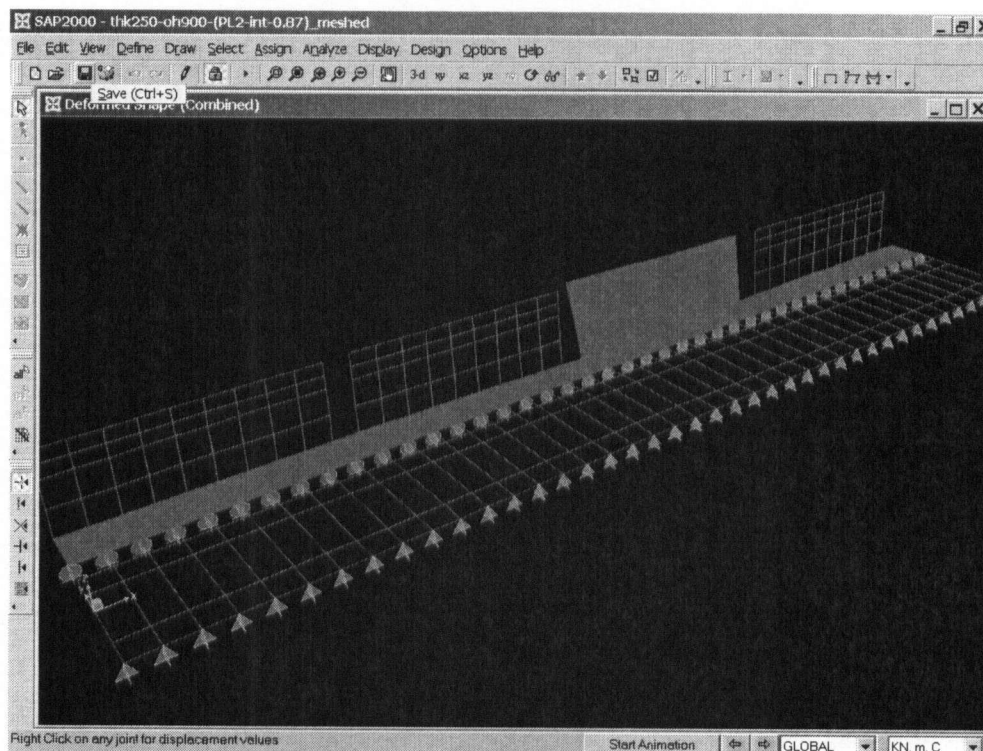
Figure 29 - Loading Condition and System Configuration for PL-2 Inner Portion
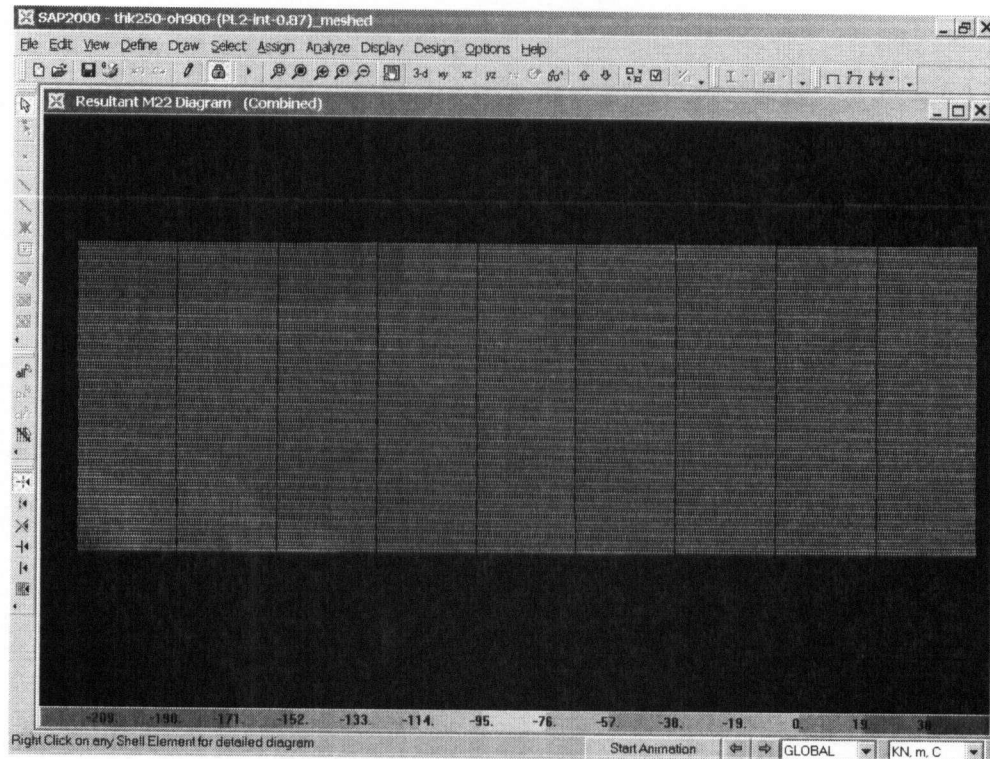
Figure 30 - Transverse Moment Intensity for PL-2 Inner Portion

For the last case of PL-2 with the barrier at the end portion, the moment

concentration is found at the bottom corner opposite where the transverse load is applied,

unlike what happened with the inner portion. The phenomenon shown in Figures 31 and

32 may seem surprising at first, but become sensible when one understands clearly the

loading conditions and configurations of the system. Since the end portion is

discontinuous, the outer most corner of the barrier would be left unsupported. Based on

the laws of physics, a force would always take the path with the highest stiffness, which

in this case is the interior side of the barrier where it is still connected firmly to the body

of the deck. In other words, the part of the barrier closest to the connection between the

barrier and the deck, but farthest from the discontinuous edge, is the area that attracts the

most forces, or moment intensity, as it is in this case. Hence, the high moment

concentration of the PL-2 end portion occurs on the interior side of the barrier. The PL-2

inner portion, on the other hand, has both sides of the barrier evenly supported by the

deck.
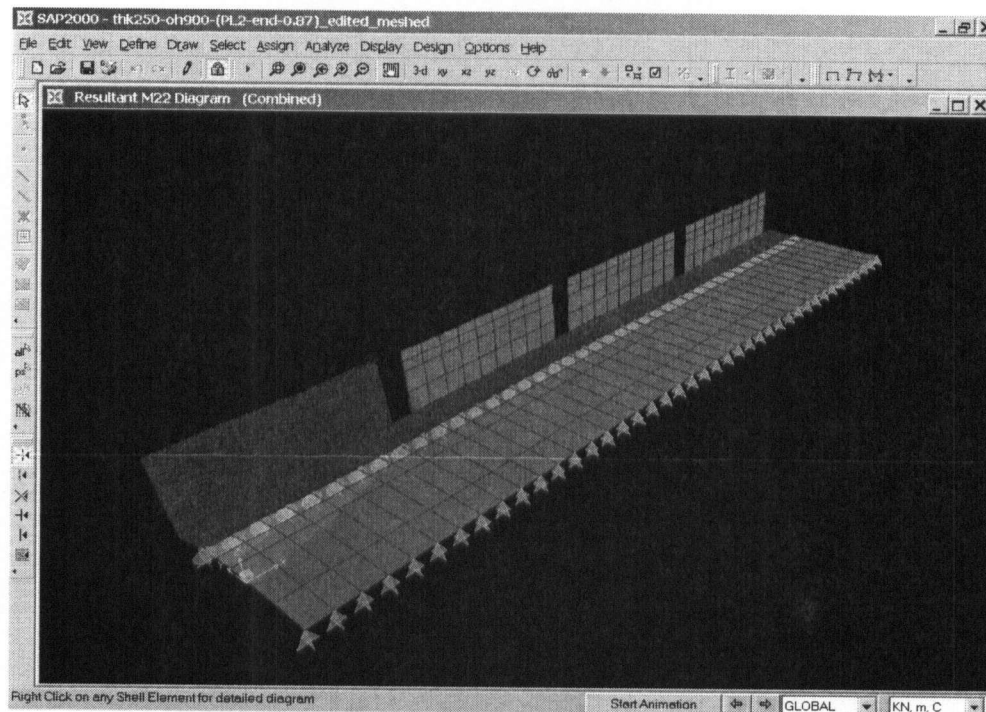
Figure 31 - Loading Condition and System Configuration for PL-2 End Portion
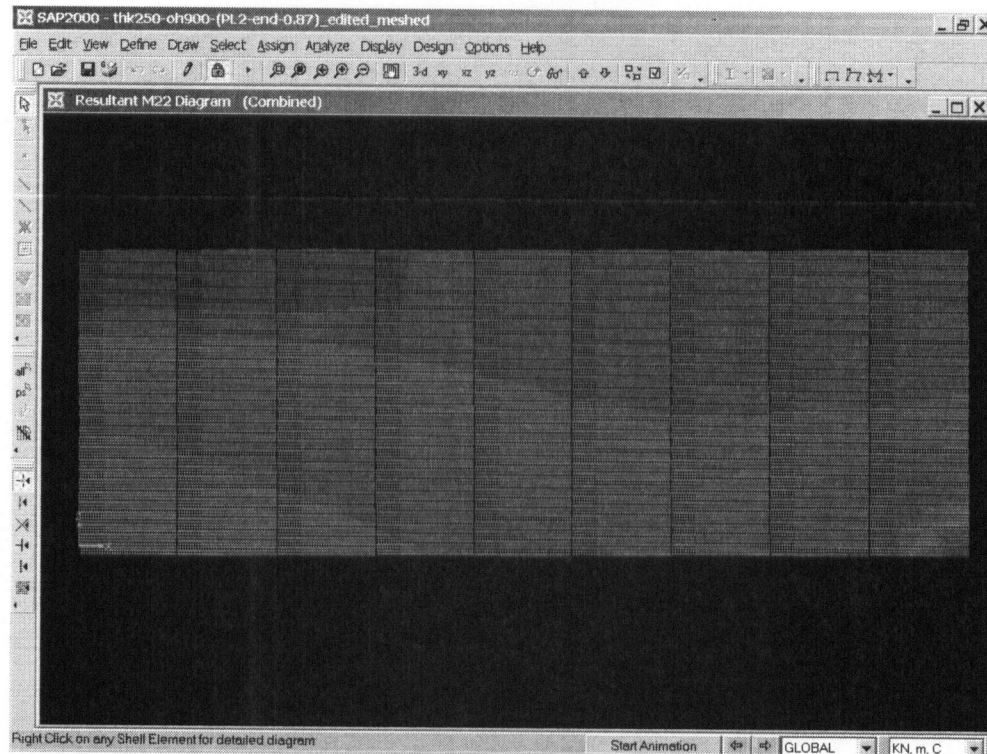
Figure 32 - Transverse Moment Intensity for PL-2 End Portion

Although the new dispersal angles are found and presented in Tables 12 - 15, it is necessary to further reduce and simplify this large amount of data into something more useful and practical to apply. It can be easily seen that some dispersal angles are more sensitive to changes in overhang distance than others. For cases where the angles act more independently of the overhang distances and have values within a reasonable range, the angles can be simplified and represented by one single dispersal angle; the mean of all relevant angles. However this method of simplification cannot be applied in those cases where the differences between angles are too great. Note that in some cases the differences between angles can be as much as two times the amount, depending on the variation caused by the overhang distance. To take into account this large change in angles, two angles for each of the 600mm and 1800mm overhang distances were given.

74

The angles between those two cantilever lengths could then be calculated using linear interpolation. Although this method cannot provide exact angles, as shown in Tables 12 - 15, it can sufficiently approximate the change of angles depending on the overhang distance. The resulting simplified angles are presented in the following tables.

Table 16 - Simplified Dispersal Angles

	Performance Level 3 – Cast-in-place Reinforced Concrete Barriers		Performance Level 2 – Precasted Reinforced Concrete Barriers	
	Inner Portion	End Portion	Inner Portion	End Portion
Barrier due to PT	31	31	-24	LI
Deck due to PT	77	50	67	LI
Deck due to PV	25	LI	65	LI
*All angles in degrees *For "LI", refer to Linear Interpolation Table #				

Table 17 - Linear Interpolation for Dispersal Angles

	PL-3 Deck End Portion due to PV	PL-2 Barrier End Portion due to PT	PL-2 Deck End Portion due to PT	PL-2 Deck End Portion due to PV
600mm	-77	8	-10	-37
1800mm	-44	-23	75	-80
*All angles in degrees				

3.5.4 Examples

Tables 18 and 19 depict the results calculated using the new dispersal angles, the current code dispersal angles, and the FEA results. The new dispersal angle results were determined using Equations (13) – (16) in the previous section.

Table 18 - Example I

Example I – PL3 with 1800mm Cantilever at Inner Portion			
	FEA Results	New Dispersal Angles	Current Dispersal Angles
Transverse moment at base of barrier due to PT (kN*m/m)	99.3	99.3	88.2
Transverse moment at deck support due to PT (kN*m/m)	22.7	22.7	50.6
Transverse moment at deck support due to PV (kN*m/m)	17	17	19.1
Transverse moment at deck support due to combined loads (kN*m/m)	39.8	39.7	69.8

Table 19 - Example II

Example II – PL3 with 1200mm Cantilever at End Portion			
	FEA Results	New Dispersal Angles	Current Dispersal Angles
Transverse moment at base of barrier due to PT (kN*m/m)	125	125	106
Transverse moment at deck support due to PT (kN*m/m)	103.5	103.5	91.2
Transverse moment at deck support due to PV (kN*m/m)	8.6	8.6	7.7
Transverse moment at deck support due to combined loads (kN*m/m)	118.8	119.9	98.9

76

Table 20 - Example III

	FEA Results	New Dispersal Angles	Current Dispersal Angles
Example III – PL2 with 1500mm Cantilever at Inner Portion			
Transverse moment at base of barrier due to PT (kN*m/m)	224	224	63.2
Transverse moment at deck support due to PT (kN*m/m)	22	22	21
Transverse moment at deck support due to PV (kN*m/m)	5.7	5.7	11.1
Transverse moment at deck support due to combined loads (kN*m/m)	31	31	32

In general, the new dispersal angles tend to generate more accurate results (closer to the FEA results) than those generated by the existing ones. The new dispersal angles also capture areas of high moment concentration, due to the more complicated structural configurations and loading mechanisms.

A free piece of software called "Response-2000" is used to carry out the section capacity calculations on a typical PL-3 Cast-In-Place barrier provided by MOT as shown in Figure 33. "Response-2000" is a very user-friendly analysis program that calculates the strength and ductility of a reinforced concrete cross-section subjected to shear, moment, and axial load. Details of this software can be found in the website provided in the "References" section of this thesis.

CONCRETE BRIDGE RAILING
F SHAPE (SBC04c)
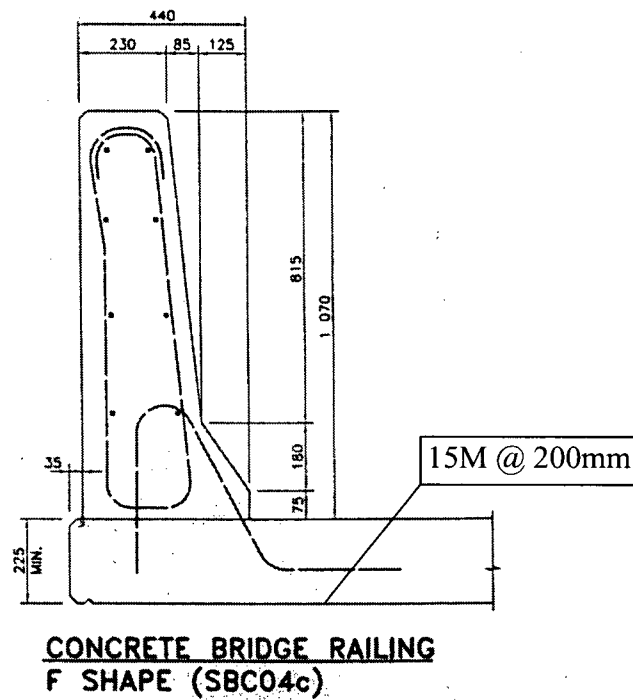
Figure 33 - Typical PL-3 Cast-In-Place Barrier

Figure 34 - Section Capacity Calculation Performed by "Response-2000"

78
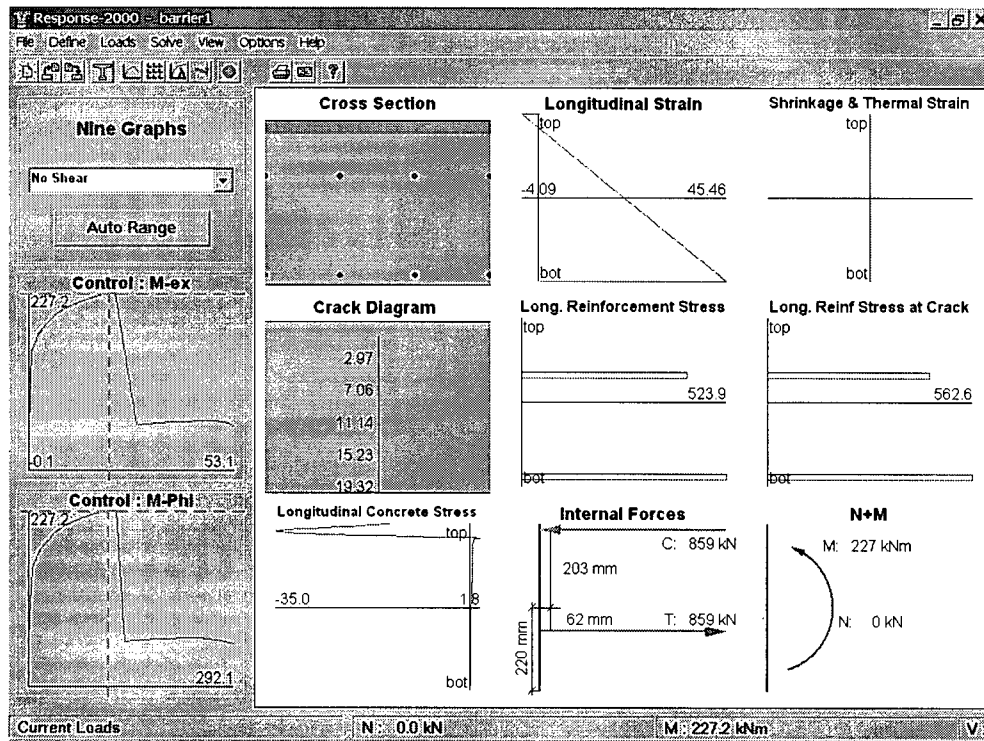
"Response-2000" has determined the flexural capacity of the typical PL-3 Cast-In-Place Barrier, which is shown in Figure 34 to be 227kN*m/m at its base. For comparison, the design loads calculated by the MMDA method can be found in Tables 18 and 19 and come out to 99.3kN*m/m and 125kN*m/m for the 1800mm inner portion and 1200mm for the end portion. Therefore, the typical PL-3 barrier that is being considered satisfies the safety requirements for both of these two examples.

The drawback of this method, however, is that it is only effective for calculating moments at critical locations, such as the bases of barriers, and deck supports. The fact that this method assumes linear load dispersions, instead of more realistic non-linear dispersions, makes it unsuitable for moment calculation done in between the end points. Again, this new dispersal angle concept is significantly different from that of the existing dispersal angle, and should be used with a strict adherence to the guidelines listed in the previous section. Overall, this method will probably be able to take designers one step closer to a safer design while requiring a minimum of effort.

Chapter 4: Conclusion

The jurisdictions reviewed in this report include *AASHTO LRFD Bridge Design Specifications*, Washington State DOT *Bridge Design Manual LRFD*, *CAN/CSA-S6-88 Design of Highway Bridges* and *CAN/CSA-S6-00 Canadian Highway Bridge Design Code*. Each of them has its own strengths and limitations. *AASHTO*, for one, is rich in technical information about the topics of traffic barriers and deck overhang designs, although the accuracy of the design method it suggests, the YLA, relies heavily on assumptions. For example, the deck overhang capacity has to be designed to exceed the flexural resistance of the barrier, or else the failure mechanism may not develop in the barrier, making the YLA invalid in this case. However, since the barrier is designed for survival instead of for the ultimate strength of the barrier itself, it is likely that the barrier is significantly over-designed and therefore will result in the deck overhang being over-designed as well.

This over-design issue is minimized by the WSDOT *Bridge Design Manual*. Seeing itself as a supplement to *AASHTO*, it offers an alternative design criterion for the deck overhang, replacing *AASHTO*'s. By suggesting that the nominal transverse barrier resistance, R_w, transferred from the barrier to the deck should be equal to 120% of the transverse loads, F_t, as specified in *AASHTO*, the over-design of the deck overhang can be prevented here. WSDOT *Bridge Design Manual* also provides a useful table of design forces for several standard traffic barriers used in Washington State, making the design procedures themselves, more consistent.

S6-00 offers a list of available design methods without specifying a standard. This may lead to confusion and cause inconsistency in designs. While the flexibility of using

80

various refined methods is something that should be kept, it would also be useful to introduce a standardized method so that there is some consistency amongst most applications for the majority of designers. The product offered by this research, the MMDA, is an ideal tool that manages to suits such purposes.

After the literature review of various jurisdictions, a discussion about the various methods of analysis that are available is also beneficial and is necessary if a better method is to be developed. *AASHTO* made use of the YLA for it power, but at the same time inherited its weaknesses. The YLA is an ultimate limit design method that approximates the ultimate capacity of a system by predicting its failure mechanism. Many assumptions must be made to ensure that the failure mechanism predicted by the YLA actually occurs and is therefore valid. While this method is powerful for systems with simple configurations and load applications, it begins reaching its limitations as soon as the system and its load applications become more complex, for example, when deck overhangs are put together with traffic barriers. Many failure mechanisms are possible for the deck overhang and the number of assumptions needed to ensure their occurrence may easily become too great to remain practical. Furthermore, YLA produces an upper bound solution, which makes the design unconservative since it becomes possible for the system to fail sooner than predicted.

FEA is a much better method for analyzing complex systems. By correctly entering the necessary parameters, system configurations, and load applications, the FEA program can carry out an analysis using whichever method the user specifies, including any of a static, dynamic, linear or non-linear analysis. By knowing the stress distribution within the deck overhang and barriers, their capacities can be designed accordingly. However, the time and human resource needed to develop an FEA is usually impractical

for the industry. Hence, the dispersal angle becomes a better tool in this case because of its efficiency.

Dispersal angles, which have been developed using FEA, allow for simple calculations to approximate the load dispersion on the deck overhang so that it can be properly designed using minimal time and effort. Although this method is convenient, the underlying theory makes it unconservative. The fact that this method assumes the load dispersion to be linear when in fact it is non-linear, as well as assuming the load distribution is uniform when it is actually a bell curve distribution, causes an overestimation of results in one area and an underestimation in another. In order to prevent this inconsistency in results, a new method called the MME was introduced.

By simulating the actual non-linearity of load dispersion with different functions for different scenarios, the MME was developed in order to determine the "maximum" moment intensities for traffic barriers and deck overhangs, ultimately yielding a safer design. However, seeing that the functions may actually be far too complicated and unfamiliar for most people, an improved version of the MME called the MMDA was developed to address those concerns.

The MMDA uses dispersal angles. These are obtained by the FEA, which is a system developed specifically for the purposes of this research. Those dispersal angles are then used to evaluate the maximum moment intensities in the barrier and deck overhang, instead of just finding the average moment intensities calculated through the use of the dispersal angle method. Using the MME as its backbone, the MMDA works in conjunction with the dispersal angle method, making it more user-friendly and easier for industries to adopt, while also eliminating any lingering weaknesses of the dispersal

angle method. Tables 16 and 17 present the results of the MMDA, which should be used in accordance with Equations (13) – (16).

Chapter 5: Recommendations and Future Developments

Due to the scope of this thesis, performance level 1 analysis is not included and it is recommended as one of the possible future research topics. Since PL-1 involves mostly post type railings, which yield significantly different load dispersions on the deck overhang than they do on the concrete parapets, it is a necessary area for further analysis.

The connections between the barriers and the decks are assumed to be continuous in the FEM, and are not seen as real, discrete connections that should be located at a particular distance apart from one another. As an extension of this research, the FEM can be modified by adding discrete connections/joints in between the barrier and the deck to reflect the true nature of the existence of anchorages/rebar. This may create a significant difference in the load dispersions generated by FEA. However, it is recommended that this be used to compare the differences between load dispersion for the FEM with and without these discrete connections.

Another recommendation for future research is a plastic analysis of the traffic barriers and deck systems in the development of an ultimate limit state design. Similar to the MMDA method, the method to be developed in evaluation of barrier and deck moment intensities for PL-1, 2, and 3 in accordance with the plastic analysis of FEA, should also require minimal time and effort. It should also be easy for designers to apply in practice. The dispersal angle method is suggested as a place to begin, but other methods are fine if they happen to satisfy the objectives. However, if other methods are proposed, the results calculated using the proposed methods and conventional dispersal angle methods should still be provided for comparison nonetheless. To then compare the

design forces calculated by the plastic analysis with those from the design examples provide by the MOT, examples should be supplied.

Reliability is another important recommendation in developing a better design method. Recall that the new dispersal angle varies with different cantilever lengths as well as with the magnitude of variation from case to case, as shown in Table 12 – 15. Instead of representing a range of dispersal angles that is within reason and which has a mean value, reliability can be applied here to determine a more representative dispersal angle. The concept of reliability is also applicable for replacing the linear interpolation method, in cases where the range of dispersal angles is too broad to be accurately represented by the mean value.

References

AASHTO LRFD Bridge Design Specifications, *American Association of State Highway and Transportation Officials*, 2004

Bentz, Evan Response-2000 [Computer software] *University of Toronto*
http://www.ecf.utoronto.ca/~bentz/r2k.htm

Bridge Design Manual LRFD, *Washington State Department of Transportation*, 2005
http://www.wsdot.wa.gov/fasc/EngineeringPublications/BDMSections.htm

Canadian Highway Bridge Design Code – CAN/CSA-S6-00, *CSA International*, 2000

Chun Hai Xiao "Analysis and Design of Bridge Deck and Barrier" *University of British Columbia*, 2004

Design of Highway Bridge – CAN/CSA-S6-88, *Canadian Standards Association* 1988

Dilger, W.H., Tadros, G.S. and Chebib, J. "Bending moments in cantilever slabs – Developments in Short and Medium Span Bridge Engineering '90" Vol 1, pp. 256-276. *Canadian Society for Civil Engineering*, Montreal, 1990

Jategaonkar, R., M.S. Cheung *"Bridge analysis using finite elements"* Montréal, *Canadian Society for Civil Engineering*, c1985

Microsoft Office 2002 [Computer software], Microsoft Corporation, © 1983-2001

Troitsky, M. S. "Orthotropic bridges theory and design [by] M. S. Troitsky" Cleveland, *James F. Lincoln Arc Welding Foundation*, 1967

Mosley, W. H. (William Henry), Bungey, J. H. "Reinforced concrete design" Basingstoke, *Macmillan Education*, 1987

Ontario Highway Bridge Design Code, Ministry of Transportation of Ontario, Downsview, Ontario, 1992.

SAP 2000 Nonlinear 8.08 [Computer software], Computers and Structures, Inc. © 1984 – 2002

Xanthakos, Petros P. "Theory and design of bridges" New York, *Wiley*, c1994

Yilmaz, Çetin., Wasti, Syed Tanvir, North Atlantic Treaty Organization. Scientific Affairs Division. "Analysis and design of bridges" Boston, *NATO Advanced Study Institute on Analysis and Design of Bridges (1982 Turkey)*, 1984

Appendix A: Simple Cantilever FEM for Determination of
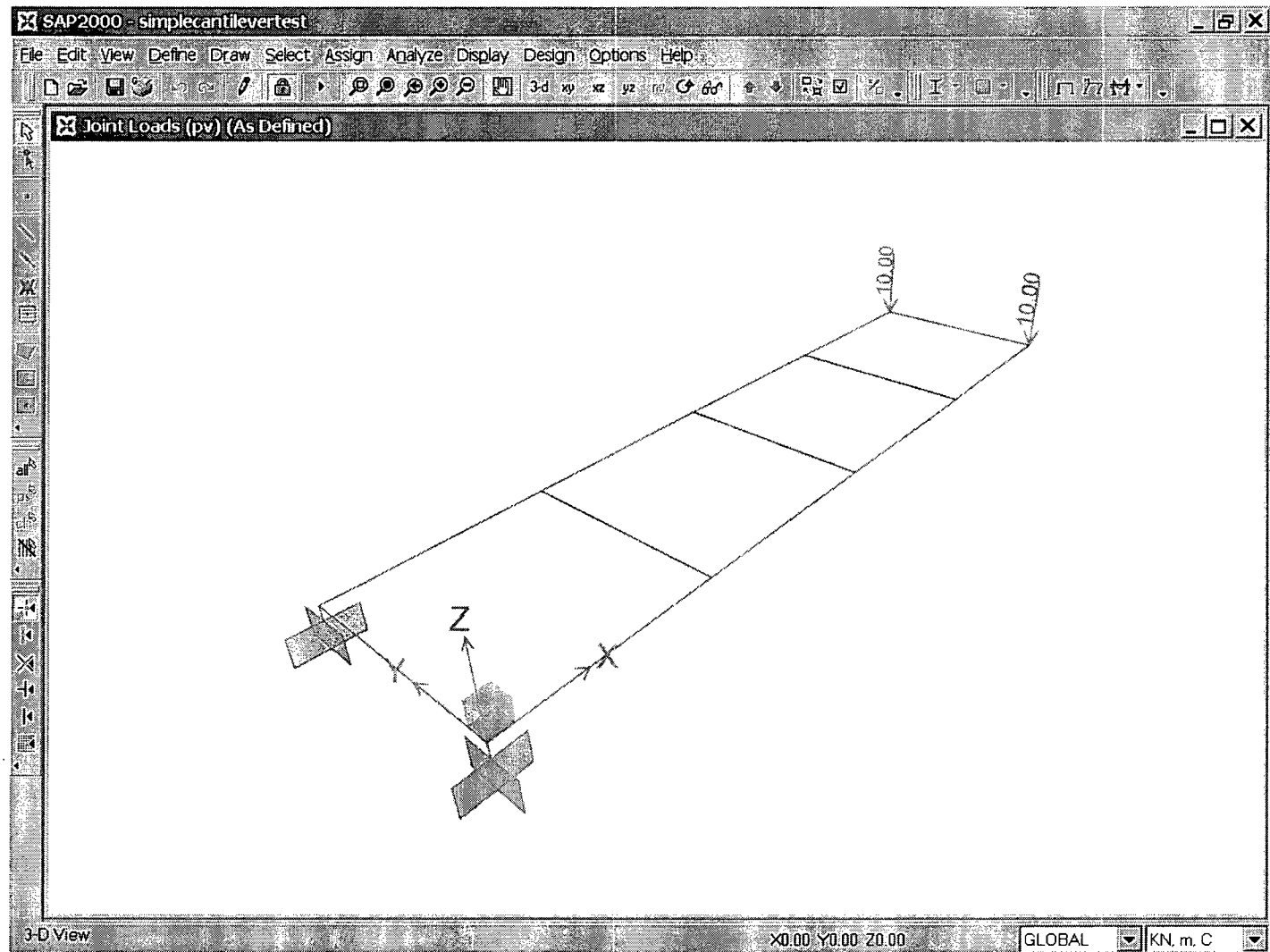
Mesh Size

Figure 35 - Simple Cantilever FEM for Determination of Mesh Size

Appendix B: Load Applications in PL-2 FEM for Inner
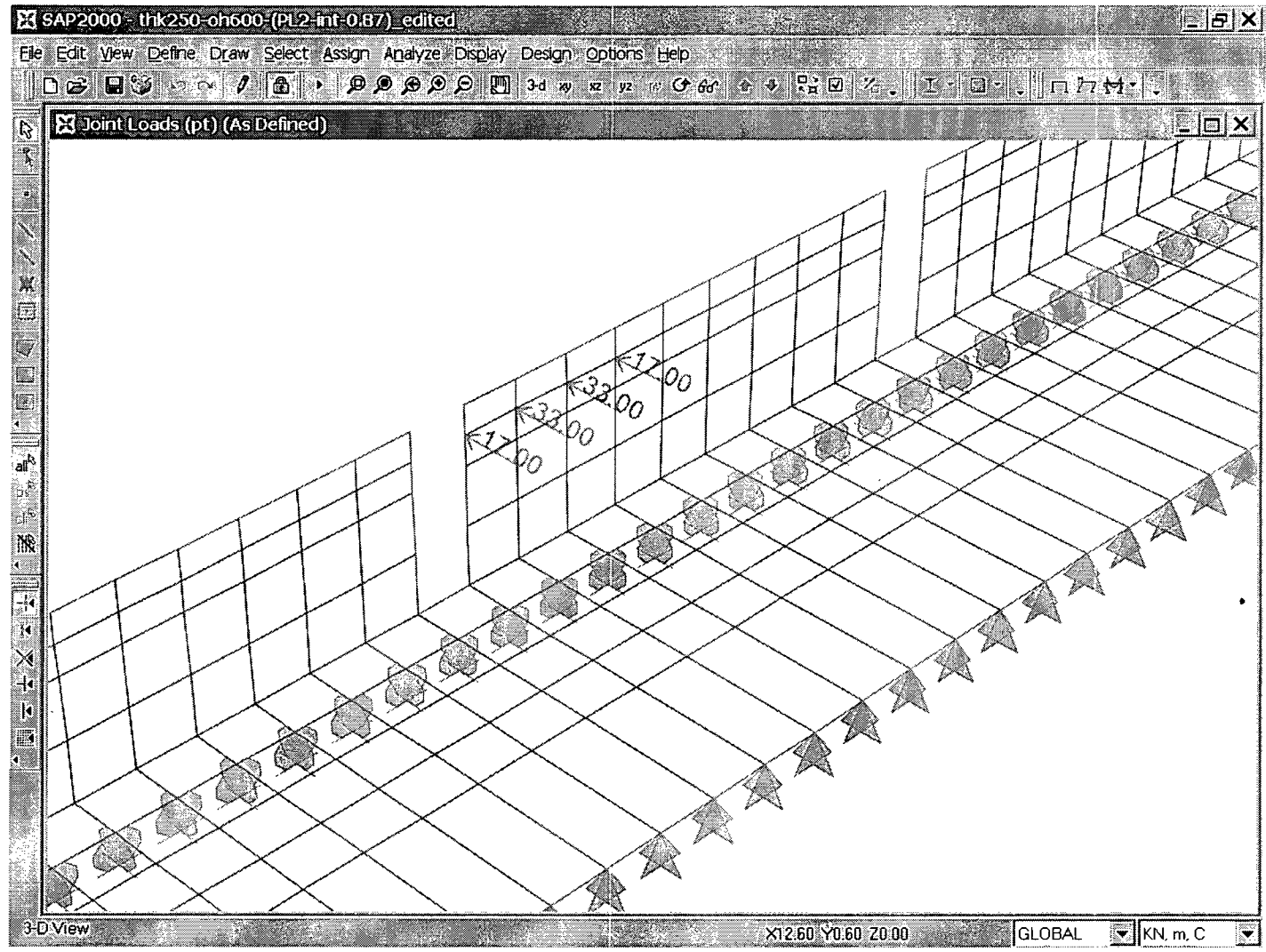
Portion

Figure 36 - PT in PL-2 FEM for Inner Portion
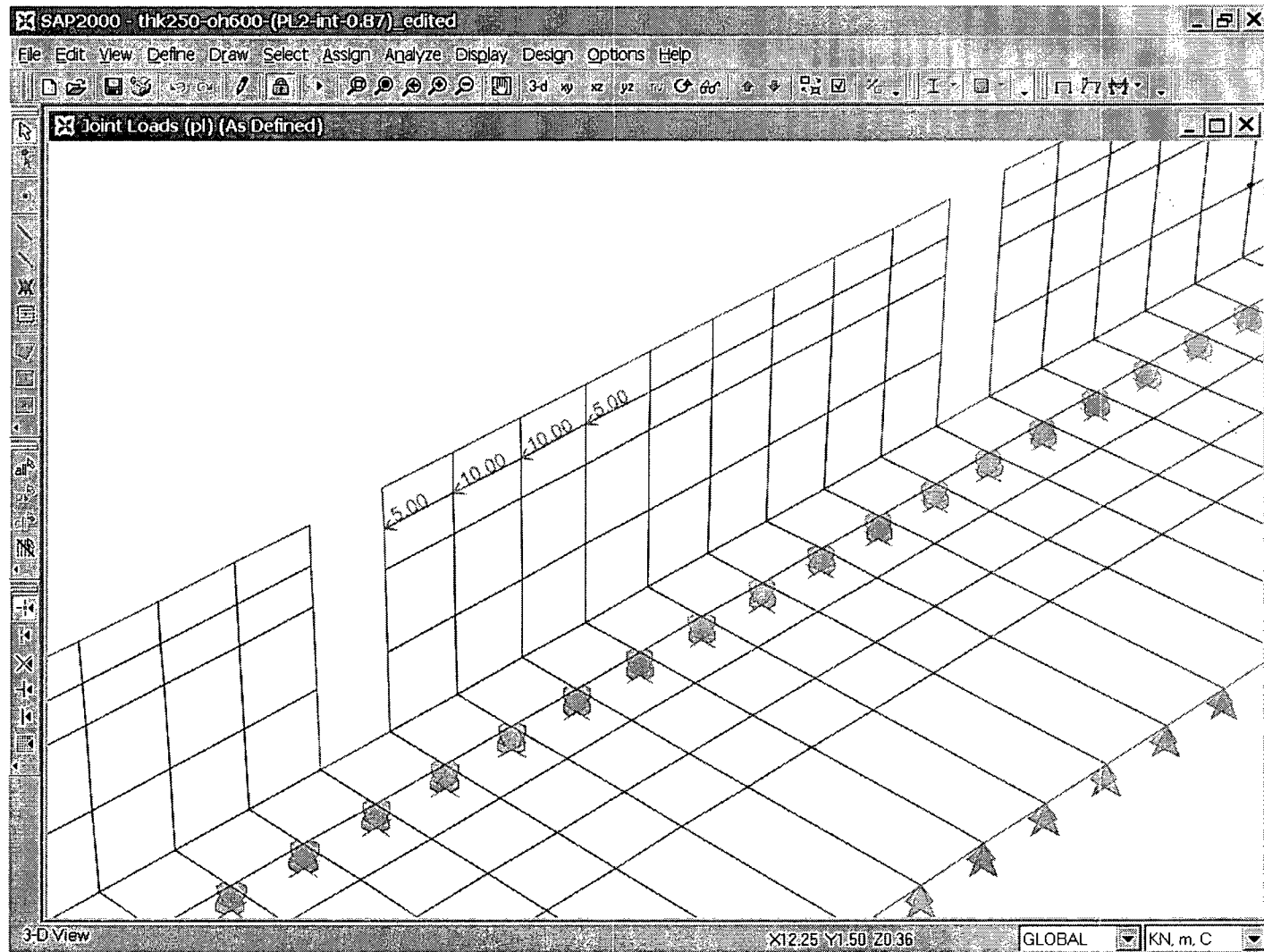
Figure 37 - PL in PL-2 FEM for Inner Portion
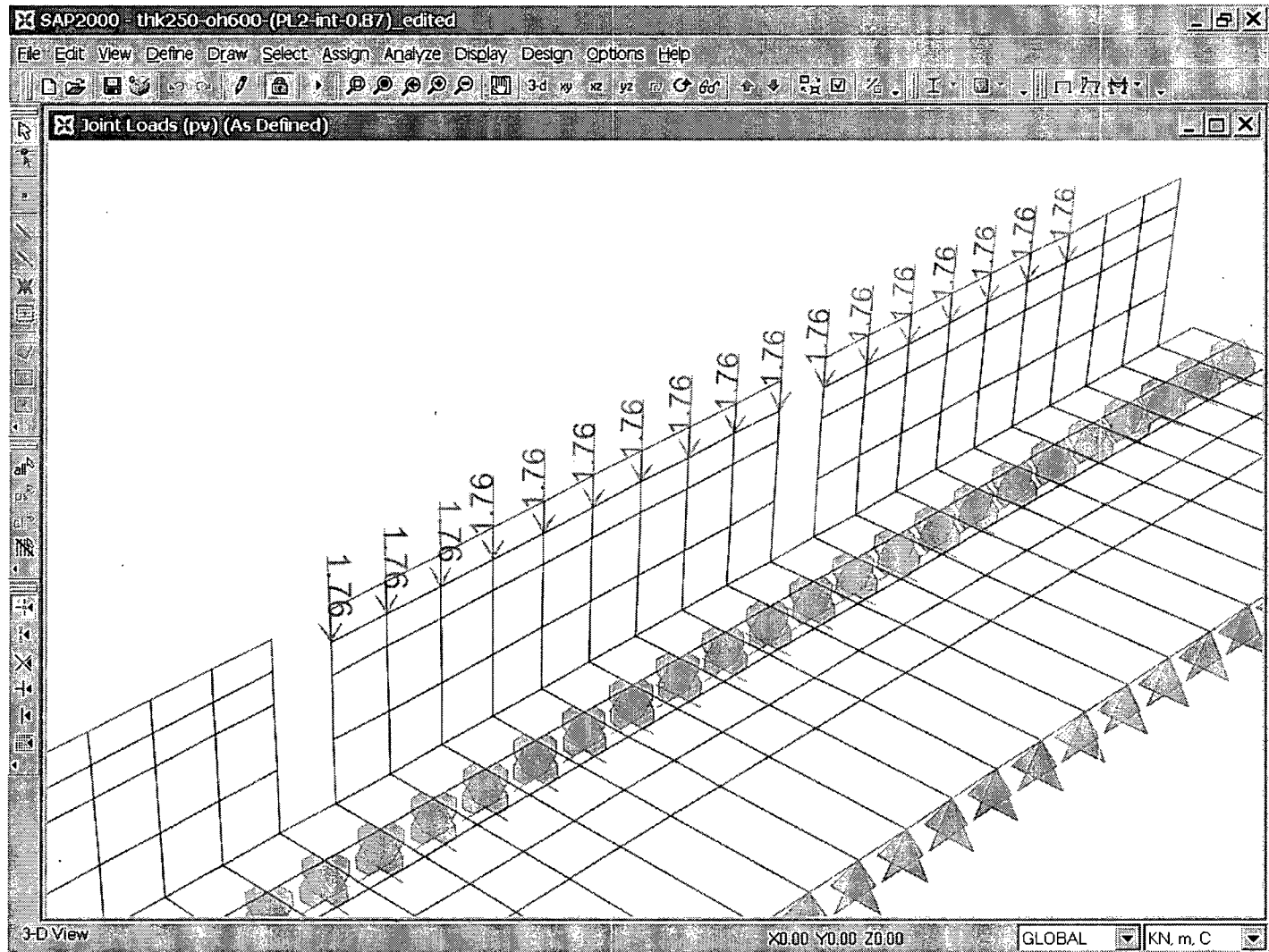
Figure 38 - PV in PL-2 FEM for Inner Portion

Appendix C: Load Applications in PL-2 FEM for End

Portion
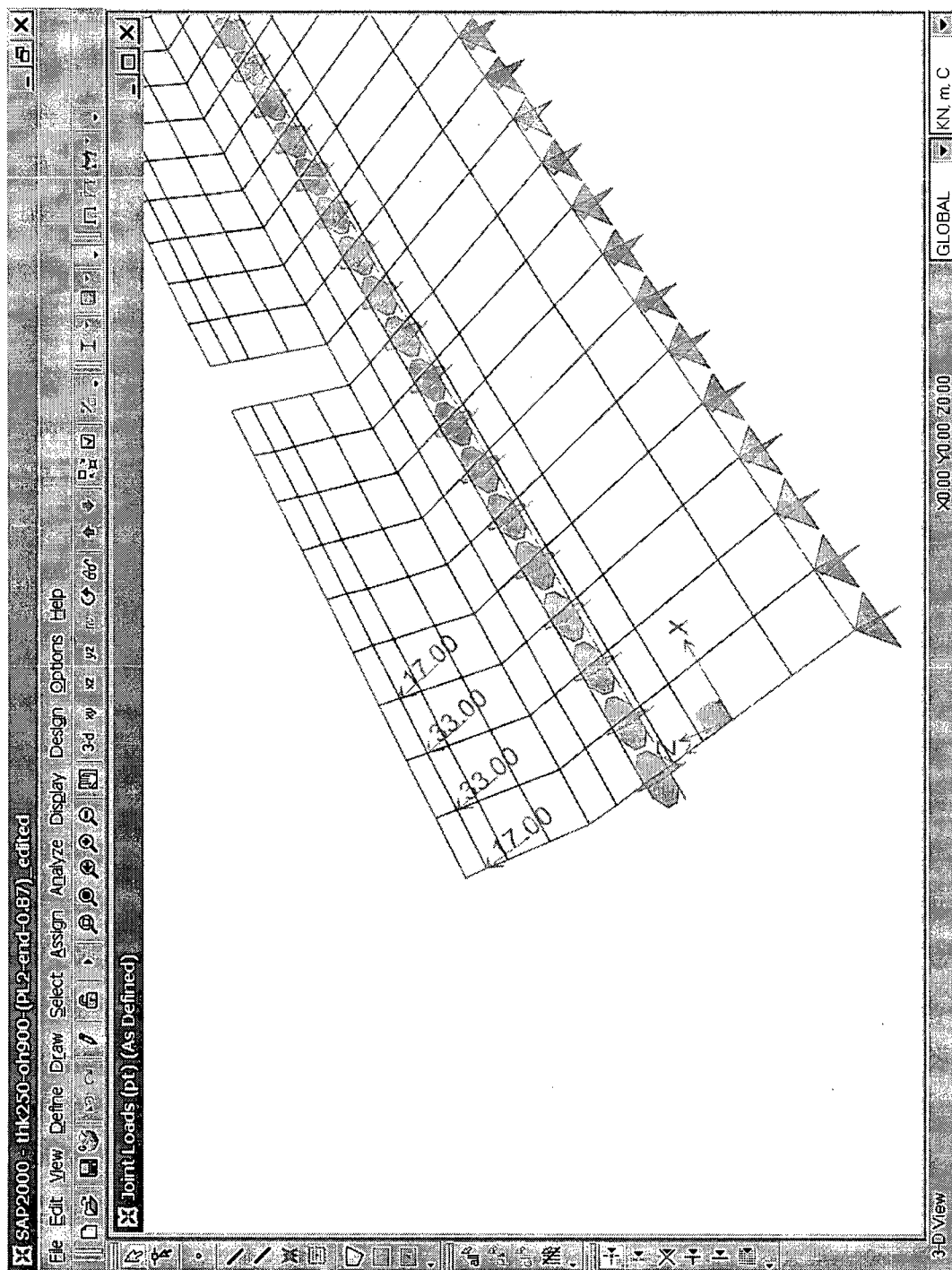
Figure 39 - PT in PL-2 FEM for End Portion

94
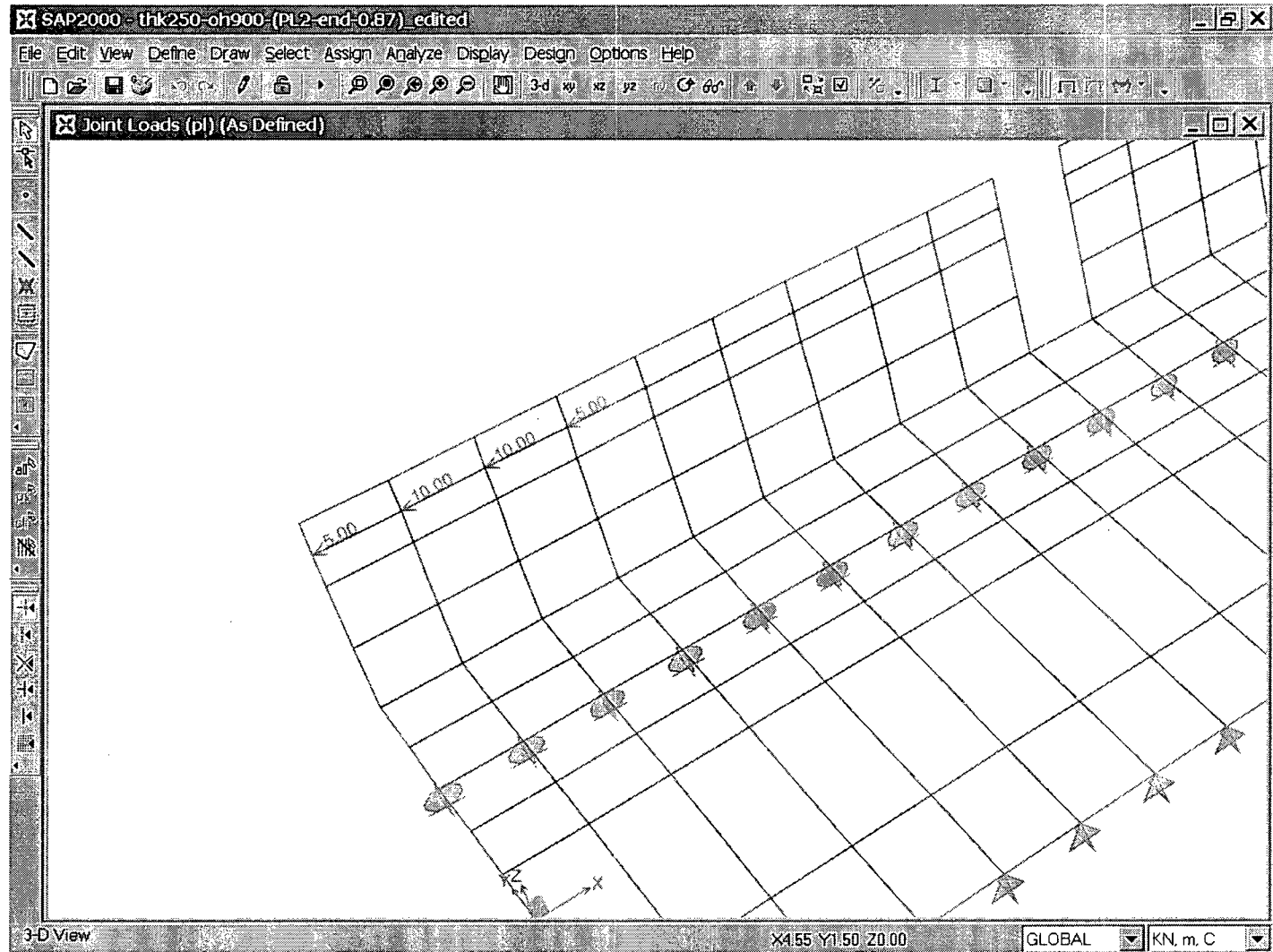
Figure 40 - PL in PL-2 FEM for End Portion
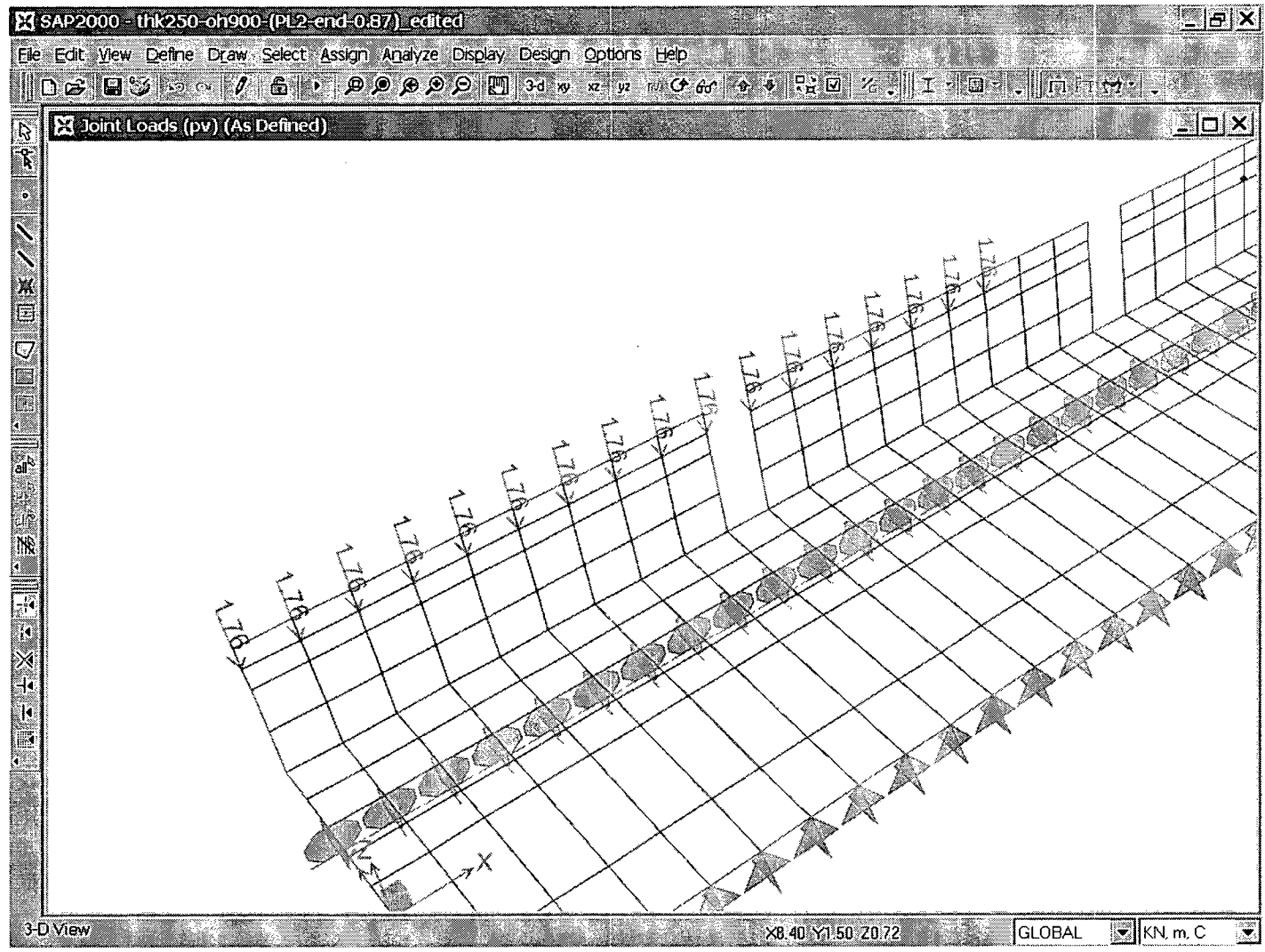
Figure 41 - PV in PL-2 FEM for End Portion

Appendix D: Load Applications in PL-3 FEM for Inner
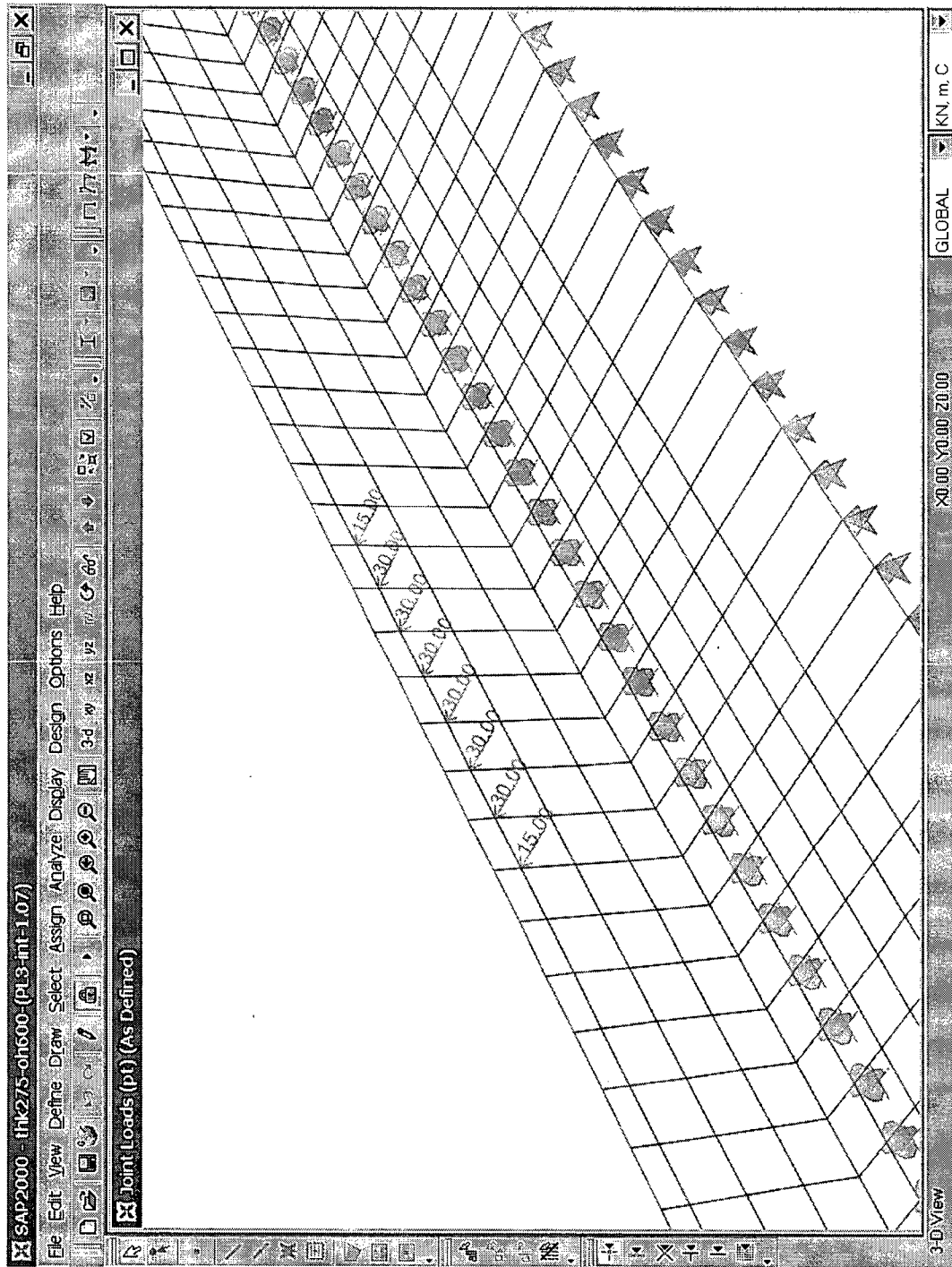
Portion

Figure 42 - PT in PL-3 FEM for Inner Portion

98
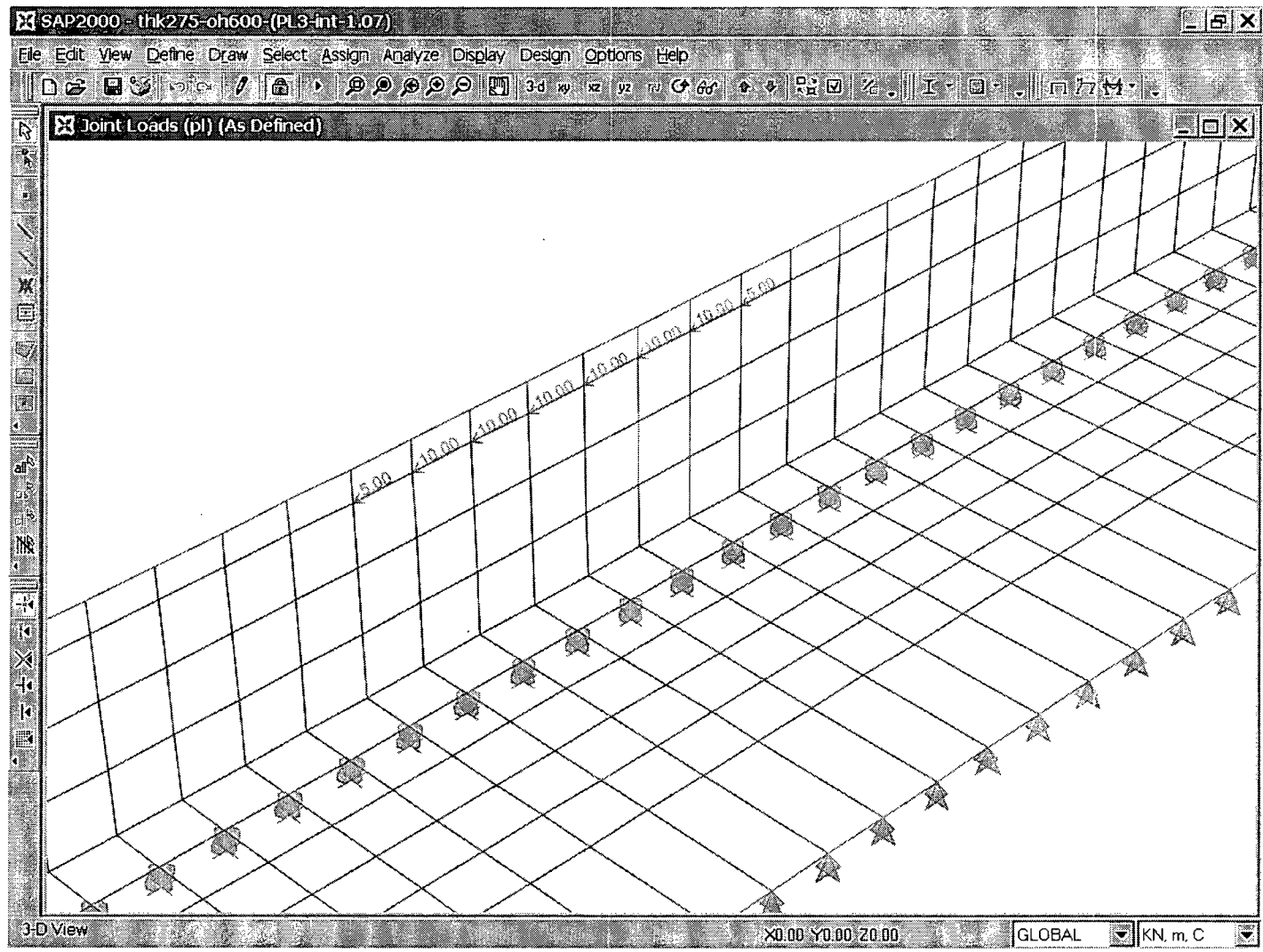
Figure 43 - PL in PL-3 FEM for Inner Portion
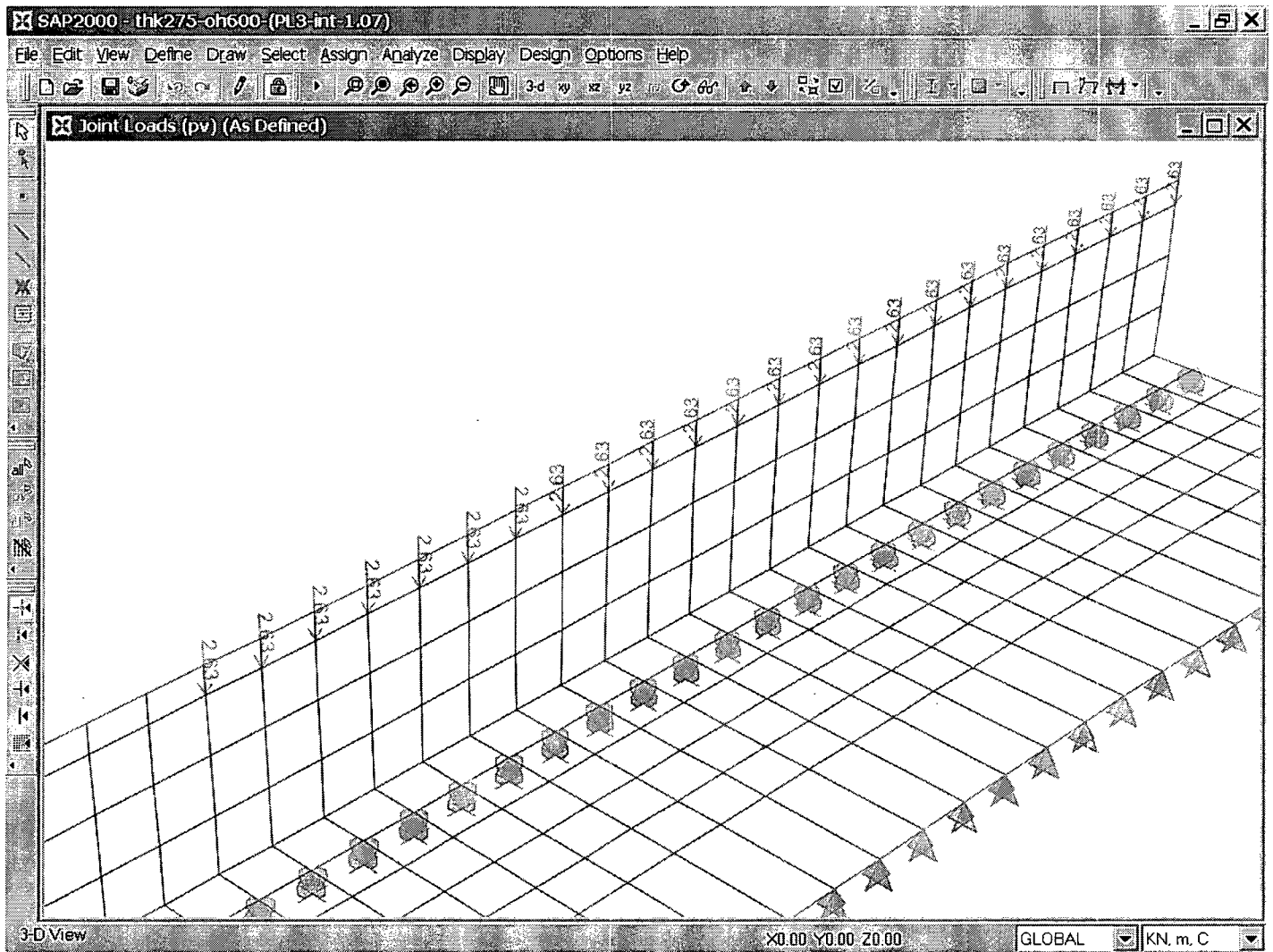
Figure 44 - PV in PL-3 FEM for Inner Portion

100

Appendix E: Load Applications in PL-3 FEM for End

Portion
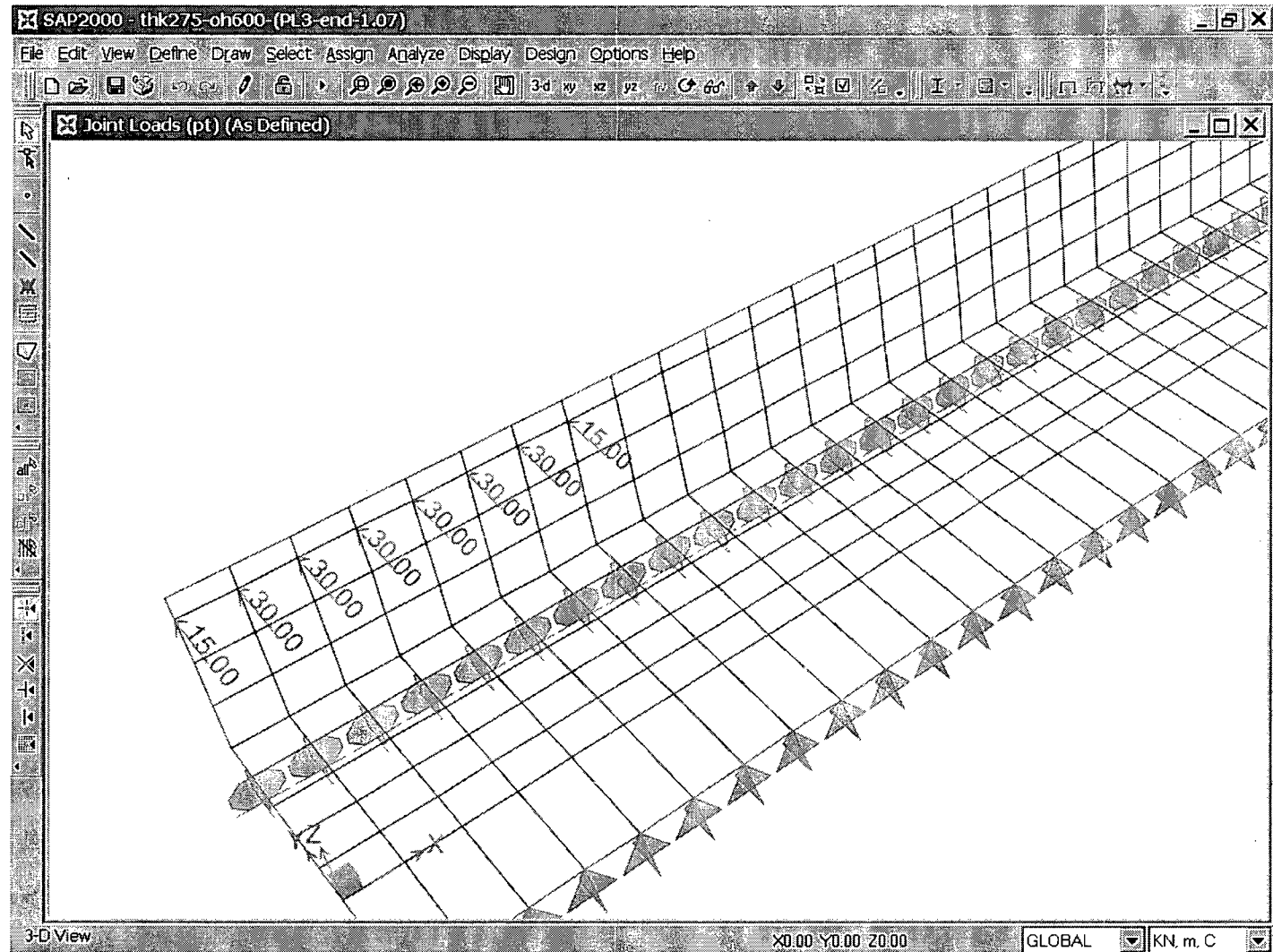
Figure 45 - PT in PL-3 FEM for End Portion

102
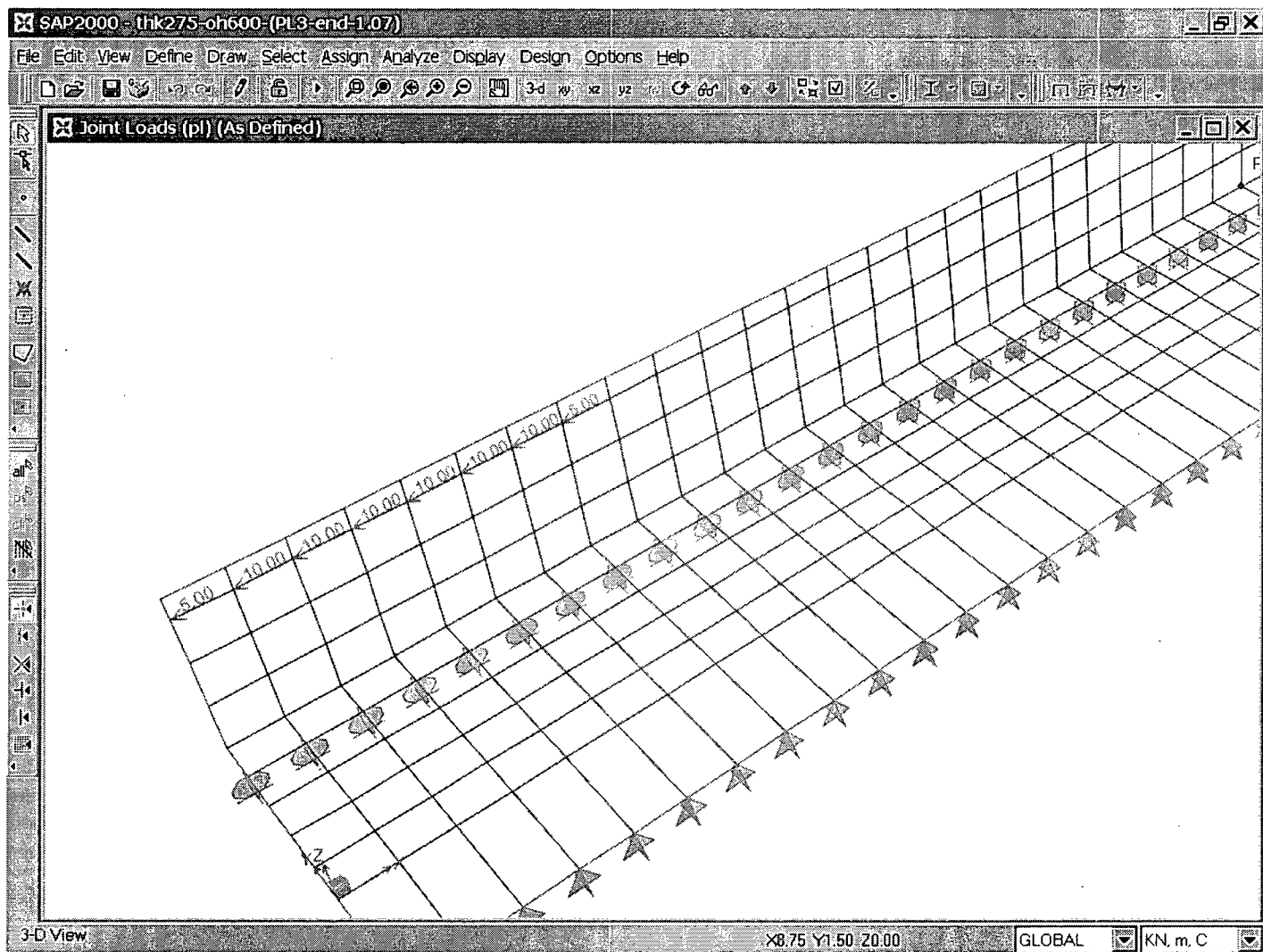
Figure 46 - PL in PL-3 FEM for End Portion

Figure 47 - PV in PL-3 FEM for End Portion

Appendix F: FEA Results and MMDA Spreadsheet for

PL-2 Inner Portion

MME Approximation for Performance Level 2 (thk250-oh600-0.87)

Internal Portion

Barrier Transverse Moment

	Due to PT	Due to Combined		New Dispersal Angle	
Distance from Barrier Top (mm)	FEA Max Negative Moment (kN*m/m)	FEA Max Negative Moment (kN*m/m)	Finite Differences	Improved Max Negative Moment(kN*m/m)	Finite Differences
0	0	-	-	0.00	0.00
180	24.7	-	-	31.68	6.98
360	41.7	-	-	69.42	27.72
540	73.5	-	-	115.12	41.62
720	98.4	-	-	171.62	73.22
870	230	-	-	230.00	0.00
sum/number of section	=		-		21.36

Approximation:

Dispersal Angle	=		-25.1	Degree

Deck Transverse Moment due to PT

New Dispersal Angle

Distance from Barrier Base (mm)	FEA Max Negative Moment (kN*m/m)	Improved Max Negative Moment(kN*m/m)	Finite Differences
0	120	115.00	-5.00
75	72	86.03	14.03
150	63	68.72	5.72
225	54	57.21	3.21
300	49	49.00	0.00
sum/number of section	=		3.59

Approximation:

Dispersal Angle	=	70.9	Degree

106

Deck Transverse Moment due to PV

Distance from Barrier Base (mm)	FEA Max Negative Moment (kN*m/m)	No-Dispersion Approximated Max Negative Moment(kN*m/m)	Finite Differences	New Dispersal Angle Approximated Max Negative Moment(kN*m/m)	Finite Differences
0	0	0.00	0.00	0.00	0.00
75	0.9	0.70	-0.20	0.66	-0.24
150	1.4	1.39	-0.01	1.26	-0.14
225	1.9	2.09	0.19	1.80	-0.10
300	2.3	2.78	0.48	2.30	0.00
sum/number of section	=		0.09		-0.10

Approximation:

Dispersal Angle = 62.5 Degree

Deck Transverse Moment due to Combined loads

Distance from Barrier Base (mm)	FEA Max Negative Moment (kN*m/m)	Code Dispersal Angle Approximated Max Negative Moment(kN*m/m)	Finite Differences	New Dispersal Angle Approximated Max Negative Moment(kN*m/m)	Finite Differences
0	121	40.75	-80.25	115.00	-6.00
75	73	39.17	-33.83	86.69	13.69
150	64	37.84	-26.16	69.98	5.98
225	58	36.70	-21.30	59.01	1.01
300	53	35.75	-17.25	51.30	-1.70
sum/number of section	=		-35.76		2.60

Table 22 - MME Approximation for PL-2 Internal Portion (thk250-oh900-0.87)

MME Approximation for Performance Level 2 (thk250-oh900-0.87)

Internal Portion

Barrier Transverse Moment

	Due to PT	Due to Combined		New Dispersal Angle	
Distance from Barrier Top (mm)	FEA Max Negative Moment (kN*m/m)	FEA Max Negative Moment (kN*m/m)	Finite Differences	Improved Max Negative Moment(kN*m/m)	Finite Differences
0	0	-	-	0.00	0.00
180	23	-	-	31.68	8.68
360	42	-	-	69.42	27.42
540	73	-	-	115.12	42.12
720	101	-	-	171.62	70.62
870	230	-	-	230.00	0.00
sum/number of section =			-		21.26

Approximation:

Dispersal Angle = -25.1 Degree

Deck Transverse Moment due to PT

		New Dispersal Angle	
Distance from Barrier Base (mm)	FEA Max Negative Moment (kN*m/m)	Improved Max Negative Moment(kN*m/m)	Finite Differences
0	120	115.00	-5.00
150	61	69.76	8.76
300	46	50.07	4.07
450	36	39.05	3.05
600	32	32.00	0.00
sum/number of section =			2.18

Approximation:

Dispersal Angle = 70.2 Degree

Deck Transverse Moment due to PV

		No-Dispersion		New Dispersal Angle	
Distance from Barrier Base (mm)	FEA Max Negative Moment (kN*m/m)	Approximated Max Negative Moment(kN*m/m)	Finite Differences	Approximated Max Negative Moment(kN*m/m)	Finite Differences
0	0	0.00	0.00	0.00	0.00
150	1.7	1.39	-0.31	1.20	-0.50
300	2	2.78	0.78	2.11	0.11
450	2.7	4.17	1.47	2.82	0.12
600	3.4	5.56	2.16	3.40	0.00
sum/number of section =			0.82		-0.05

Approximation:

Dispersal Angle = 71.1 Degree

Deck Transverse Moment due to Combined loads

		Code Dispersal Angle		New Dispersal Angle	
Distance from Barrier Base (mm)	FEA Max Negative Moment (kN*m/m)	Approximated Max Negative Moment(kN*m/m)	Finite Differences	Approximated Max Negative Moment(kN*m/m)	Finite Differences
0	121	40.75	-80.25	115.00	-6.00
150	61	37.84	-23.16	70.96	9.96
300	48	35.75	-12.25	52.18	4.18
450	41	34.26	-6.74	41.87	0.87
600	38	33.24	-4.76	35.40	-2.60
sum/number of section =			-25.43		1.28

Table 23 - MME Approximation for PL-2 Internal Portion (thk250-oh1200-0.87)

MME Approximation for Performance Level 2 (thk250-oh1200-0.87)

Internal Portion .

Barrier Transverse Moment

	Due to PT	Due to Combined		New Dispersal Angle	
Distance from Barrier Top (mm)	FEA Max Negative Moment (kN*m/m)	FEA Max Negative Moment (kN*m/m)	Finite Differences	Improved Max Negative Moment(kN*m/m)	Finite Differences
0	0	-	-	0.00	0.00
180	22	-	-	31.51	9.51
360	41	-	-	68.58	27.58
540	71	-	-	112.82	41.82
720	98	-	-	166.56	68.56
870	221	-	-	221.00	0.00
sum/number of section =			-		21.07

Approximation:

Dispersal Angle = -23.6 Degree

Deck Transverse Moment due to PT

		New Dispersal Angle	
Distance from Barrier Base (mm)	FEA Max Negative Moment (kN*m/m)	Improved Max Negative Moment(kN*m/m)	Finite Differences
0	121	110.50	-10.50
225	54	58.13	4.13
450	37	39.43	2.43
675	28	29.84	1.84
900	24	24.00	0.00
sum/number of section =		-0.42	

Approximation:

Dispersal Angle = 69.5 Degree

110

Deck Transverse Moment due to PV

Distance from Barrier Base (mm)	FEA Max Negative Moment (kN*m/m)	No-Dispersion		New Dispersal Angle	
		Approximated Max Negative Moment(kN*m/m)	Finite Differences	Approximated Max Negative Moment(kN*m/m)	Finite Differences
0	0	0.00	0.00	0.00	0.00
225	2.1	2.09	-0.01	1.70	-0.40
450	2.6	4.17	1.57	2.88	0.28
675	3.6	6.26	2.66	3.74	0.14
900	4.4	8.35	3.95	4.40	0.00
sum/number of section =			1.63		0.01

Approximation:

Dispersal Angle = 69.9 Degree

Deck Transverse Moment due to Combined loads

Distance from Barrier Base (mm)	FEA Max Negative Moment (kN*m/m)	Code Dispersal Angle		New Dispersal Angle	
		Approximated Max Negative Moment(kN*m/m)	Finite Differences	Approximated Max Negative Moment(kN*m/m)	Finite Differences
0	122	40.75	-81.25	110.50	-11.50
225	55	36.70	-18.30	59.83	4.83
450	40	34.26	-5.74	42.32	2.32
675	33	32.87	-0.13	33.58	0.58
900	33	32.20	-0.80	28.40	-4.60
sum/number of section =			-21.24		-1.67

MME Approximation for Performance Level 2 (thk250-oh1500-0.87)

Internal Portion

Barrier Transverse Moment

	Due to PT	Due to Combined		New Dispersal Angle	
Distance from Barrier Top (mm)	FEA Max Negative Moment (kN*m/m)	FEA Max Negative Moment (kN*m/m)	Finite Differences	Improved Max Negative Moment(kN*m/m)	Finite Differences
0	0	-	-	0.00	0.00
180	24	-	-	31.57	7.57
360	41	-	-	68.86	27.86
540	71	-	-	113.60	42.60
720	98	-	-	168.26	70.26
870	224	-	-	224.00	0.00
sum/number of section	=		-		21.18

Approximation:

Dispersal Angle   =   -24.1   Degree

Deck Transverse Moment due to PT

		New Dispersal Angle	
Distance from Barrier Base (mm)	FEA Max Negative Moment (kN*m/m)	Improved Max Negative Moment(kN*m/m)	Finite Differences
0	120	112.00	-8.00
300	54	55.37	1.37
600	35	36.78	1.78
900	26	27.53	1.53
1200	22	22.00	0.00
sum/number of section	=		-0.66

Approximation:

Dispersal Angle   =   66.0   Degree

Deck Transverse Moment due to PV

		No-Dispersion		New Dispersal Angle	
Distance from Barrier Base (mm)	FEA Max Negative Moment (kN*m/m)	Approximated Max Negative Moment(kN*m/m)	Finite Differences	Approximated Max Negative Moment(kN*m/m)	Finite Differences
0	0	0.00	0.00	0.00	0.00
300	2.3	2.78	0.48	2.25	-0.05
600	3.5	5.56	2.06	3.77	0.27
900	4.7	8.35	3.65	4.87	0.17
1200	5.7	11.13	5.43	5.70	0.00
sum/number of section	=		2.32		0.08

Approximation:

Dispersal Angle	=		65.4	Degree

Deck Transverse Moment due to Combined loads

		Code Dispersal Angle		New Dispersal Angle	
Distance from Barrier Base (mm)	FEA Max Negative Moment (kN*m/m)	Approximated Max Negative Moment(kN*m/m)	Finite Differences	Approximated Max Negative Moment(kN*m/m)	Finite Differences
0	120	40.75	-79.25	112.00	-8.00
300	55	35.75	-19.25	57.62	2.62
600	40	33.24	-6.76	40.55	0.55
900	33	32.20	-0.80	32.40	-0.60
1200	31	32.08	1.08	27.70	-3.30
sum/number of section	=		-21.00		-1.75

113

MME Approximation for Performance Level 2 (thk250-oh1800-0.87)

Internal Portion

Barrier Transverse Moment

	Due to PT	Due to Combined		New Dispersal Angle	
Distance from Barrier Top (mm)	FEA Max Negative Moment (kN*m/m)	FEA Max Negative Moment (kN*m/m)	Finite Differences	Improved Max Negative Moment(kN*m/m)	Finite Differences
0	0	-	-	0.00	0.00
180	24	-	-	31.63	7.63
360	41	-	-	69.14	28.14
540	71	-	-	114.37	43.37
720	98	-	-	169.94	71.94
870	227	-	-	227.00	0.00
sum/number of section	=		-		21.58

Approximation:

Dispersal Angle   =   -24.6   Degree

Deck Transverse Moment due to PT

New Dispersal Angle

Distance from Barrier Base (mm)	FEA Max Negative Moment (kN*m/m)	Improved Max Negative Moment(kN*m/m)	Finite Differences
0	119	113.50	-5.50
375	49	50.59	1.59
750	31	32.55	1.55
1125	23	23.99	0.99
1500	19	19.00	0.00
sum/number of section	=		-0.27

Approximation:

Dispersal Angle   =   65.2   Degree

Deck Transverse Moment due to PV

Distance from Barrier Base (mm)	FEA Max Negative Moment (kN*m/m)	No-Dispersion		New Dispersal Angle	
		Approximated Max Negative Moment(kN*m/m)	Finite Differences	Approximated Max Negative Moment(kN*m/m)	Finite Differences
0	0	0.00	0.00	0.00	0.00
375	2.9	3.48	0.58	2.77	-0.13
750	4.4	6.95	2.55	4.61	0.21
1125	5.8	10.43	4.63	5.92	0.12
1500	6.9	13.91	7.01	6.90	0.00
sum/number of section	=		2.95		0.04

Approximation:

Dispersal Angle	=	61.8	Degree

Deck Transverse Moment due to Combined loads

Distance from Barrier Base (mm)	FEA Max Negative Moment (kN*m/m)	Code Dispersal Angle		New Dispersal Angle	
		Approximated Max Negative Moment(kN*m/m)	Finite Differences	Approximated Max Negative Moment(kN*m/m)	Finite Differences
0	119	40.75	-78.25	113.50	-5.50
375	55	34.94	-20.06	53.37	-1.63
750	40	32.58	-7.42	37.16	-2.84
1125	33	32.05	-0.95	29.91	-3.09
1500	29	32.60	3.60	25.90	-3.10
sum/number of section	=		-20.62		-3.23

Appendix G: FEA Results and MMDA Spreadsheet for

PL-2 End Portion

Table 26 - MME Approximation for PL-2 End Portion (thk250-oh600-0.87)

MME Approximation for Performance Level 2 (thk250-oh600-0.87)

End Portion

Barrier Transverse Moment

Distance from Barrier Top (mm)	Due to PT FEA Max Negative Moment (kN*m/m)	Due to Combined FEA Max Negative Moment (kN*m/m)	Finite Differences	New Dispersal Angle Improved Max Negative Moment(kN*m/m)	Finite Differences
0	0	-	-	0.00	0.00
180	28	-	-	28.50	0.50
360	46	-	-	55.77	9.77
540	59	-	-	81.88	22.88
720	59	-	-	106.92	47.92
870	127	-	-	127.00	0.00
			-		11.58

Dispersal Angle	=	7.5 Degree

Deck Transverse Moment due to PT

		New Dispersal Angle	
Distance from Barrier Base (mm)	FEA Max Negative Moment (kN*m/m)	Improved Max Negative Moment(kN*m/m)	Finite Differences
0	66	63.50	-2.50
75	67	63.87	-3.13
150	65	64.24	-0.76
225	63	64.62	1.62
300	65	65.00	0.00
			-0.95

Dispersal Angle	=	-10.2 Degree

Deck Transverse Moment due to PV

Distance from Barrier Base (mm)	FEA Max Negative Moment (kN*m/m)	No-Dispersion		New Dispersal Angle	
		Approximated Max Negative Moment(kN*m/m)	Finite Differences	Approximated Max Negative Moment(kN*m/m)	Finite Differences
0	0	0.00	0.00	0.00	0.00
75	0.4	0.70	0.30	0.70	0.30
150	1	1.39	0.39	1.42	0.42
225	1.9	2.09	0.19	2.15	0.25
300	2.9	2.78	-0.12	2.90	0.00
			0.15		0.19

Dispersal Angle   =   -36.7 Degree

Deck Transverse Moment due to Combined loads

Distance from Barrier Base (mm)	FEA Max Negative Moment (kN*m/m)	Code Dispersal Angle		New Dispersal Angle	
		Approximated Max Negative Moment(kN*m/m)	Finite Differences	Approximated Max Negative Moment(kN*m/m)	Finite Differences
0	68	64.52	-3.48	63.50	-4.50
75	67	62.33	-4.67	64.57	-2.43
150	66	60.39	-5.61	65.66	-0.34
225	66	58.67	-7.33	66.77	0.77
300	71	57.14	-13.86	67.90	-3.10
			-6.99		-1.92

Table 27 - MME Approximation for PL-2 End Portion (thk250-oh900-0.87)

MME Approximation for Performance Level 2 (thk250-oh900-0.87)

End Portion

Barrier Transverse Moment

	Due to PT	Due to Combined		New Dispersal Angle	
Distance from Barrier Top (mm)	FEA Max Negative Moment (kN*m/m)	FEA Max Negative Moment (kN*m/m)	Finite Differences	Improved Max Negative Moment(kN*m/m)	Finite Differences
0	0	-	-	0.00	0.00
180	25	-	-	29.78	4.78
360	43	-	-	60.88	17.88
540	55	-	-	93.39	38.39
720	61	-	-	127.41	66.41
870	157	-	-	157.00	0.00
			-		18.21

Dispersal Angle	=	-7.1 Degree

Deck Transverse Moment due to PT

		New Dispersal Angle	
Distance from Barrier Base (mm)	FEA Max Negative Moment (kN*m/m)	Improved Max Negative Moment(kN*m/m)	Finite Differences
0	75	78.50	3.50
150	65	72.13	7.13
300	63	66.71	3.71
450	59	62.05	3.05
600	58	58.00	0.00
			3.48

Dispersal Angle	=	48.0 Degree

Deck Transverse Moment due to PV

Distance from Barrier Base (mm)	FEA Max Negative Moment (kN*m/m)	No-Dispersion		New Dispersal Angle	
		Approximated Max Negative Moment(kN*m/m)	Finite Differences	Approximated Max Negative Moment(kN*m/m)	Finite Differences
0	0	0.00	0.00	0.00	0.00
150	1.2	1.39	0.19	1.41	0.21
300	2.7	2.78	0.08	2.84	0.14
450	4.2	4.17	-0.03	4.30	0.10
600	5.8	5.56	-0.24	5.80	0.00
			0.00		0.09

Dispersal Angle   =   -20.5   Degree

Deck Transverse Moment due to Combined loads

Distance from Barrier Base (mm)	FEA Max Negative Moment (kN*m/m)	Code Dispersal Angle		New Dispersal Angle	
		Approximated Max Negative Moment(kN*m/m)	Finite Differences	Approximated Max Negative Moment(kN*m/m)	Finite Differences
0	83	64.52	-18.48	78.50	-4.50
150	64	60.39	-3.61	73.53	9.53
300	65	57.14	-7.86	69.55	4.55
450	67	54.56	-12.44	66.36	-0.64
600	68	52.53	-15.47	63.80	-4.20
			-11.57		0.95

Table 28 - MME Approximation for PL-2 End Portion (thk250-oh1200-0.87)

MME Approximation for Performance Level 2 (thk250-oh1200-0.87)

End Portion

Barrier Transverse Moment

Distance from Barrier Top (mm)	Due to PT — FEA Max Negative Moment (kN*m/m)	Due to Combined — FEA Max Negative Moment (kN*m/m)	Finite Differences	New Dispersal Angle — Improved Max Negative Moment(kN*m/m)	Finite Differences
0	0	-	-	0.00	0.00
180	24	-	-	30.46	6.46
360	40	-	-	63.79	23.79
540	59	-	-	100.44	41.44
720	56	-	-	140.90	84.90
870	178	-	-	178.00	0.00
			-		22.37

Dispersal Angle = -14.1 Degree

Deck Transverse Moment due to PT

Distance from Barrier Base (mm)	FEA Max Negative Moment (kN*m/m)	New Dispersal Angle — Improved Max Negative Moment(kN*m/m)	Finite Differences
0	84	89.00	5.00
150	57	75.56	18.56
300	55	65.65	10.65
450	53	58.03	5.03
600	52	52.00	0.00
			7.85

Dispersal Angle = 63.1 Degree

Deck Transverse Moment due to PV

Distance from Barrier Base (mm)	FEA Max Negative Moment (kN*m/m)	No-Dispersion		New Dispersal Angle	
		Approximated Max Negative Moment(kN*m/m)	Finite Differences	Approximated Max Negative Moment(kN*m/m)	Finite Differences
0	0	0.00	0.00	0.00	0.00
150	1.3	1.39	0.09	1.51	0.21
300	3.1	2.78	-0.32	3.28	0.18
450	5.4	4.17	-1.23	5.41	0.01
600	8	5.56	-2.44	8.00	0.00
			-0.78		0.08

Dispersal Angle = -70.3 Degree

Deck Transverse Moment due to Combined loads

Distance from Barrier Base (mm)	FEA Max Negative Moment (kN*m/m)	Code Dispersal Angle		New Dispersal Angle	
		Approximated Max Negative Moment(kN*m/m)	Finite Differences	Approximated Max Negative Moment(kN*m/m)	Finite Differences
0	97	64.52	-32.48	89.00	-8.00
150	62	60.39	-1.61	77.06	15.06
300	63	57.14	-5.86	68.93	5.93
450	66	54.56	-11.44	63.44	-2.56
600	68	52.53	-15.47	60.00	-8.00
			-13.37		0.49

Table 29 - MME Approximation for PL-2 End Portion (thk250-oh1500-0.87)

MME Approximation for Performance Level 2 (thk250-oh1500-0.87)

End Portion

Barrier Transverse Moment

	Due to PT	Due to Combined		New Dispersal Angle	
Distance from Barrier Top (mm)	FEA Max Negative Moment (kN*m/m)	FEA Max Negative Moment (kN*m/m)	Finite Differences	Improved Max Negative Moment(kN*m/m)	Finite Differences
0	0	-	-	0.00	0.00
180	22	-	-	31.02	9.02
360	37	-	-	66.30	29.30
540	59	-	-	106.80	47.80
720	55	-	-	153.75	98.75
870	199	-	-	199.00	0.00
			-		26.41

Dispersal Angle = -19.4 Degree

Deck Transverse Moment due to PT

		New Dispersal Angle	
Distance from Barrier Base (mm)	FEA Max Negative Moment (kN*m/m)	Improved Max Negative Moment(kN*m/m)	Finite Differences
0	88	99.50	11.50
150	61	77.78	16.78
300	55	63.84	8.84
450	49	54.14	5.14
600	47	47.00	0.00
			8.45

Dispersal Angle = 70.1 Degree

Deck Transverse Moment due to PV					
		No-Dispersion		New Dispersal Angle	
Distance from Barrier Base (mm)	FEA Max Negative Moment (kN*m/m)	Approximated Max Negative Moment(kN*m/m)	Finite Differences	Approximated Max Negative Moment(kN*m/m)	Finite Differences
0	0	0.00	0.00	0.00	0.00
150	2	1.39	-0.61	1.59	-0.41
300	3.4	2.78	-0.62	3.69	0.29
450	6.7	4.17	-2.53	6.63	-0.07
600	11	5.56	-5.44	11.00	0.00
			-1.84		-0.04

Dispersal Angle   =   -77.6 Degree

Deck Transverse Moment due to Combined loads					
		Code Dispersal Angle		New Dispersal Angle	
Distance from Barrier Base (mm)	FEA Max Negative Moment (kN*m/m)	Approximated Max Negative Moment(kN*m/m)	Finite Differences	Approximated Max Negative Moment(kN*m/m)	Finite Differences
0	106	64.52	-41.48	99.50	-6.50
150	51	60.39	9.39	79.37	28.37
300	52	57.14	5.14	67.54	15.54
450	55	54.56	-0.44	60.77	5.77
600	66	52.53	-13.47	58.00	-8.00
			-8.17		7.04

Table 30 - MME Approximation for PL-2 End Portion (thk250-oh1800-0.87)

MME Approximation for Performance Level 2 (thk250-oh1800-0.87)					
End Portion					
Barrier Transverse Moment					
	Due to PT	Due to Combined		*New Dispersal Angle*	
Distance from Barrier Top (mm)	FEA Max Negative Moment (kN*m/m)	FEA Max Negative Moment (kN*m/m)	Finite Differences	Improved Max Negative Moment(kN*m/m)	Finite Differences
0	0	-	-	0.00	0.00
180	26	-	-	31.42	5.42
360	41	-	-	68.19	27.19
540	57	-	-	111.77	54.77
720	71	-	-	164.28	93.28
870	217	-	-	217.00	0.00
			-		25.81
Dispersal Angle	=		-23.0	Degree	

Deck Transverse Moment due to PT			
New Dispersal Angle			
Distance from Barrier Base (mm)	FEA Max Negative Moment (kN*m/m)	Improved Max Negative Moment(kN*m/m)	Finite Differences
0	91	108.50	17.50
150	45	77.73	32.73
300	44	60.56	16.56
450	44	49.60	5.60
600	42	42.00	0.00
			14.48
Dispersal Angle	=	74.5	Degree

Deck Transverse Moment due to PV					
		No-Dispersion		*New Dispersal Angle*	
Distance from Barrier Base (mm)	FEA Max Negative Moment (kN*m/m)	Approximated Max Negative Moment(kN*m/m)	Finite Differences	Approximated Max Negative Moment(kN*m/m)	Finite Differences
0	0	0.00	0.00	0.00	0.00
150	1.5	1.39	-0.11	1.64	0.14
300	3.7	2.78	-0.92	3.98	0.28
450	7.5	4.17	-3.33	7.61	0.11
600	14	5.56	-8.44	14.00	0.00
			-2.56		0.11

Dispersal Angle = -79.7 Degree

Deck Transverse Moment due to Combined loads					
		Code Dispersal Angle		*New Dispersal Angle*	
Distance from Barrier Base (mm)	FEA Max Negative Moment (kN*m/m)	Approximated Max Negative Moment(kN*m/m)	Finite Differences	Approximated Max Negative Moment(kN*m/m)	Finite Differences
0	112	64.52	-47.48	108.50	-3.50
150	65	60.39	-4.61	79.37	14.37
300	63	57.14	-5.86	64.54	1.54
450	62	54.56	-7.44	57.21	-4.79
600	62	52.53	-9.47	56.00	-6.00
			-14.97		0.32

Appendix H: FEA Results and MMDA Spreadsheet for

PL-3 Inner Portion

MME Approximation for Performance Level 3 (thk275-oh600-1.07)

Internal Portion

Barrier Transverse Moment

	Due to PT	Due to Combined		New Dispersal Angle	
Distance from Barrier Top (mm)	FEA Max Negative Moment (kN*m/m)	FEA Max Negative Moment (kN*m/m)	Finite Differences	Improved Max Negative Moment(kN*m/m)	Finite Differences
0	0	-	-	0.00	0.00
180	17.1	-	-	24.55	7.45
360	37.5	-	-	45.33	7.83
540	56.7	-	-	63.14	6.44
720	72.9	-	-	78.58	5.68
900	87.1	-	-	92.10	5.00
1070	103.4	-	-	103.40	0.00
sum/number of section =			-		4.63

Approximation:

Dispersal Angle   =   31.2   Degree

Deck Transverse Moment due to PT

		New Dispersal Angle	
Distance from Barrier Base (mm)	FEA Max Negative Moment (kN*m/m)	Improved Max Negative Moment(kN*m/m)	Finite Differences
0	103.4	103.40	0.00
75	91.4	89.41	-1.99
150	82.7	78.76	-3.94
225	73.3	70.37	-2.93
300	63.6	63.60	0.00
sum/number of section =			-1.77

Approximation:

Dispersal Angle   =   75.5   Degree

128

Deck Transverse Moment due to PV

Distance from Barrier Base (mm)	FEA Max Negative Moment (kN*m/m)	No-Dispersion		New Dispersal Angle	
		Approximated Max Negative Moment(kN*m/m)	Finite Differences	Approximated Max Negative Moment(kN*m/m)	Finite Differences
0	0	0.00	0.00	0.00	0.00
75	0.87	0.96	0.09	0.95	0.08
150	1.83	1.91	0.08	1.88	0.05
225	2.8	2.87	0.07	2.80	0.00
300	3.7	3.83	0.13	3.70	0.00
sum/number of section	=		0.07		0.03

Approximation:

Dispersal Angle	=		34.1	Degree

Deck Transverse Moment due to Combined loads

Distance from Barrier Base (mm)	FEA Max Negative Moment (kN*m/m)	Code Dispersal Angle		New Dispersal Angle	
		Approximated Max Negative Moment(kN*m/m)	Finite Differences	Approximated Max Negative Moment(kN*m/m)	Finite Differences
0	103.6	88.28	-15.32	103.40	-0.20
75	92.3	86.08	-6.22	90.36	-1.94
150	84.6	84.09	-0.51	80.64	-3.96
225	76.2	82.29	6.09	73.17	-3.03
300	67.5	80.68	13.18	67.30	-0.20
sum/number of section	=		-0.56		-1.87

Table 32 - MME Approximation for PL-3 Internal Portion (thk275-oh900-1.07)

MME Approximation for Performance Level 3 (thk275-oh900-1.07)					
Barrier Transverse Moment					
	Due to PT	Due to Combined		*New Dispersal Angle*	
Distance from Barrier Top (mm)	FEA Max Negative Moment (kN*m/m)	FEA Max Negative Moment (kN*m/m)	Finite Differences	Improved Max Negative Moment(kN*m/m)	Finite Differences
0	0	-	-	0.00	0.00
180	17.2	-	-	24.58	7.38
360	37.6	-	-	45.42	7.82
540	56.9	-	-	63.33	6.43
720	73.4	-	-	78.87	5.47
900	87.7	-	-	92.49	4.79
1070	103.9	-	-	103.90	0.00
sum/number of section	=		-		4.56

Approximation:

Dispersal Angle = 30.8 Degree

Deck Transverse Moment due to PT			
New Dispersal Angle			
Distance from Barrier Base (mm)	FEA Max Negative Moment (kN*m/m)	Improved Max Negative Moment(kN*m/m)	Finite Differences
0	103.9	103.90	0.00
150	85.6	76.49	-9.11
300	70.5	60.53	-9.97
450	56.3	50.07	-6.23
600	42.7	42.70	0.00
sum/number of section	=		-5.06

Approximation:

Dispersal Angle = 77.2 Degree

Deck Transverse Moment due to PV

Distance from Barrier Base (mm)	FEA Max Negative Moment (kN*m/m)	No-Dispersion		New Dispersal Angle	
		Approximated Max Negative Moment(kN*m/m)	Finite Differences	Approximated Max Negative Moment(kN*m/m)	Finite Differences
0	0	0.00	0.00	0.00	0.00
150	1.68	1.91	0.23	1.88	0.20
300	3.5	3.83	0.33	3.71	0.21
450	5.4	5.74	0.34	5.48	0.08
600	7.2	7.65	0.45	7.20	0.00
sum/number of section	=		0.27		0.10

Approximation:

Dispersal Angle = 32.0 Degree

Deck Transverse Moment due to Combined loads

Distance from Barrier Base (mm)	FEA Max Negative Moment (kN*m/m)	Code Dispersal Angle		New Dispersal Angle	
		Approximated Max Negative Moment(kN*m/m)	Finite Differences	Approximated Max Negative Moment(kN*m/m)	Finite Differences
0	103.9	88.28	-15.62	103.90	0.00
150	87.3	84.09	-3.21	78.38	-8.92
300	74	80.68	6.68	64.23	-9.77
450	61.8	77.92	16.12	55.55	-6.25
600	50.1	75.70	25.60	49.90	-0.20
sum/number of section	=		5.91		-5.03

Table 33 - MME Approximation for PL-3 Internal Portion (thk275-oh1200-1.07)

MME Approximation for Performance Level 3 (thk275-oh1200-1.07)

Barrier Transverse Moment

	Due to PT	Due to Combined		New Dispersal Angle	
Distance from Barrier Top (mm)	FEA Max Negative Moment (kN*m/m)	FEA Max Negative Moment (kN*m/m)	Finite Differences	Improved Max Negative Moment(kN*m/m)	Finite Differences
0	0	0	0	0.00	0.00
180	17.2	17.1	-0.1	24.51	7.31
360	37.5	37.4	-0.1	45.21	7.71
540	56.7	56.6	-0.1	62.92	6.22
720	73	72.9	-0.1	78.24	5.24
900	87	86.9	-0.1	91.62	4.62
1070	102.8	102.7	-0.1	102.80	0.00
sum/number of section	=		-0.09		4.44

Approximation:

Dispersal Angle	=	31.6	Degree

Deck Transverse Moment due to PT

New Dispersal Angle

Distance from Barrier Base (mm)	FEA Max Negative Moment (kN*m/m)	Improved Max Negative Moment(kN*m/m)	Finite Differences
0	102.8	102.80	0.00
150	86.8	75.65	-11.15
300	74.3	59.84	-14.46
450	62.9	49.50	-13.40
600	52.4	42.21	-10.19
750	42.4	36.79	-5.61
900	32.6	32.60	0.00
sum/number of section	=		-7.83

Approximation:

Dispersal Angle	=	77.3	Degree

Deck Transverse Moment due to PV

		No-Dispersion		New Dispersal Angle	
Distance from Barrier Base (mm)	FEA Max Negative Moment (kN*m/m)	Approximated Max Negative Moment(kN*m/m)	Finite Differences	Approximated Max Negative Moment(kN*m/m)	Finite Differences
0	0	0.00	0.00	0.00	0.00
150	1.6	1.91	0.31	1.89	0.29
300	3.4	3.83	0.43	3.73	0.33
450	5.2	5.74	0.54	5.54	0.34
600	7	7.65	0.65	7.30	0.30
750	8.9	9.56	0.66	9.02	0.12
900	10.7	11.48	0.78	10.70	0.00
sum/number of section =			0.48		0.20

Approximation:

Dispersal Angle   =   25.8   Degree

Deck Transverse Moment due to Combined loads

		Code Dispersal Angle		New Dispersal Angle	
Distance from Barrier Base (mm)	FEA Max Negative Moment (kN*m/m)	Approximated Max Negative Moment(kN*m/m)	Finite Differences	Approximated Max Negative Moment(kN*m/m)	Finite Differences
0	102.7	88.28	-14.42	102.80	0.10
150	88.5	84.09	-4.41	77.54	-10.96
300	77.7	80.68	2.98	63.58	-14.12
450	68	77.92	9.92	55.04	-12.96
600	59.4	75.70	16.30	49.51	-9.89
750	51.2	73.92	22.72	45.81	-5.39
900	43.2	72.52	29.32	43.30	0.10
sum/number of section =			8.92		-7.59

Table 34 - MME Approximation for PL-3 Internal Portion (thk275-oh1500-1.07)

MME Approximation for Performance Level 3 (thk275-oh1500-1.07)

Barrier Transverse Moment

	Due to PT	Due to Combined		New Dispersal Angle	
Distance from Barrier Top (mm)	FEA Max Negative Moment (kN*m/m)	FEA Max Negative Moment (kN*m/m)	Finite Differences	Improved Max Negative Moment(kN*m/m)	Finite Differences
0	0	-	-	0.00	0.00
180	17	-	-	24.42	7.42
360	37.3	-	-	44.88	7.58
540	56.3	-	-	62.28	5.98
720	72.3	-	-	77.25	4.95
900	85.8	-	-	90.27	4.47
1070	101.1	-	-	101.10	0.00
sum/number of section	=				4.34

Approximation:

Dispersal Angle	=		32.8	Degree	

Deck Transverse Moment due to PT

New Dispersal Angle

Distance from Barrier Base (mm)	FEA Max Negative Moment (kN*m/m)	Improved Max Negative Moment(kN*m/m)	Finite Differences
0	101.1	101.10	0.00
150	86.5	74.28	-12.22
300	75.5	58.71	-16.79
450	65.6	48.53	-17.07
600	56.8	41.36	-15.44
750	48.6	36.04	-12.56
900	41	31.93	-9.07
1050	33.5	28.66	-4.84
1200	26	26.00	0.00
sum/number of section	=		-9.78

Approximation:

Dispersal Angle	=		77.6	Degree

Deck Transverse Moment due to PV

Distance from Barrier Base (mm)	FEA Max Negative Moment (kN*m/m)	No-Dispersion		New Dispersal Angle	
		Approximated Max Negative Moment(kN*m/m)	Finite Differences	Approximated Max Negative Moment(kN*m/m)	Finite Differences
0	0	0.00	0.00	0.00	0.00
150	1.5	1.91	0.41	1.89	0.39
300	3.3	3.83	0.53	3.74	0.44
450	5.1	5.74	0.64	5.54	0.44
600	6.9	7.65	0.75	7.31	0.41
750	8.6	9.56	0.96	9.04	0.44
900	10.4	11.48	1.08	10.73	0.33
1050	12.2	13.39	1.19	12.38	0.18
1200	14	15.30	1.30	14.00	0.00
sum/number of section =			0.48		0.29

Approximation:

Dispersal Angle   =   24.9   Degree

Deck Transverse Moment due to Combined loads

Distance from Barrier Base (mm)	FEA Max Negative Moment (kN*m/m)	Code Dispersal Angle		Combined Modifications	
		Approximated Max Negative Moment(kN*m/m)	Finite Differences	Approximated Max Negative Moment(kN*m/m)	Finite Differences
0	100.9	88.28	-12.62	101.10	0.20
150	88.1	84.09	-4.01	76.17	-11.93
300	78.8	80.68	1.88	62.45	-16.35
450	70.7	77.92	7.22	54.08	-16.62
600	63.6	75.70	12.10	48.67	-14.93
750	57.2	73.92	16.72	45.08	-12.12
900	51.3	72.52	21.22	42.66	-8.64
1050	45.6	71.45	25.85	41.04	-4.56
1200	40	70.66	30.66	40.00	0.00
sum/number of section =			4.72		-9.44

MME Approximation for Performance Level 3 (thk275-oh1800-1.07)

Barrier Transverse Moment

	Due to PT	Due to Combined		*New Dispersal Angle*	
Distance from Barrier Top (mm)	FEA Max Negative Moment (kN*m/m)	FEA Max Negative Moment (kN*m/m)	Finite Differences	Improved Max Negative Moment(kN*m/m)	Finite Differences
0	0	-	-	0.00	0.00
180	17.1	-	-	24.31	7.21
360	37.2	-	-	44.52	7.32
540	56	-	-	61.59	5.59
720	72.2	-	-	76.19	3.99
900	85.1	-	-	88.83	3.73
1070	99.3	-	-	99.30	0.00
sum/number of section	=				3.98

Approximation:

Dispersal Angle	=	34.1	Degree

Deck Transverse Moment due to PT

New Dispersal Angle

Distance from Barrier Base (mm)	FEA Max Negative Moment (kN*m/m)	Improved Max Negative Moment(kN*m/m)	Finite Differences
0	99.3	99.30	0.00
300	76.1	59.29	-16.81
600	59.6	42.26	-17.34
900	45.9	32.83	-13.07
1200	33.9	26.84	-7.06
1500	22.7	22.70	0.00
sum/number of section	=		-9.05

Approximation:

Dispersal Angle	=	77.0	Degree

Deck Transverse Moment due to PV

		No-Dispersion		New Dispersal Angle	
Distance from Barrier Base (mm)	FEA Max Negative Moment (kN*m/m)	Approximated Max Negative Moment(kN*m/m)	Finite Differences	Approximated Max Negative Moment(kN*m/m)	Finite Differences
0	0	0.00	0.00	0.00	0.00
300	3.3	3.83	0.53	3.73	0.43
600	6.7	7.65	0.95	7.29	0.59
900	10.1	11.48	1.38	10.67	0.57
1200	13.6	15.30	1.70	13.91	0.31
1500	17	19.13	2.13	17.00	0.00
sum/number of section	=		1.1125		0.32

Approximation:

Dispersal Angle	=	26.6	Degree

Deck Transverse Moment due to Combined loads

		Code Dispersal Angle		Combined Modifications	
Distance from Barrier Base (mm)	FEA Max Negative Moment (kN*m/m)	Approximated Max Negative Moment(kN*m/m)	Finite Differences	Approximated Max Negative Moment(kN*m/m)	Finite Differences
0	99.1	88.28	-10.82	99.30	0.20
300	79.4	80.68	1.28	63.02	-16.38
600	66.2	75.70	9.50	49.55	-16.65
900	56	72.52	16.52	43.51	-12.49
1200	47.5	70.66	23.16	40.75	-6.75
1500	39.8	69.76	29.96	39.70	-0.10
sum/number of section	=		11.60		-8.70

Appendix I: FEA Results and MMDA Spreadsheet for PL-

3 End Portion

Table 36 - MME Approximation for PL-3 End Portion (thk275-oh600-1.07)

MME Approximation for Performance Level 3 (thk275-oh600-1.07)					
End Portion					
Barrier Transverse Moment					
	Due to PT	Due to Combined		*New Dispersal Angle*	
Distance from Barrier Top (mm)	FEA Max Negative Moment (kN*m/m)	FEA Max Negative Moment (kN*m/m)	Finite Differences	Improved Max Negative Moment(kN*m/m)	Finite Differences
0	0	-	-	0.00	0.00
180	22.4	-	-	25.73	3.33
360	46.6	-	-	49.53	2.93
540	68.5	-	-	71.60	3.10
720	87	-	-	92.13	5.13
900	107	-	-	111.27	4.27
1070	128.2	-	-	128.20	0.00
			-		2.68
Dispersal Angle	=		28.4	Degree	
Deck Transverse Moment due to PT					
New Dispersal Angle					
Distance from Barrier Base (mm)	FEA Max Negative Moment (kN*m/m)	Improved Max Negative Moment(kN*m/m)	Finite Differences		
0	128.2	128.20	0.00		
75	123	126.05	3.05		
150	120	123.96	3.96		
225	120	121.95	1.95		
300	120	120.00	0.00		
			1.79		
Dispersal Angle	=		34.2	Degree	

Deck Transverse Moment due to PV					
		No-Dispersion		*New Dispersal Angle*	
Distance from Barrier Base (mm)	FEA Max Negative Moment (kN*m/m)	Approximated Max Negative Moment(kN*m/m)	Finite Differences	Approximated Max Negative Moment(kN*m/m)	Finite Differences
0	0	0.00	0.00	0.00	0.00
75	1.05	0.96	-0.09	0.98	-0.07
150	2.08	1.91	-0.17	2.02	-0.06
225	3.19	2.87	-0.32	3.13	-0.06
300	4.3	3.83	-0.48	4.30	0.00
			-0.21		-0.04

Dispersal Angle = -77.2 Degree

Deck Transverse Moment due to Combined loads					
		Code Dispersal Angle		*New Dispersal Angle*	
Distance from Barrier Base (mm)	FEA Max Negative Moment (kN*m/m)	Approximated Max Negative Moment(kN*m/m)	Finite Differences	Approximated Max Negative Moment(kN*m/m)	Finite Differences
0	127.9	106.45	-21.45	128.20	0.30
75	123.4	105.23	-18.17	127.03	3.63
150	122.9	104.09	-18.81	125.99	3.09
225	126	103.04	-22.96	125.08	-0.92
300	129	102.06	-26.94	124.30	-4.70
			-21.66		0.28

Table 37 - MME Approximation for PL-3 End Portion (thk275-oh900-1.07)

MME Approximation for Performance Level 3 (thk275-oh900-1.07)

Barrier Transverse Moment

Distance from Barrier Top (mm)	Due to PT FEA Max Negative Moment (kN*m/m)	Due to Combined FEA Max Negative Moment (kN*m/m)	Finite Differences	New Dispersal Angle Improved Max Negative Moment(kN*m/m)	Finite Differences
0	0	-	-	0.00	0.00
180	22	-	-	25.59	3.59
360	45.9	-	-	49.03	3.13
540	67.3	-	-	70.56	3.26
720	85.8	-	-	90.41	4.61
900	104.5	-	-	108.78	4.28
1070	124.9	-	-	124.90	0.00
			-		2.69

Dispersal Angle	=		31.6	Degree

Deck Transverse Moment due to PT

New Dispersal Angle

Distance from Barrier Base (mm)	FEA Max Negative Moment (kN*m/m)	Improved Max Negative Moment(kN*m/m)	Finite Differences
0	124.9	124.90	0.00
150	106.77	118.76	11.99
300	106.66	113.20	6.54
450	104.55	108.13	3.58
600	103.5	103.50	0.00
			4.42

Dispersal Angle	=		46.5	Degree

Deck Transverse Moment due to PV					
		No-Dispersion		*New Dispersal Angle*	
Distance from Barrier Base (mm)	FEA Max Negative Moment (kN*m/m)	Approximated Max Negative Moment(kN*m/m)	Finite Differences	Approximated Max Negative Moment(kN*m/m)	Finite Differences
0	0	0.00	0.00	0.00	0.00
150	2.05	1.91	-0.14	1.97	-0.08
300	4.11	3.83	-0.29	4.05	-0.06
450	6.27	5.74	-0.53	6.25	-0.02
600	8.59	7.65	-0.94	8.59	0.00
			-0.38		-0.03

Dispersal Angle = -65.44 Degree

Deck Transverse Moment due to Combined loads					
		Code Dispersal Angle		*Combined Modifications*	
Distance from Barrier Base (mm)	FEA Max Negative Moment (kN*m/m)	Approximated Max Negative Moment(kN*m/m)	Finite Differences	Approximated Max Negative Moment(kN*m/m)	Finite Differences
0	123.7	106.45	-17.25	124.90	1.20
150	115.8	104.09	-11.71	120.73	4.93
300	111.86	102.06	-9.80	117.24	5.38
450	114.7	100.33	-14.37	114.38	-0.32
600	118.8	98.85	-19.95	112.09	-6.71
			-14.6		0.90

142

Table 38 - MME Approximation for PL-3 End Portion (thk275-oh1200-1.07)

MME Approximation for Performance Level 3 (thk275-oh1200-1.07)

Barrier Transverse Moment

	Due to PT	Due to Combined		New Dispersal Angle	
Distance from Barrier Top (mm)	FEA Max Negative Moment (kN*m/m)	FEA Max Negative Moment (kN*m/m)	Finite Differences	Improved Max Negative Moment(kN*m/m)	Finite Differences
0	0	0	0	0.00	0.00
180	21.5	21.2	-0.3	25.62	4.12
360	45.7	45	-0.7	49.12	3.42
540	67.5	65.7	-1.8	70.75	3.25
720	85.5	84.7	-0.8	90.73	5.23
900	104	103	-1	109.23	5.23
1070	125.5	123	-2.5	125.50	0.00
			-1.01		3.03

Dispersal Angle	=	31.0	Degree

Deck Transverse Moment due to PT

		New Dispersal Angle	
Distance from Barrier Base (mm)	FEA Max Negative Moment (kN*m/m)	Improved Max Negative Moment(kN*m/m)	Finite Differences
0	125.5	125.50	0.00
150	114	118.32	4.32
300	106	111.92	5.92
450	105	106.17	1.17
600	101	100.99	-0.01
750	95	96.28	1.28
900	92	92.00	0.00
			1.81

Dispersal Angle	=	50.9	Degree

		Deck Transverse Moment due to PV				
		No-Dispersion			*New Dispersal Angle*	
Distance from Barrier Base (mm)	FEA Max Negative Moment (kN*m/m)	Approximated Max Negative Moment(kN*m/m)	Finite Differences		Approximated Max Negative Moment(kN*m/m)	Finite Differences
0	0	0.00	0.00		0.00	0.00
150	2	1.91	-0.09		1.95	-0.05
300	4.03	3.83	-0.21		3.98	-0.05
450	6.13	5.74	-0.39		6.09	-0.04
600	8.32	7.65	-0.67		8.30	-0.02
750	10.57	9.56	-1.01		10.60	0.03
900	13	11.48	-1.53		13.00	0.00
			-0.56			-0.02

Dispersal Angle	=	-57.4	Degree

		Deck Transverse Moment due to Combined loads				
		Code Dispersal Angle			*Combined Modifications*	
Distance from Barrier Base (mm)	FEA Max Negative Moment (kN*m/m)	Approximated Max Negative Moment(kN*m/m)	Finite Differences		Approximated Max Negative Moment(kN*m/m)	Finite Differences
0	123	106.45	-16.55		125.50	2.50
150	115	104.09	-10.91		120.27	5.27
300	110	102.06	-7.94		115.90	5.90
450	112	100.33	-11.67		112.26	0.26
600	114	98.85	-15.15		109.28	-4.72
750	111	97.61	-13.39		106.88	-4.12
900	113	96.58	-16.42		105.00	-8.00
			-13.14			-0.41

Table 39 - MME Approximation for PL-3 End Portion (thk275-oh1500-1.07)

MME Approximation for Performance Level 3 (thk275-oh1500-1.07)

Barrier Transverse Moment

	Due to PT	Due to Combined		New Dispersal Angle	
Distance from Barrier Top (mm)	FEA Max Negative Moment (kN*m/m)	FEA Max Negative Moment (kN*m/m)	Finite Differences	Improved Max Negative Moment(kN*m/m)	Finite Differences
0	0	-	-	0.00	0.00
180	21.7	-	-	25.60	3.90
360	45.3	-	-	49.04	3.74
540	67.1	-	-	70.59	3.49
720	84.7	-	-	90.46	5.76
900	103.5	-	-	108.85	5.35
1070	125	-	-	125.00	0.00
					3.18

Dispersal Angle	=	31.5 Degree

Deck Transverse Moment due to PT

		New Dispersal Angle	
Distance from Barrier Base (mm)	FEA Max Negative Moment (kN*m/m)	Improved Max Negative Moment(kN*m/m)	Finite Differences
0	125	125.00	0.00
150	112.4	116.79	4.39
300	103.7	109.59	5.89
450	101.3	103.23	1.93
600	98	97.56	-0.44
750	93.8	92.49	-1.31
900	89.1	87.91	-1.19
1050	82.8	83.77	0.97
1200	80	80.00	0.00
			1.14

Dispersal Angle	=	55.1 Degree

Deck Transverse Moment due to PV

Distance from Barrier Base (mm)	FEA Max Negative Moment (kN*m/m)	No-Dispersion		Modification Factor	
		Approximated Max Negative Moment(kN*m/m)	Finite Differences	Approximated Max Negative Moment(kN*m/m)	Finite Differences
0	0	0.00	0.00	0.00	0.00
150	1.8	1.91	0.11	1.94	0.14
300	3.9	3.83	-0.07	3.95	0.05
450	6	5.74	-0.26	6.02	0.02
600	8.3	7.65	-0.65	8.16	-0.14
750	10.5	9.56	-0.94	10.38	-0.12
900	12.6	11.48	-1.13	12.67	0.07
1050	14.8	13.39	-1.41	15.04	0.24
1200	17.5	15.30	-2.20	17.50	0.00
			-0.33		0.03

Dispersal Angle	=	-51.5	Degree

Deck Transverse Moment due to Combined loads

Distance from Barrier Base (mm)	FEA Max Negative Moment (kN*m/m)	Code Dispersal Angle		Combined Modifications	
		Approximated Max Negative Moment(kN*m/m)	Finite Differences	Approximated Max Negative Moment(kN*m/m)	Finite Differences
0	121.8	106.45	-15.35	125.00	3.20
150	112.6	104.09	-8.51	118.73	6.13
300	106.9	102.06	-4.84	113.54	6.64
450	107.3	100.33	-6.97	109.25	1.95
600	108.1	98.85	-9.25	105.72	-2.38
750	107.9	97.61	-10.29	102.86	-5.04
900	106.9	96.58	-10.32	100.58	-6.32
1050	103.8	95.74	-8.06	98.81	-4.99
1200	104.8	95.07	-9.73	97.50	-7.30
			-7.28		-0.90

Table 40 - MME Approximation for PL-3 End Portion (thk275-oh1800-1.07)

MME Approximation for Performance Level 3 (thk275-oh1800-1.07)

Barrier Transverse Moment

	Due to PT	Due to Combined		Modification Factor	
Distance from Barrier Top (mm)	FEA Max Negative Moment (kN*m/m)	FEA Max Negative Moment (kN*m/m)	Finite Differences	Improved Max Negative Moment(kN*m/m)	Finite Differences
0	0	-	-	0.00	0
180	21.8	-	-	25.56	3.76
360	45.5	-	-	48.89	3.39
540	66.6	-	-	70.27	3.67
720	84.4	-	-	89.94	5.54
900	102.9	-	-	108.09	5.19
1070	124	-	-	124.00	0.00
					3.08

Dispersal Angle	=		32.5	Degree

Deck Transverse Moment due to PT

		Modification Factor	
Distance from Barrier Base (mm)	FEA Max Negative Moment (kN*m/m)	Improved Max Negative Moment(kN*m/m)	Finite Differences
0	124	124.00	0.00
300	103.3	107.75	4.45
600	96.8	95.27	-1.53
900	89	85.38	-3.62
1200	80	77.35	-2.65
1500	70.7	70.70	0.00
			-0.56

Dispersal Angle	=		57.14	Degree

Deck Transverse Moment due to PV

Distance from Barrier Base (mm)	FEA Max Negative Moment (kN*m/m)	No-Dispersion		Modification Factor	
		Approximated Max Negative Moment(kN*m/m)	Finite Differences	Approximated Max Negative Moment(kN*m/m)	Finite Differences
0	0	0.00	0.00	0.00	0.00
300	3.8	3.83	0.03	3.92	0.12
600	8	7.65	-0.35	8.03	0.03
900	12.7	11.48	-1.23	12.35	-0.35
1200	16.9	15.30	-1.60	16.90	0.00
1500	21.7	19.13	-2.58	21.70	0.00
			-0.95		-0.03

Dispersal Angle = -43.5 Degree

Deck Transverse Moment due to Combined loads

Distance from Barrier Base (mm)	FEA Max Negative Moment (kN*m/m)	Code Dispersal Angle		Combined Modifications	
		Approximated Max Negative Moment(kN*m/m)	Finite Differences	Approximated Max Negative Moment(kN*m/m)	Finite Differences
0	120	106.45	-13.55	124.00	4.00
300	105.7	102.06	-3.64	111.67	5.97
600	105.7	98.85	-6.85	103.30	-2.40
900	105	96.58	-8.42	97.73	-7.27
1200	102.8	95.07	-7.73	94.25	-8.55
1500	99.6	94.20	-5.40	92.40	-7.20
			-7.60		-2.57

148

Appendix J: Sample Transverse Moment Due to Design

Loads Plots

PL3-Barrier-oh1800-PT-Inner

Max Negative Moment (kN*m/m) vs *Distance from Barrier Top (mm)*

Legend: ◆ FEA ■ Code Disperal Angle △ New Dispersal Angle
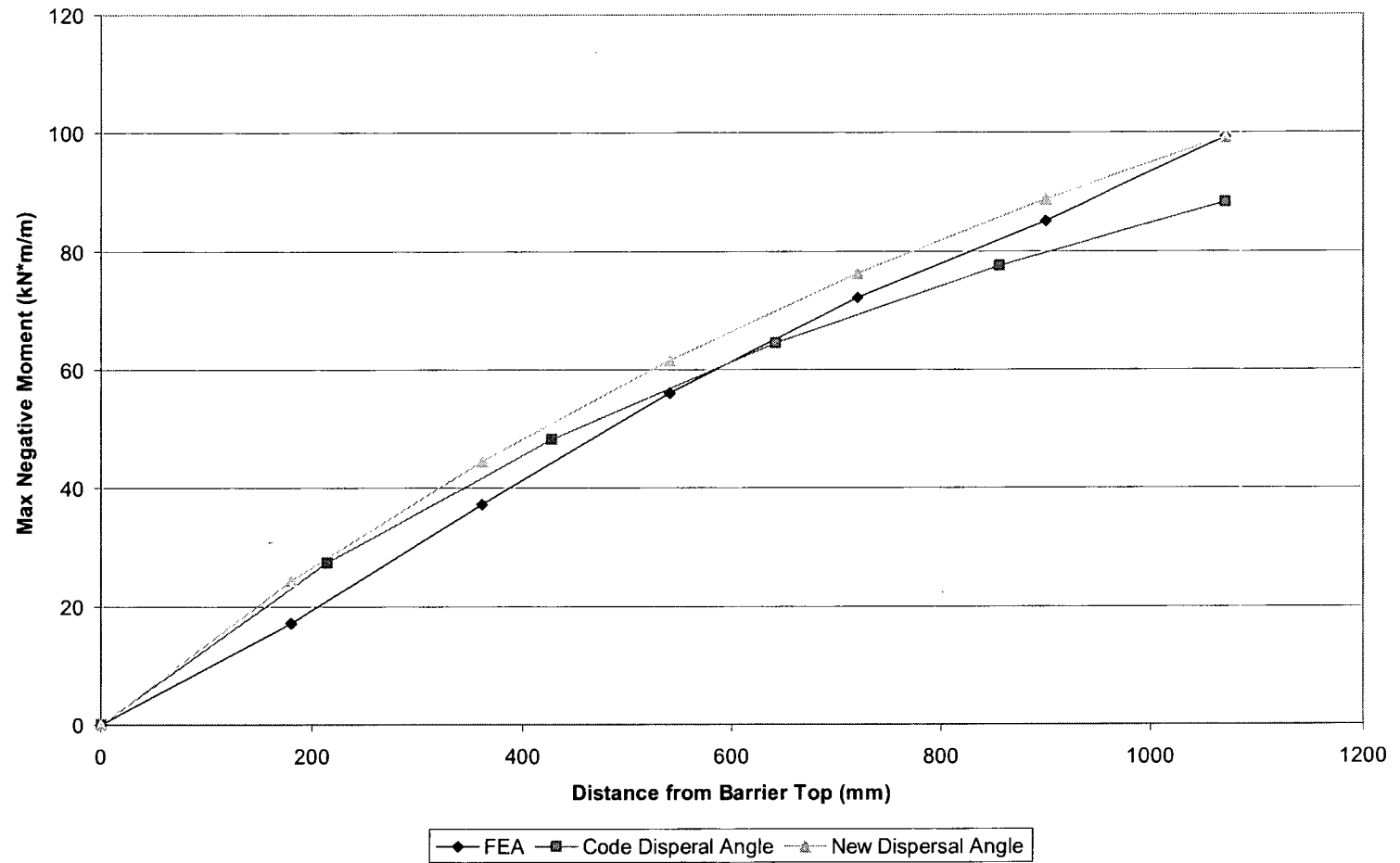
Figure 48 - Sample Plot of PT for PL-3 Barrier Internal Portion with 1800mm Overhang

PL3-Deck-oh1800-PT-Inner

Figure 49 - Sample Plot of PT for PL-3 Deck Internal Portion with 1800mm Overhang

151
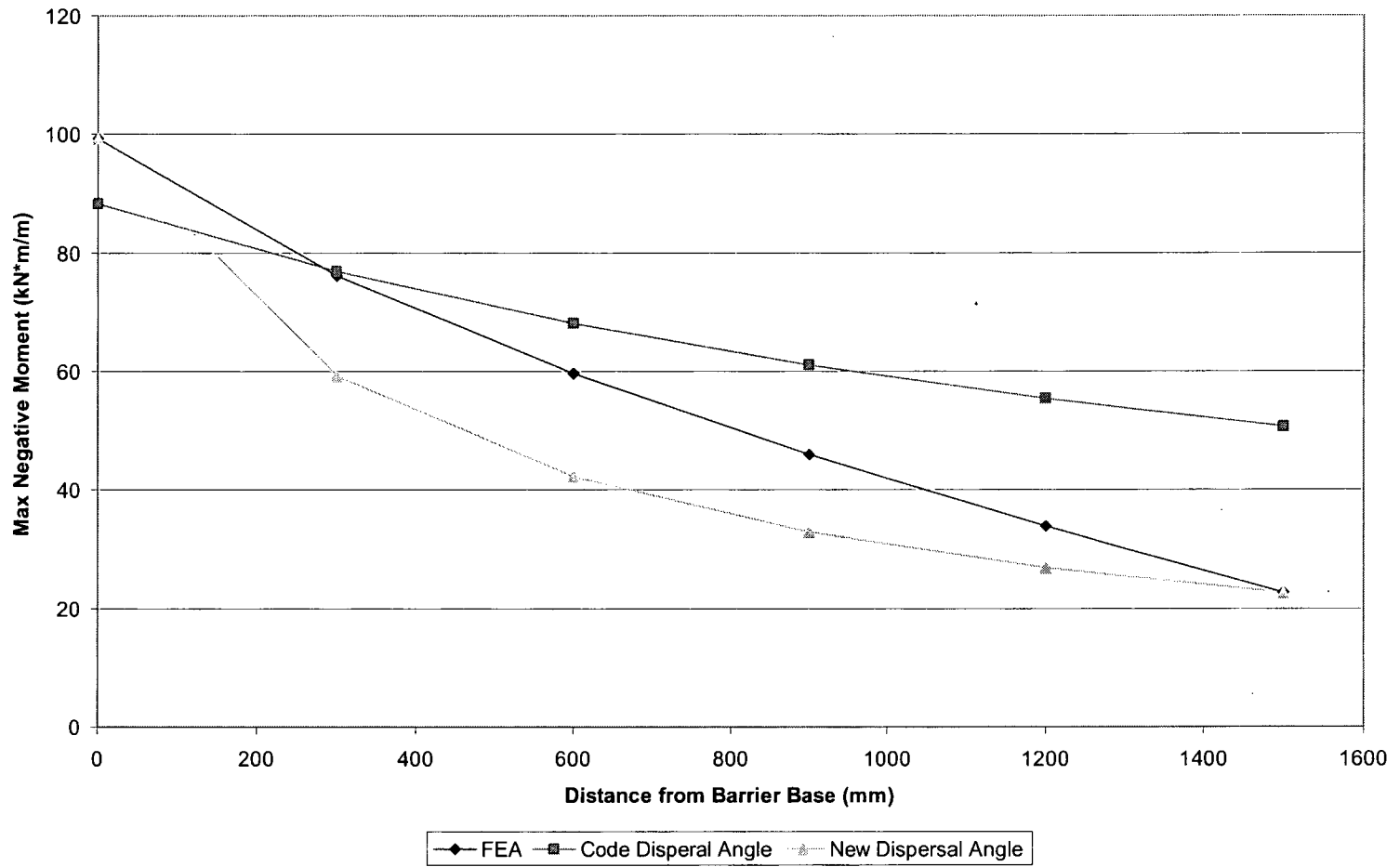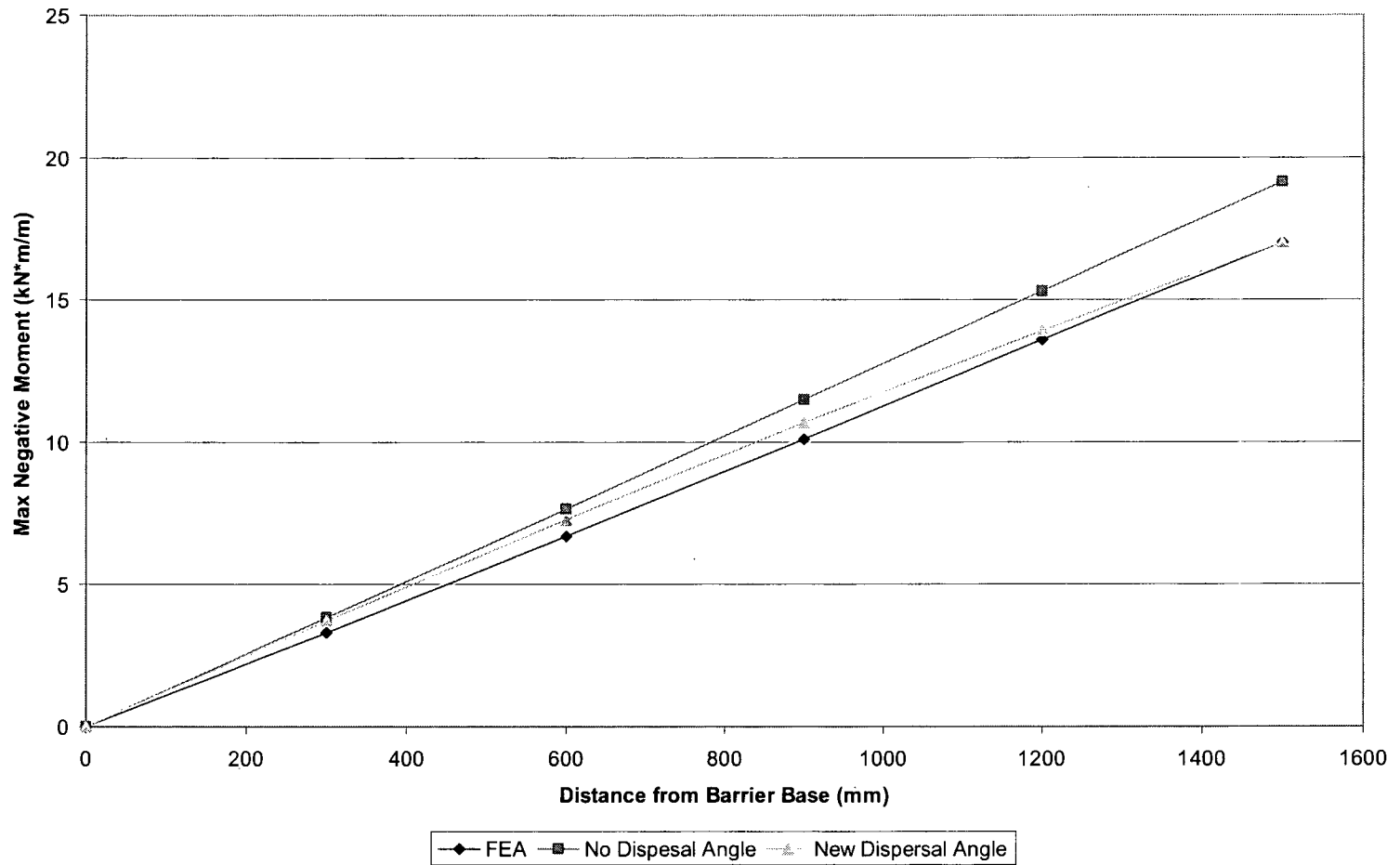
PL3-Deck-oh1800-PV-Inner

Figure 50 - Sample Plot of PV for PL-3 Deck Internal Portion with 1800mm Overhang

152

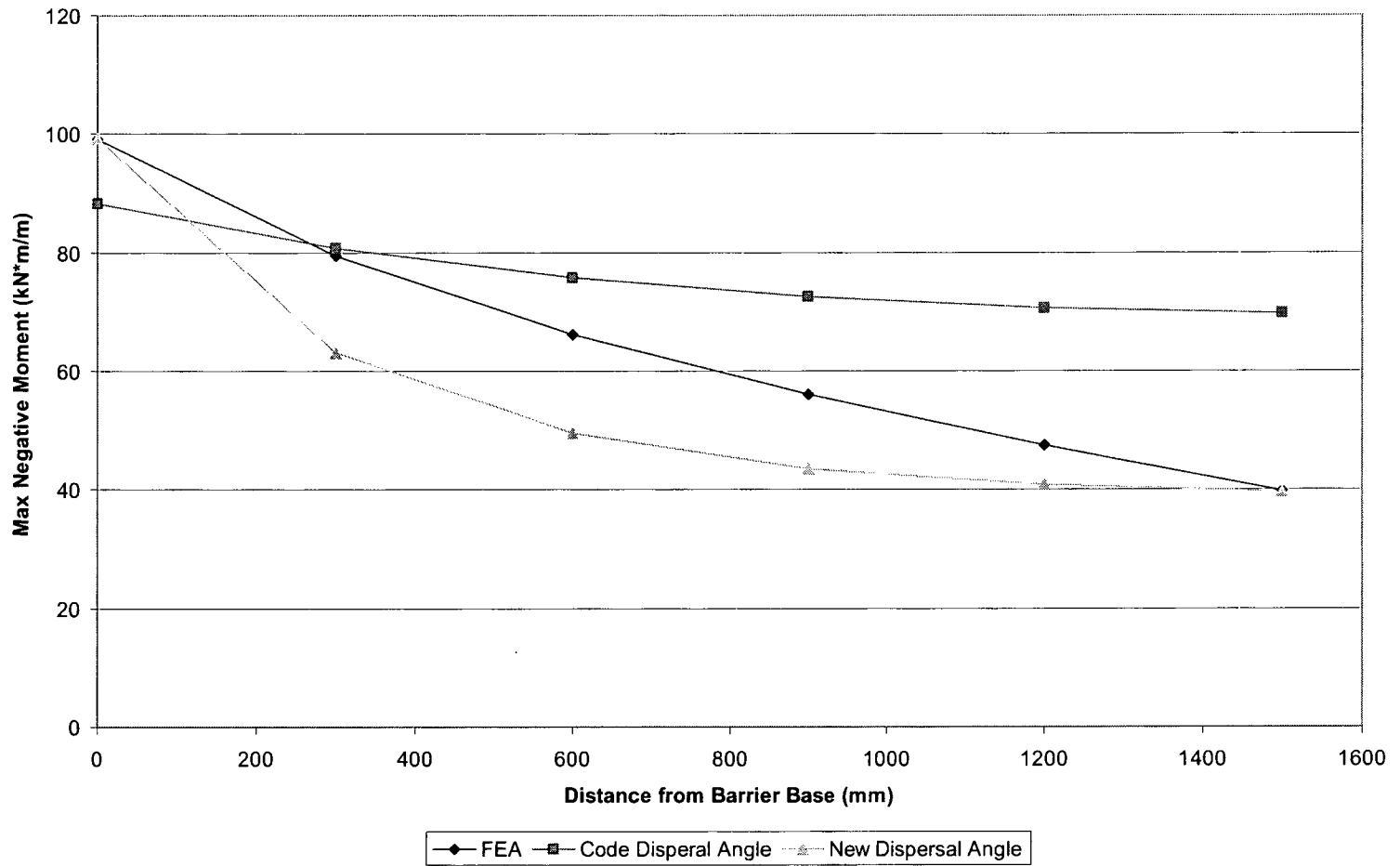**PL3-Deck-oh1800-Combined-Inner**

Figure 51 - Sample Plot of Combined Loads for PL-3 Deck Internal Portion with 1800mm Overhang

153

Appendix K: Spreadsheet for Moment Calculations

Using Dispersal Angle Method

Table 41 - Spreadsheet for Moment Calculations Using Dispersal Angle Method

PROJECT	**MoT - Joe Wong**			SECTION	1
TITLE	**Transverse Moments on Bridge Barrier and Deck**			DATE	12/06/2005
FILE	MMEv3.xls			TIME	6:01 PM

INPUT PARAMETERS

Loads

Target performance level	PL	=		=	3
Live load factor	fl	=		=	1.7
Overhang Distance	oh	=		=	1800

Barrier Type

i.)Steel Bridge Railings (PL-1) =

Post spacing	d	=		=	1200 [mm]
Width of Post Base	wp	=		=	300 [mm]

CALCULATIONS

Depth of cantilever portion	dd	= oh-DemoApplication!G19/2		=	1500 [mm]

Loads

Transverse load	Pt	= If(PL=1,50,if(PL=2,100,if(PL=3,210,"Error")))		=	210 [kN]
Longitudinal load	Pl	= If(PL=1,20,if(PL=2,30,if(PL=3,70,"Error")))		=	70 [kN]
Vertical load	Py	= If(PL=1,10,if(PL=2,30,if(PL=3,90,"Error")))		=	90 [kN]
Height of impact	h	= If(PL=1,750,if(PL=2,870,if(PL=3,1070,"Error")))		=	1070 [mm]
Barrier length for transverse and longituduenal loads	Lt	= If(PL=1,1200,if(PL=2,1050,if(PL=3,2400,"Error")))		=	2400 [mm]
Barrier length for vertical loads	Lv	= If(PL=1,5500,if(PL=2,5500,if(PL=3,12000,"Error")))		=	12000 [mm]
Factored transverse load	FPt	= Pt*fl		=	357 [kN]
Factored longitudinal load	FPl	= Pl*fl		=	119 [kN]
Factored vertical load	FPy	= Py*fl		=	153 [kN]
Factored moment due to transverse load (N.A. for PL-1)	Mt	= FPt*h		=	381990 [kN*mm]

Dispersal Angle of Barrier

Moment @ inner portion	thetami	= If(PL=1,"N.A.",if(PL=2,56,if(PL=3,42,"Error")))		=	42 [degree]
Tensile force @ inner portion	thetati	= If(PL=1,"N.A.",if(PL=2,25,if(PL=3,3,"Error")))		=	3 [degree]
Moment @ end portion	thetame	= If(PL=1,"N.A.",if(PL=2,55,if(PL=3,48,"Error")))		=	48 [degree]
Tensile force @ end portion	thetate	= If(PL=1,"N.A.",if(PL=2,8,if(PL=3,0,"Error")))		=	0 [degree]

Dispersal Length @ Barrier Base

Moment @ inner portion	Ltmi	= Lt+2*h*tan(radians(thetami))		=	4326.86 [mm]
Tensile force @ inner portion	Ltti	= Lt+2*h*tan(radians(thetati))		=	2512.15 [mm]
Moment @ end portion	Ltme	= Lt+h*tan(radians(thetame))		=	3588.36 [mm]
Tensile force @ end portion	Ltte	= Lt+h*tan(radians(thetate))		=	2400.00 [mm]

Dispersal Angle of Deck

Moment @ inner portion	thetaid	= If(PL=1,55,if(PL=2,55,if(PL=3,47,"Error")))		=	47 [degree]
Tensile force @ inner portion	thetatd	= If(PL=1,20,if(PL=2,20,if(PL=3,10,"Error")))		=	10 [degree]
Moment @ end portion	thetaed	= If(PL=1,55,if(PL=2,55,if(PL=3,45,"Error")))		=	45 [degree]
Tensile force @ end portion	thetafe	= If(PL=1,8,if(PL=2,8,if(PL=3,0,"Error")))		=	0 [degree]
Vertical for both portions	thetavd	=	0 =		0.00 [degree]

INTERNAL PORTION

Barrier

ii.) Cast-in-place Concrete Barrier (PL-3) or Precast Concrete Barrier (PL-2)

Distance from barrier top @ section:

0	h0	= 0*h		=	0.00 [mm]
1	h1	= 0.2*h		=	214.00 [mm]
2	h2	= 0.4*h		=	428.00 [mm]
3	h3	= 0.6*h		=	642.00 [mm]
4	h4	= 0.8*h		=	856.00 [mm]
5	h5	= h		=	1070.00 [mm]

Transverse moment due to transverse load @ section:

0	mh0	= FPt*h0		=	0
1	mh1	= FPt*h1		=	76398
2	mh2	= FPt*h2		=	152796
3	mh3	= FPt*h3		=	229194
4	mh4	= FPt*h4		=	305592
5	mh5	= FPt*h5		=	381990

Dispersal length @ section:

0	d0	= Lt+2*h0*tan(radians(thetami))		=	2400.00
1	d1	= Lt+2*h1*tan(radians(thetami))		=	2785.37
2	d2	= Lt+2*h2*tan(radians(thetami))		=	3170.75
3	d3	= Lt+2*h3*tan(radians(thetami))		=	3556.12
4	d4	= Lt+2*h4*tan(radians(thetami))		=	3941.49
5	d5	= Lt+2*h5*tan(radians(thetami))		=	4326.86

Transverse moment distribution @ section:

0	md0	= mh0/d0		=	0.00
1	md1	= mh1/d1		=	27.43
2	md2	= mh2/d2		=	48.19
3	md3	= mh3/d3		=	64.45
4	md4	= mh4/d4		=	77.53
5	md5	= mh5/d5		=	88.28

Deck
i.) Steel Bridge Railings (PL-1)

Traverse load per post   Ptp $=$ $=$

     $=$ if(Lt<d,FPt,if(Lt<2*d,FPt/2,if(Lt<3*d,FPt/3,"Error"))) $=$ 119.00   [kN]

Vertical load per post   if(Lv<d,FPy,if(Lv<2*d,FPy/2,if(Lv<3*d,FPy/3,if(Lv<4*d,

     Pyp   FPy/4,if(Lv<5*d,FPy/5,if(Lv<6*d,FPy/6,if(Lv<7*d,FPy/7,

     $=$ if(Lv<8*d,FPy/8,"Error"))))))) $=$ Error   [kN]

Moment due to transverse load   Mtp $=$ Ptp*h $=$ 1.27E+05 [kN*mm]

Moment due to vertical load   Myp $=$ Pyp*0 $=$ #VALUE!   [kN*mm/mm]

Distance @ sections

0	dd0	$=$ 0*dd	$=$	0	[mm]
1	dd1	$=$ 0.2*dd	$=$	300	[mm]
2	dd2	$=$ 0.4*dd	$=$	600	[mm]
3	dd3	$=$ 0.6*dd	$=$	900	[mm]
4	dd4	$=$ 0.8*dd	$=$	1200	[mm]
5	dd5	$=$ dd	$=$	1500	[mm]

Dispersal length of transverse moment

At 0*dd	D0	$=$ wp	$=$	300.00	[mm]
At 0.2*dd	D1	$=$ 0.2*dd*tan(radians(thetaid))*2+wp	$=$	943.42	[mm]
At 0.4*dd	D2	$=$ 0.4*dd*tan(radians(thetaid))*2+wp	$=$	1586.84	[mm]
At 0.6*dd	D3	$=$ 0.6*dd*tan(radians(thetaid))*2+wp	$=$	2230.26	[mm]
At 0.8*dd	D4	$=$ 0.8*dd*tan(radians(thetaid))*2+wp	$=$	2873.68	[mm]
At dd	D5	$=$ dd*tan(radians(thetaid))*2+wp	$=$	3517.11	[mm]

Transverse moment distribution

At 0*dd	Mdtp0	$=$ Mtp/wp	$=$	424.43	[kN*mm/mm]
At 0.2*dd	Mdtp1	$=$ Mtp/D1	$=$	134.97	[kN*mm/mm]
At 0.4*dd	Mdtp2	$=$ Mtp/D2	$=$	80.24	[kN*mm/mm]
At 0.6*dd	Mdtp3	$=$ Mtp/D3	$=$	57.09	[kN*mm/mm]
At 0.8*dd	Mdtp4	$=$ Mtp/D4	$=$	44.31	[kN*mm/mm]
At dd	Mdtp5	$=$ Mtp/D5	$=$	36.20	[kN*mm/mm]

Dispersal length of vertical load

At 0*dd	Dv0	$=$ wp	$=$	300.00	[mm]
At 0.2*dd	Dv1	$=$ 0.2*dd*tan(radians(thetavd))*2+wp	$=$	300.00	[mm]
At 0.4*dd	Dv2	$=$ 0.4*dd*tan(radians(thetavd))*2+wp	$=$	300.00	[mm]
At 0.6*dd	Dv3	$=$ 0.6*dd*tan(radians(thetavd))*2+wp	$=$	300.00	[mm]
At 0.8*dd	Dv4	$=$ 0.8*dd*tan(radians(thetavd))*2+wp	$=$	300.00	[mm]
At dd	Dv5	$=$ dd*tan(radians(thetavd))*2+wp	$=$	300.00	[mm]

Moment due to vertical load

At 0*dd	Mv0	$=$ Pyp*0*dd	$=$	#VALUE!	[kN*mm]
At 0.2*dd	Mv1	$=$ Pyp*0.2*dd	$=$	#VALUE!	[kN*mm]
At 0.4*dd	Mv2	$=$ Pyp*0.4*dd	$=$	#VALUE!	[kN*mm]
At 0.6*dd	Mv3	$=$ Pyp*0.6*dd	$=$	#VALUE!	[kN*mm]
At 0.8*dd	Mv4	$=$ Pyp*0.8*dd	$=$	#VALUE!	[kN*mm]
At dd	Mv5	$=$ Pyp*dd	$=$	#VALUE!	[kN*mm]

Moment distribution due to vertical load

At 0*dd	Mdv0	$=$ Mv0/Dv0	$=$	#VALUE!	[kN*mm/mm]
At 0.2*dd	Mdv1	$=$ Mv1/Dv1	$=$	#VALUE!	[kN*mm/mm]
At 0.4*dd	Mdv2	$=$ Mv2/Dv2	$=$	#VALUE!	[kN*mm/mm]
At 0.6*dd	Mdv3	$=$ Mv3/Dv3	$=$	#VALUE!	[kN*mm/mm]
At 0.8*dd	Mdv4	$=$ Mv4/Dv4	$=$	#VALUE!	[kN*mm/mm]
At dd	Mdv5	$=$ Mv5/Dv5	$=$	#VALUE!	[kN*mm/mm]

Total Moment

At 0*dd	Mtt0	$=$ Mdv0+Mdtp0	$=$	#VALUE!	[kN*mm/mm]
At 0.2*dd	Mtt1	$=$ Mdv1+Mdtp1	$=$	#VALUE!	[kN*mm/mm]
At 0.4*dd	Mtt2	$=$ Mdv2+Mdtp2	$=$	#VALUE!	[kN*mm/mm]
At 0.6*dd	Mtt3	$=$ Mdv3+Mdtp3	$=$	#VALUE!	[kN*mm/mm]
At 0.8*dd	Mtt4	$=$ Mdv4+Mdtp4	$=$	#VALUE!	[kN*mm/mm]
At dd	Mtt5	$=$ Mdv5+Mdtp5	$=$	#VALUE!	[kN*mm/mm]

ii.) Cast-in-place Concrete Barrier (PL-3) or Precast Concrete Barrier (PL-2)

Distance @ sections

0	dd0ii	$= 0*dd$	=	0 [mm]
1	dd1ii	$= 0.2*dd$	=	300 [mm]
2	dd2ii	$= 0.4*dd$	=	600 [mm]
3	dd3ii	$= 0.6*dd$	=	900 [mm]
4	dd4ii	$= 0.8*dd$	=	1200 [mm]
5	dd5ii	$= dd$	=	1500 [mm]

Dispersal length of transverse moment

At 0*dd	D0ii	$= Ltmi$	=	4326.86 [mm]
At 0.2*dd	D1ii	$= 0.2*dd*tan(radians(thetaid))*2+Ltmi$	=	4970.29 [mm]
At 0.4*dd	D2ii	$= 0.4*dd*tan(radians(thetaid))*2+Ltmi$	=	5613.71 [mm]
At 0.6*dd	D3ii	$= 0.6*dd*tan(radians(thetaid))*2+Ltmi$	=	6257.13 [mm]
At 0.8*dd	D4ii	$= 0.8*dd*tan(radians(thetaid))*2+Ltmi$	=	6900.55 [mm]
At dd	D5ii	$= dd*tan(radians(thetaid))*2+Ltmi$	=	7543.97 [mm]

Transverse moment distribution

At 0*dd	Mdtp0ii	$= Mt/D0ii$	=	88.28 [kN*mm/mm]
At 0.2*dd	Mdtp1ii	$= Mt/D1ii$	=	76.85 [kN*mm/mm]
At 0.4*dd	Mdtp2ii	$= Mt/D2ii$	=	68.05 [kN*mm/mm]
At 0.6*dd	Mdtp3ii	$= Mt/D3ii$	=	61.05 [kN*mm/mm]
At 0.8*dd	Mdtp4ii	$= Mt/D4ii$	=	55.36 [kN*mm/mm]
At dd	Mdtp5ii	$= Mt/D5ii$	=	50.64 [kN*mm/mm]

Moment due to vertical load

At 0*dd	Mv0ii	$= FPy*0*dd$	=	0 [kN*mm]
At 0.2*dd	Mv1ii	$= FPy*0.2*dd$	=	45900 [kN*mm]
At 0.4*dd	Mv2ii	$= FPy*0.4*dd$	=	91800 [kN*mm]
At 0.6*dd	Mv3ii	$= FPy*0.6*dd$	=	137700 [kN*mm]
At 0.8*dd	Mv4ii	$= FPy*0.8*dd$	=	183600 [kN*mm]
At dd	Mv5ii	$= FPy*dd$	=	229500 [kN*mm]

Dispersal length of vertical load

At 0*dd	Dv0ii	$= Lv$	=	12000.00 [mm]
At 0.2*dd	Dv1ii	$= 0.2*dd*tan(radians(thetavd))*2+Lv$	=	12000.00 [mm]
At 0.4*dd	Dv2ii	$= 0.4*dd*tan(radians(thetavd))*2+Lv$	=	12000.00 [mm]
At 0.6*dd	Dv3ii	$= 0.6*dd*tan(radians(thetavd))*2+Lv$	=	12000.00 [mm]
At 0.8*dd	Dv4ii	$= 0.8*dd*tan(radians(thetavd))*2+Lv$	=	12000.00 [mm]
At dd	Dv5ii	$= dd*tan(radians(thetavd))*2+Lv$	=	12000.00 [mm]

Moment distribution due to vertical load

At 0*dd	Mdv0ii	$= Mv0ii/Dv0ii$	=	0.00 [kN*mm/mm]
At 0.2*dd	Mdv1ii	$= Mv1ii/Dv1ii$	=	3.83 [kN*mm/mm]
At 0.4*dd	Mdv2ii	$= Mv2ii/Dv2ii$	=	7.65 [kN*mm/mm]
At 0.6*dd	Mdv3ii	$= Mv3ii/Dv3ii$	=	11.48 [kN*mm/mm]
At 0.8*dd	Mdv4ii	$= Mv4ii/Dv4ii$	= ·	15.30 [kN*mm/mm]
At dd	Mdv5ii	$= Mv5ii/Dv5ii$	=	19.13 [kN*mm/mm]

Total Moment

At 0*dd	Mtt0ii	$= Mdv0ii+Mdtp0ii$	=	88.28 [kN*mm/mm]
At 0.2*dd	Mtt1ii	$= Mdv1ii+Mdtp1ii$	=	80.68 [kN*mm/mm]
At 0.4*dd	Mtt2ii	$= Mdv2ii+Mdtp2ii$	=	75.70 [kN*mm/mm]
At 0.6*dd	Mtt3ii	$= Mdv3ii+Mdtp3ii$	=	72.52 [kN*mm/mm]
At 0.8*dd	Mtt4ii	$= Mdv4ii+Mdtp4ii$	=	70.66 [kN*mm/mm]
At dd	Mtt5ii	$= Mdv5ii+Mdtp5ii$	=	69.76 [kN*mm/mm]

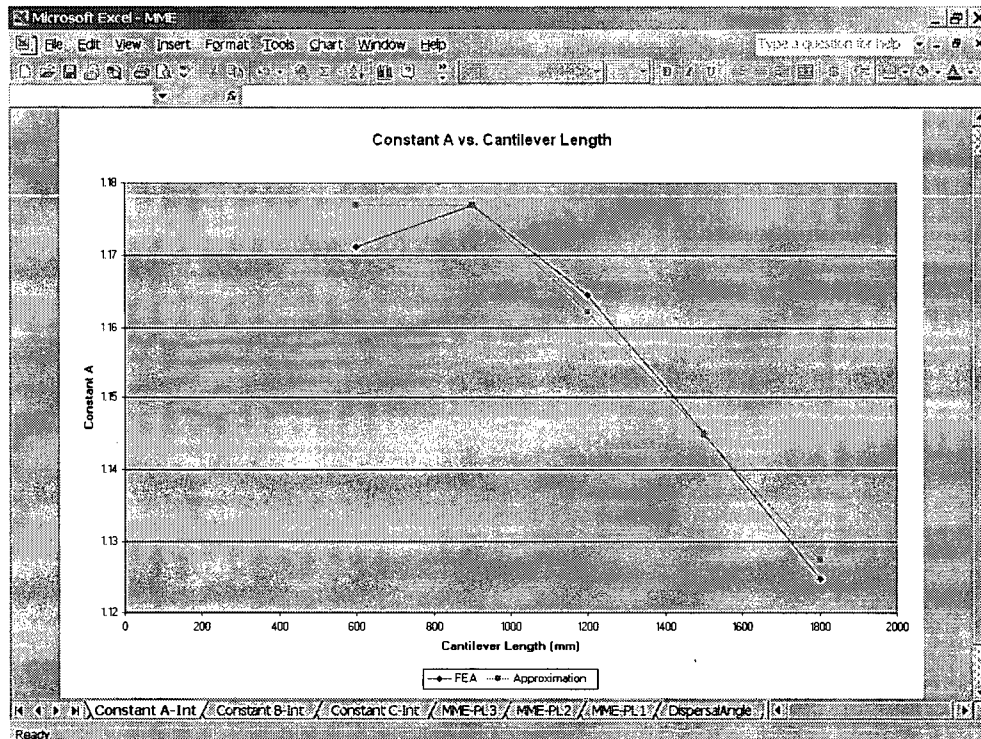# Appendix L: Constants vs. Cantilever Length

Relationship for MME

Figure 52 - Constant A vs. Cantilever Length Plot for MME

Figure 53 - Spreadsheet MME Calculations for Constant A

159

Figure 54 - Constant B vs. Cantilever Length Plot for MME

Figure 55 - Spreadsheet MME Calculations for Constant B

160

Figure 56 - Constant C vs. Cantilever Length Plot for MME

Figure 57 - Spreadsheet MME Calculations for Constant C

161

DEPARTMENT OF CIVIL ENGINEERING
UNIVERSITY OF BRITISH COLUMBIA

CHECKLIST
FOR GRADUATING GRADUATE STUDENTS

o   **Apply for Graduation** either on-line at
http://students.ubc.ca/current/graduation.cm?page=apply (Deadline dates are found in the Calendar). Inform the Graduate Secretary that you have applied for graduation.

o   **Submission of Theses**

For PhD dissertations, the requirement is as follows.
The department <u>does not</u> require a hard copy for archiving in the CEME Reading Room. PhD dissertations will be available to UBC users through the ProQuest distribution service via the UBC Library. Any copies required by you and your supervisor should be agreed upon by both of you. It is the responsibility of the student to produce all of the copies required.

For MASc theses, the requirements are as follows.
The department <u>does not</u> require a hard copy for archiving in the CEME Reading Room. The Reading Room is rapidly filling with MASc theses and many of these have become badly worn through use by subsequent students. The new requirement is for a CD version of your thesis in PDF format. The department will be making MASc theses available to UBC users through our web site. Note that MASc theses are not readily available via any other means, as the UBC Library stores copies only in microfiche form and MASc theses are not distributed through ProQuest. Any copies required by you and your supervisor should be agreed upon by both of you. It is the responsibility of the student to produce all of the copies required.

If you do not have the Adobe Acrobat software required to convert your word processor document to PDF, it is available in the graduate computer lab downstairs in CEME. A word processor document is not adequate because it is not a read-only file.

o   **Desk and office area** must be cleaned, and the Department's Graduate Secretary advised of your departure.

o   **Lockers** must be cleared out and advise the CEGSS.

o   **Lab work area** must be cleaned and left tidy, including the disposal of all samples, and the return of lab keys, equipment, tools and instrumentation to the Machine Shop or Lab Manager.

o   **Computer accounts:** "Home" directory should be cleaned out and the Computer Laboratory Manager advised of your departure.

o   Advise the Department office of your forwarding address and have someone check your **mailbox** after your leave. If you request the Department office to forward your mail this will be done for 3 months only.

o   Return all **copy cards** to the CEGSS copy card representative for refund.

o   Return all **books** and **periodicals** to the Library and Reading Room.

o   Return all **keys** to Parking & Security Access Control Centre and present receipt to the Department office for a refund.